Improving Predictions for Camber in Precast, Prestressed Concrete Bridge Girders

Hang Thi Nguyet Nguyen

A thesis
submitted in partial fulfillment of the
requirements for the degree of

Master of Science in Civil Engineering

University of Washington

2014

Committee:

John F. Stanton

Marc O. Eberhard

Program Authorized to Offer Degree:
Civil and Environmental Engineering

University of Washington

Abstract

Improving predictions for camber in precast, prestressed concrete bridge girders.

Hang Thi Nguyet Nguyen

Chair of the Supervisory Committee:
Professor of Structural Engineering and Mechanics - John F. Stanton
Department of Civil and Environmental Engineering
Professor of Structural Engineering and Mechanics - Marc O. Eberhard
Department of Civil and Environmental Engineering

Most of the modern medium-span bridges in the United States are constructed with precast, prestressed concrete girders. An accurate estimate of girder camber is important for all parties involved in the precast concrete industry for several reasons. The most important reason is that achieving vertical alignment, and casting the deck, becomes much more difficult if the cambers of two adjacent girders in the bridge are not the same, since the girders are generally too large to make the correction by brute force. In addition, any uncertainty of the estimated camber in the precast, prestressed concrete girders can lead to construction delays and can increase material and labor costs. However, the prediction and control of camber over time is difficult, because camber varies with many parameters, such as the concrete properties, curing methods, and temperature variations.

The goal of this research is to improve the methods to predict camber in precast, prestressed concrete girders, with an emphasis on determining the effect of temperature on camber both

during curing and in service. The research focused on monitoring and collecting fabrication camber to calibrate the current models for predicting camber. Temperature histories at release and service were also recorded to examine the effect of fabrication temperatures on initial camber and the effect of daily temperature variations on service camber.

Two models were developed to predict daily camber changes under solar radiation based on ambient temperature data. The predictions of the models correlate well with the data collected during the research.

ACKNOWLEDGEMENTS

I would like to thank to Vietnam Education Foundation (VEF) for bringing me a great change to study in the US. Thanks to the P.C. Bridge Endowed Fellowship for giving me funding to pursue my studies at the University of Washington.

I would like to thank to professors John F. Stanton and Marc O. Eberhard for their inspiration, friendship and guidance. I would also like to thank to Professor Greg Miller for helping me out with the programing stuff and his kind help whenever I needed.

Special thanks go to David D. Chapman, Chief Engineer at Concrete Technology Corporation (CTC) and engineers, workers at CTC for their great support during my time of working there.

Thanks to the many graduate students at More Hall: Olafur Haraldsson, Saura Jost, Todd Janes, Travis Thonstad, Bo-Shiuan Wang, Ching Ji who helped me and made my student life more joyful.

Last but not the least, I would like to thank my husband, Hung for all the love, support and encouragement. Graciously, thanks to my family for all their love and support over the years. Thank you for always being with me.

Table of Contents

List of Figures

List of Tables

1 INTRODUCTION

Most modern, medium span bridges in the US are constructed with precast, prestressed concrete girders. In precast concrete bridge girders, camber or upward deflection is normally defined as a combination of the flexural upward deflection caused by the eccentric axial compression and the downward deflection due to gravity loads. An accurate estimate of camber is important for all parties involved in the precast concrete industry for several reasons. Bridge engineers are interested because they compute theoretical cambers, which determine the depth of the cast-in-place "pad" topping under the desk and more importantly, because they set the vertical alignment between two adjacent girders based on the predicted camber. Contractors are concerned because they prepare their bids by estimating the quantities of labor and material needed to construct the bridge according to the engineer's plans. The uncertainty in the estimated camber in precast, prestressed concrete girders can lead to problems during construction.

If the camber is larger than predicted, the top of the girder may conflict with the bottom reinforcement in the bridges deck. If the camber is lower than estimated, the contractor must increase the depth of the pad, resulting in additional material requirements and loads on the bridge. Moreover, if the top surfaces of two adjacent girders are not located in their planned vertical locations, placing the deck forms and steel could be difficult because the girders are generally too large to make the correction by brute force. Therefore, if the actual camber of the girder is different from predicted, it can lead to construction delays and increased material and labor costs.

However, the prediction and control of camber over time is difficult because camber varies with a number of parameters, such as concrete properties, curing methods, and temperature variations. The purpose of this study is improve the methods for predicting camber in precast, prestressed concrete girders, with an emphasis on determining the effect of temperature on camber both during curing and in service.

1.1 Previous Work

An accurate estimate of camber is important for all parties involved in the precast concrete industry. Many researchers have focused on improving methods of predicting camber. The following sections review some of the main research studies relevant to the present study.

1.1.1 Effects of Temperature Variations on Precast, Prestressed Concrete Bridge Girders

Barr et al. (2005) mostly focused on the effects of temperature variations on the change of strand stress and camber. He conducted experiments and recorded temperatures, strains and cambers for five girders in a prestressed concrete bridge and a matching test girder in Washington State over three years. The measurements were used to study strand stress and camber change caused by elevated curing temperature during fabrication and variations in service conditions. Barr pointed out that for the five girders that they investigated, high curing temperature reduced the calculated prestressing stress from the original design values at release by 3% to 7%, reduced the initial camber by 26% to 40% and increased the service bottom stress by 60% of the allowable tension stress.

1.1.2 Improving Predictions for Camber in Precast, Prestressed Concrete Bridge Girders

Rosa et al. (2007), a research group from the University of Washington, researched camber using field measurements, material testing and various predictive models. The primary goal of the research was to propose a new or modified camber prediction methodology that reduced errors in camber predictions.

In order to evaluate the camber prediction methods, Rosa measured cambers on eight WF74 girders for the Snake Lake Bridge project in Washington. Next, he took measurements on W83G girders fabricated at Central Premix Prestress Co. (CPM) in Washington. Cambers were monitored for 28 days in the fabrication yard. Additionally, measurements were taken on 91 girders from the Keys Road Project in Yakima, Washington. For this set of girders, he focused on the change in camber due to the release of temporary prestressing strands, deck placement, and time-dependent deflection after placing the deck. In addition, he collected camber readings for 110 girders from various projects fabricated during the previous 11 years.

Rosa developed a program that allowed the user to input the desired parameters to create better camber predictions. He calibrated the program by comparing the predicted and measured cambers of the 146 girders in the database, which were produced by Concrete Technology Corporation (CTC) and Central Premix Prestress Co. (CPM), both directly after release and at a later time. The results show that predicted camber is sensitive to the predicted stress losses, and that the 2006 AASHTO Specifications lead to much better camber estimates than the 2004 provision did. In addition, to achieve the best match, correction factors were recommended to the prediction equations. Specifically, the adjustment factor for the elastic modulus using the AASHTO 2006 was 1.15. Selecting the factor as $E_c = 1.15$ led to an optimization for the creep coefficient factor of 1.4. Rosa recommended using 1.4 times the value given by the AASHTO LRFD 2006 equation for predicting the creep coefficient.

1.1.3 Precast, Prestressed Girder Camber Variability

Tadros et al. (2011) took camber measurements at prestress transfer and several later stages for 382 pretensioned concrete bridge girders from various fabricators and states. They examined the camber variations including the compressive concrete strength, the concrete elastic modulus, the debonding and transfer length, the temperature of strands, the girder production schedule and the curing method. They proposed two models for predicting camber in prestressed concrete bridge girders. One was the approximate method and the other one was the refined method. Tadros et al. pointed out that camber predictions should account for the fact that the concrete strength at transfer and at 28 days is typically higher than the specified values. They also affirmed that curing methods significantly affect the transfer camber.

1.1.4 Validation of Prestressed Concrete I-Beam Deflection and Camber Estimates

Cullen et al. (2012) collected extensive historical fabrication data for 1067 precast girders produced between 2006 and 2010, of which 768 girders were monitored at the time of erection. Various factors that affect the release camber were investigated, including concrete strength and modulus of elasticity, and variations in the strand prestress force.

Cullen et al. found that on average, the measured release camber was only 74% of the predicted value. In addition, the measured camber at erection for the 768 girders was only 83.5%, on average, of the design value. All the calculations followed the Minnesota Department

of Transportation (MnDOT) Specifications (2012) for camber prediction. Cullen et al. examined various factors that affect the release camber, including the compressive concrete strength, the elastic modulus, and variations of prestress force in the strands. They found that the actual concrete strength at release was, on average, 15% higher than the design value. Also, the MnDOT model to estimate elastic modulus underestimated the actual elastic modulus. Cullen showed that the Pauw (1960) model (which is used by AASHTO LRFD 2010 Bridge Design Specification (prov. 5.4.2.4)) provided the best predictions for the concrete elastic modulus. The errors between calculated and measured cambers were significantly reduced by using Pauw's model rather than the ACI 363 equation currently used by the MnDOT in the camber calculations. Cullen at el. (2012) also analyzed the effects of thermal changes during curing and showed that they caused an average reduction in strand stress at release of approximately 3%.

1.2 Research Objectives

The accurate prediction of camber growth is difficult because of the many variables that affect it, such as concrete properties, methods of curing, design assumptions, weather conditions. The primary goal of this research is to improve the methods for predicting camber in precast, prestressed concrete girders. The research focused on monitoring, collecting fabrication camber to calibrate the current models for predicting camber. Temperature histories at release and service were also recorded to examine their effects on initial and in service camber respectively. The following specific objectives were considered:

- Evaluating the effect of using actual rather than design concrete strength for predicting camber.
- Evaluating common models for predicting elastic modulus.
- Evaluating the effect of thermal on camber change in various times by monitoring thermal histories of girders at release and at service condition.
- Providing recommendations to improve current methods of predicting camber.

1.3 Organization of Thesis

This thesis is organized as follows:

- Chapter 2 provides information of the girders that Rosa at el. (2007) monitored and collected from two fabricators in Washington State.
- Chapter 3 describes camber monitoring of nine girders from the Alaska Way Viaduct project in Seattle.
- Chapter 4 compares measured and design concrete strengths and evaluates the effect on camber of using actual instead of the design concrete strength on camber.
- Chapter 5 presents calibrations of current models used to predict the concrete elastic modulus.
- Chapter 6 presents internal temperature monitoring histories from two WF100 girders in storage conditions and evaluates the effect of daily temperature variations on camber. Two models were developed for predicting camber change under the effect of daily temperature variations.
- Chapter 7 shows histories of internal temperature during and after curing for six girders cast at Concrete Technology Corporation in Tacoma and Central Premix in Spokane. The chapter concentrates on analyzing the effect of heating the strand before it bonds to the concrete and the effect on camber of thermal gradient at bonding times. The results help to explain the large errors between predicted and measured release camber for the CPM girders.
- Chapter 8 summarizes the research and its conclusion. It also provides recommendations for future calculations in predicting camber.

2 ROSA'S CAMBER DATABASE

This study used Rosa's camber database to calibrate the effect of concrete compressive strength and the effect of elastic modulus on camber. Therefore, this chapter will briefly describe Rosa's camber database.

Rosa et al. (2007) collected girder properties and camber data for 146 girders from two fabricators in Washington State. Most of these girders (103) were fabricated by Concrete Technology Corporation (CTC), in Tacoma, Washington, and the others (43) were cast by Central Premix Prestress Co. (CPM), in Spokane, Washington. The girders varied in cross section, length, concrete strength, curing history and number of prestressing strands. The following sections summarize the properties of the girders in Rosa's camber database.

2.1 Data Collection from Concrete Technology Corporation (CTC)

The 103 girders from CTC came from four projects.

Eight girders were fabricated as part of the Snake Lake Bridge project and were monitored by Rosa over time. Those girders were monitored from Aug 29, 2005 to Oct 28, 2005. All of the girders had W74G sections and were 135-feet long. The information was useful for calibrating time-varying camber models. Concrete material testing for the six of eight girders was performed concurrently in the materials lab at University of Washington (UW) in Seattle, Washington. The material tests provided values of the actual compressive strength, measured elastic modulus, as well as the shrinkage and creep properties of the concrete. These properties were then compared with the predicted values to evaluate the accuracy of the prediction equations.

The other 95 CTC girders were fabricated over an 11-year period. The information for these three projects was gathered from the company's files. This information included the camber at release and a one later time.

- Black Lake Bridge Project: This project included 66 W74 girders, which had lengths ranging from 65 to 131 feet.

- The 277th St Bridge project: The project included 16 girders with W50G sections. All girders had the same length (96 feet).
- Cedar River Bridge project: This project included 13 WF74 girders. The girders all had one of three lengths: 95, 120 or 128 feet.

2.2 Data Collection from Central Premix Prestress Co. (CPM)

The Rosa camber database included girder properties and camber data for 43 girders from two projects.

- Keys Road Bridge Project: The data mostly was used to evaluate the effects of the release of temporary stands and deck placement on camber. Detailed field camber monitoring was conducted on 28 girders cast in the CTC for the Keys Road Bridge project in Yakima, Washington from Nov 30, 2005 to Nov 13, 2006. This monitoring was described in Chapter 6 of Rosa at el. (2007). All the measured girders had a W83 cross section and were approximately 178-feet long.
- Yakima River Bridge Project: This project included 15 W83G girders. All the girders were 171 feet long.

2.3 Summary of Girder Properties

This section summarizes the key information for the 146 girders in Rosa's camber database.

Table 2-1 shows number of girders according to cross-section type. The sections in the database are the most commonly used sections in Washington State. The population distributions for girder length and section type are summarized in Figure 2-1. As shown in the table and figure, the W74 girders dominated the Rosa's database.

Table 2-1. Number of Girders with Each Cross-Section Type

	Number of girders			
	W50G	W74G	WF74G	W83G
CTC	16	74	13	0
CPM	0	0	0	43
Total	**16**	**74**	**13**	**43**

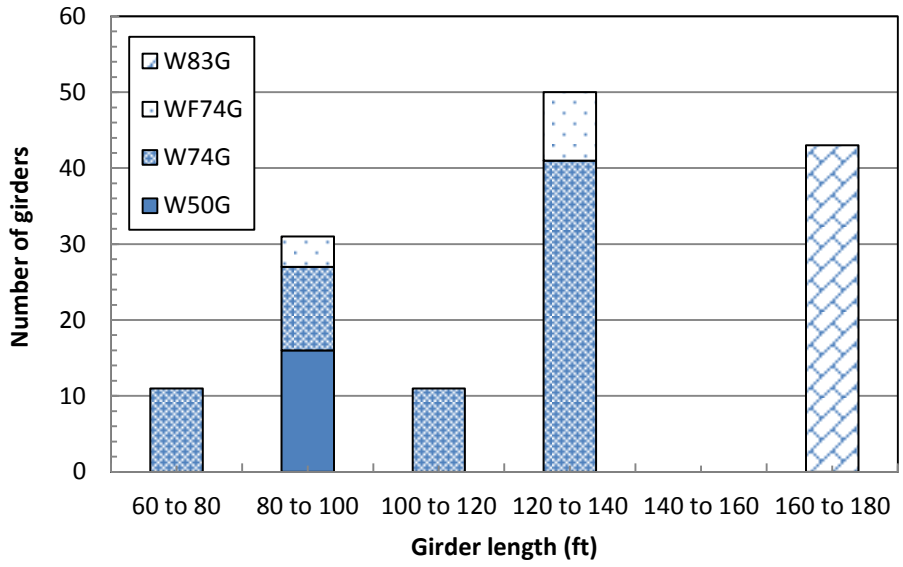

Figure 2-1. Number of Girders for Each Section

Information about the time at release is important to predicting camber, because it affects the girder stiffness. Usually, girders are released after 0.6 to 1 days after casting. However, girders cast on Friday are usually cured over the weekend and released on Monday morning of the following week. In addition, some girders that were cast on Monday through Thursday; also have extended curing periods due to unexpected conditions, such as bad weather or interruptions in fabricator operations. Those changes might make delay the release time and make the concrete more mature. Table 2-2 presents the number of girder with each release time, the time between concrete casting and release of the prestressing strand from the abutments.

Table 2-2. Number of Girders for Each Range of Release Time

	Number of girders			
	up to 1 days	1 to 2 days	2 to 3 days	more than 3 days
CTC	81	1	19	2
CPM	26	7	7	3
Total	**107**	**8**	**26**	**5**

Seasonal variations might be also important. Cambers of the girders that have the same properties but are cast during different seasons may differ. For example, CPM uses outdoor casting beds. In the winter months, the air temperature drops below freezing, creating significant temperature gradients between the top and the bottom of the girders. CTC has indoor casting

beds; however, girders are still subjected to a variety of ambient temperatures. Table 2-3 shows the number of girders cast in each calendar month.

Table 2-3. Number of Girders Cast in Each Month

	Number of girders											
	Jan	Feb	Mar	Apr	May	Jun	Jul	Aug	Sep	Oct	Nov	Dec
CTC	20	17	23	19	5	11	0	2	6	0	0	0
CPM	0	0	0	0	0	0	0	1	5	20	13	4
Total	20	17	23	19	5	11	0	3	11	20	13	4

Table 2-4 shows the number of girders for each range of release concrete strength. For this set of girders, girders cast by CPM had, on average, higher release concrete strength than those cast by CTC.

Table 2-4. Number of Girders for Each Range of Design Release Concrete Strength

	Number of girders			
	5 to 6 ksi	6 to 7 ksi	7 to 8 ksi	8 to 9 ksi
CTC	48	35	20	0
CPM	0	0	40	3
Total	**48**	**35**	**60**	**3**

2.4 Summary

Chapter 2 provides key information for 146 girders from Rosa et al.(2007), cast by the two fabricators in Washington State. The girders in the database varied in the type of cross sections, release time, length of girders, concrete strength and the number of prestressing strands. More information was presented in Rosa's report (2007).

3 CAMBER MEASUREMENTS – ALASKA WAY GIRDERS

3.1 Purpose

To investigate the changes of camber due to time-dependent effects (e.g., concrete compressive strength, temperature, elastic modulus, creep, shrinkage), nine girders were monitored at Concrete Technology Co. (CTC) from Jan 10, 2012 until May 18, 2012. The data collected were compared with calculated cambers using currently available methods for predicting initial and long-term camber to study the suitability of those models for high-strength, pre-stressed concrete and long-span girders.

3.2 Beam Configuration and Material Properties

Camber histories were collected for the Alaska Way Viaduct project at CTC's fabrication yard in Tacoma, Washington. All of the girders were WF100 sections and were 205.29 feet long. Figure 3-1 and 3-2 depict the cross section of the girders and the prestressing layout.

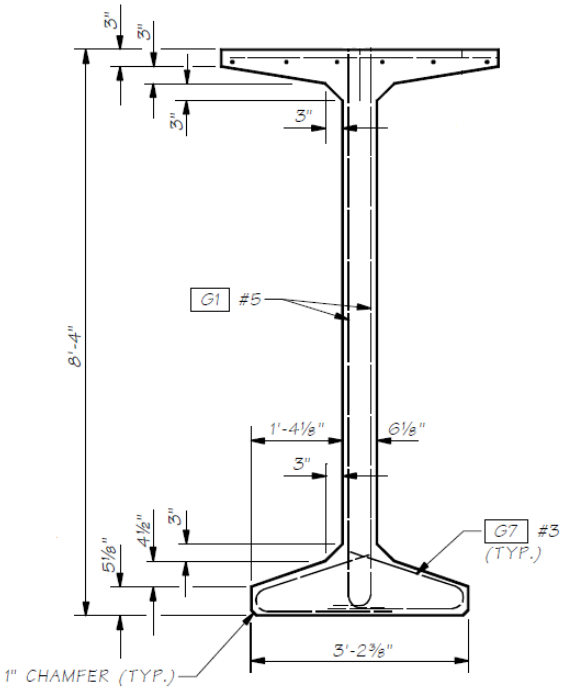

Figure 3-1. WF100 Cross Section (Fabricated in CTC)

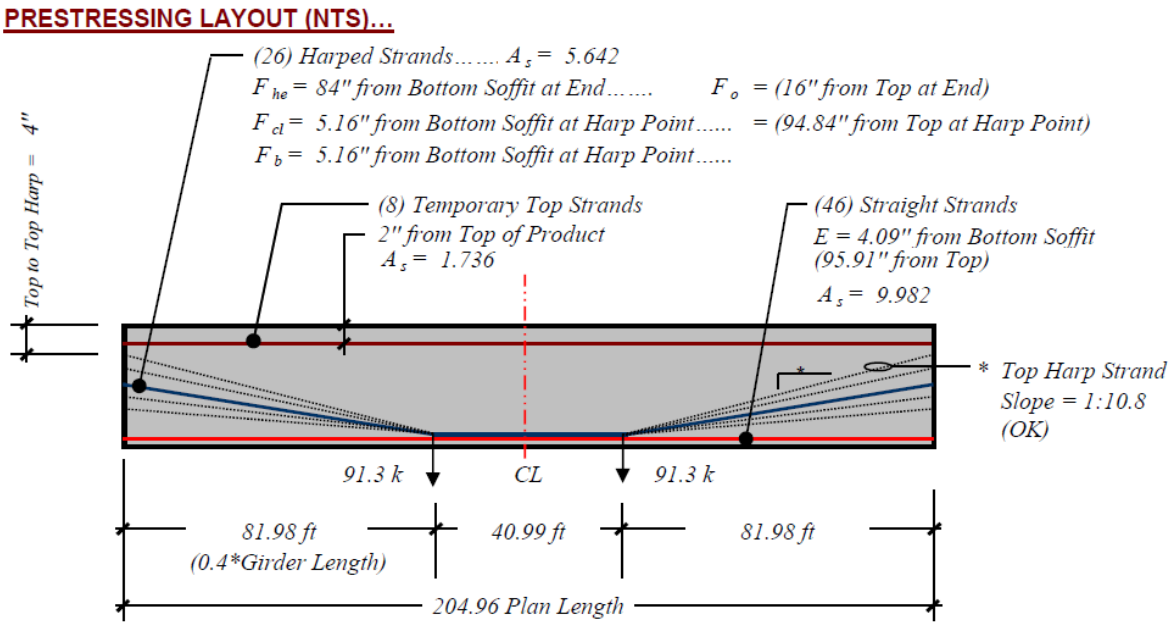

Figure 3-2. Prestressing Layout (G95C-X)

Nine girders were monitored. Eight were interior girders of type G95C, and the one exterior girder was designated type G96C. Some of the interior girders had an additional letter in the name to define them uniquely. The properties of the G95C and G96C girders differed slightly, as shown in Table 3-1:

Table 3-1. G95C-X and G96 Properties

Items	G95C (G95C-X)	G96C
Quantity	8	1
Length (ft)	205.29	205.29
Straight Strands	46	46
Harped Strands	**26**	**28**
Temporary Top Strands	8	8
Specified Release Strength (ksi)	**7.5**	**8**
Design 28-Day Strength (ksi)	10	10
CTC Concrete Mix Design	**#140**	**#190**

Individual girder concrete properties are provided in Table 3-2.

Table 3-2. Individual Girder Properties

Cast Date	Mark No.	Release Age (days)	Concrete Maturity (^{o}F hours)	Measured Concrete Strength At Release (psi)	Measured Concrete Strength At 28 Days (psi)
1/10/2012	G95C	0.67	1482	7,845	11,960
1/11/2012	G95C	0.67	1496	8,385	12,657
1/12/2012	G95C	0.50	1464	7,615	11,810
1/13/2012	G95C	2.40	5394	8,290	11,185
1/16/2012	G95C-B	0.67	1624	7,570	11,295
1/17/2012	G96C	1.50	4268	10,920	11,987
1/23/2012	G95C-P	0.67	1519	7,660	11,895
1/24/2012	G95C-M	0.67	1634	8,120	11,855
1/25/2012	G95C-L	0.67	1625	7,790	11,655

The mark G95C girder that was cast on Jan 13, 2012 and Girder G96C were both considered “weekend girders”. Girder G95C (1/13/2012) was cast on a Friday and released on a Monday the following week, resulting in 2.5 days of curing before release. Girder G96C was cast on a Tuesday and was scheduled to be released on the following day. However due to heavy snowstorm, CTC had to suspend operations on Wednesday. Consequently, the release of Girder G96C was delayed until the second day. Such “weekend girders” had the benefit of longer curing times, but they were also cured at lower temperatures. However, the longer curing times more than compensated for the lower temperatures, so the concrete in those two girders was much more mature at release than the concrete in the other girders.

3.3 Measurement Procedure.

The initial camber measurements were all taken by CTC staff members immediately after release. For these readings, the girders were hanging from the crane above the casting bed, and were supported 19 feet from each end. CTC used a tape to measure the distance from the casting bed to the bottom of each girder at both ends and at the middle. The camber was calculated by taking the average of the end readings and subtracting them from the mid-span reading. This procedure relies on the bed’s being straight.

Later, when the girders were moved to the storage yard, the girders were supported on heavy timbers, located 8 feet from each end. Deflections in the girders were then measured by both the University of Washington (UW) researchers and CTC staff members, using a rotating laser level. The laser level was placed on a surveying tripod set up near the middle of each girder (if measurements were conducted by UW researchers) or near one end of each girder (if CTC staff measured deflections). The accuracy of the laser level is ±1/8 in. per 100 feet. Therefore, for girders with a length of 205.29 feet, an error of ±1/4 in. could be expected.

Camber was initially monitored at intervals of about 3 days and then at longer intervals (1-2 weeks) as the rate of camber change decreased.

Both UW and CTC used the laser to establish long term camber value. However, CTC used a tape measure to measure the distance from the reference point to laser spot and took camber readings on only one side of the girder, but UW used a wooden template to measure the distance from another reference point to the laser spot and measured those elevations for both faces of the girders and averaged the two. The wooden template was manufactured to fit the section of a WF100 girder, as shown in Figure 3-3. The template was in contact with the web and the bottom flange. This template worked under the assumption that the thickness of WF100 bottom flanges was constant. Two scales were attached to the template so that the researchers could easily read data from any location of the laser level and at both sides of the girders. The measurements were taken at two ends of each girder and mid-span. The data then were used to calculate measured camber.

Figure 3-3. Wooden Template

The times at which the two parties took readings were also different. Whereas CTC generally measured camber in the morning, UW usually took the readings in the afternoon. Therefore, one should expect some discrepancies between the CTC and UW measurements due to solar radiation effects (those effects will be discussed in Chapter 6 of this study) and due to concrete creep and strand relaxation. However, because the readings were taken between January and May, the solar radiation effects were much less important than they would have been if the readings had been taken during the summer.

3.4 Observed Camber at Release.

The measured initial cambers are plotted in the Figure 3-4 against release concrete strength of the girders. Figure 3-4 shows that the initial camber tended to decrease with increasing concrete strength at release. However, this trend depends entirely on the value of the camber measured for Girder G96C. Note that, although this girder had the smallest camber, it had two extra harped strands compared to the other eight girders.

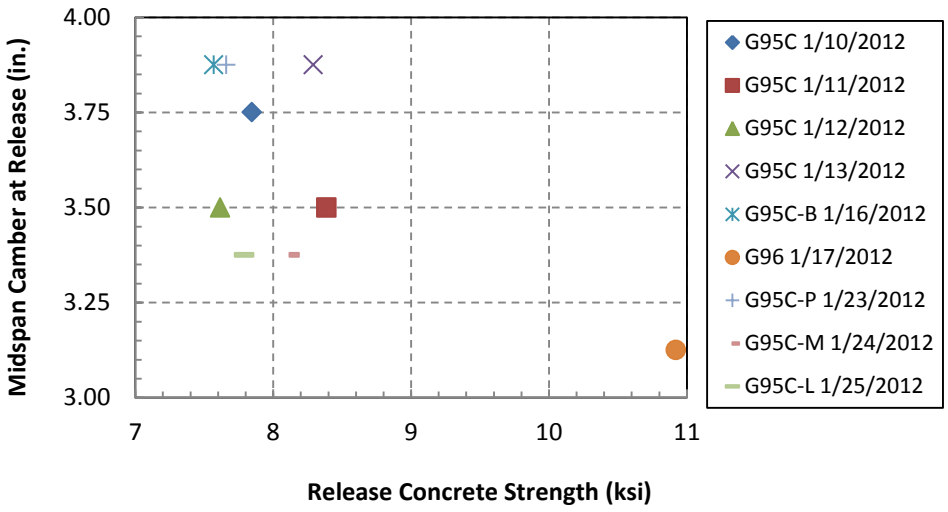

Figure 3-4. Alaska Way Viaduct Girders Release Camber vs. Release Concrete Strength

Figure 3-5 shows the mid-span camber at release plotted against the release age of the girders. It would be expected that girders which have longer release age, corresponding with higher concrete maturity (as shown in Table 3-2), should have less camber than the others since concrete strength and elastic modulus rise with concrete maturity. However, any trend in the plot depends entirely on the two weekend girders, and respectively, they had the largest and smallest cambers of any of the girders. Because the difference in camber errors of those two girders was significantly larger than the expected measurement error, it is believed that it was caused by other factors such as temperature during curing. It is also important to note that the release strength of the G95 weekend girder was similar to that of the other G95 girders and smaller than the G96 release strength.

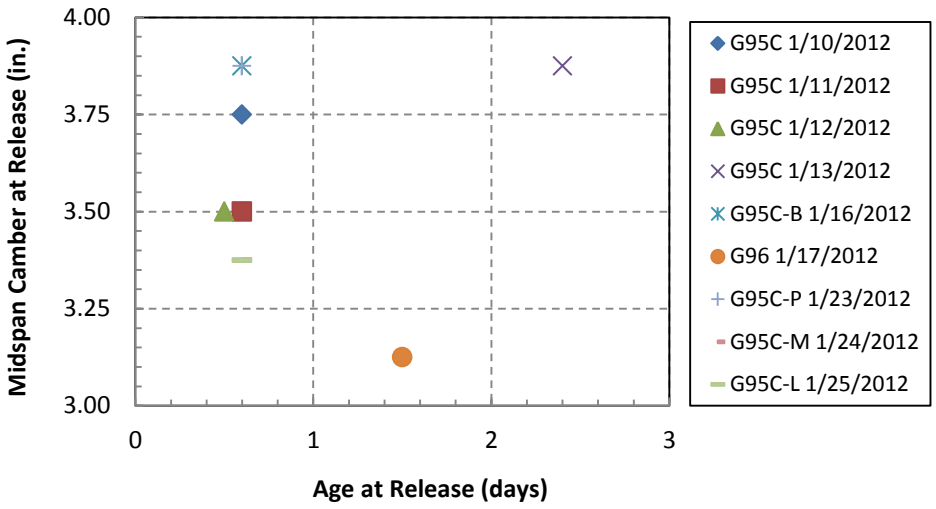

Figure 3-5. Alaska Way Viaduct Girders Release Camber at Midspan vs. Age at Release

Each release camber measurement was also compared with the release camber calculated using the program written by Rosa (2007). The calculations used measured concrete strength, the AASHTO 2005 models for elastic modulus, creep and shrinkage, and the AASHTO 2005 refined method for prestress loss. The predicted camber took into account the same boundary condition as the measured camber (supports 19 ft. from each end). Figure 3-6 shows the camber error (which is defined as the measured value (Δ_m) minus the predicted one (Δ_p)) at release against concrete strength at release. A negative error means that the measured upward camber is smaller than the calculated camber. This was the case for all investigated girders.

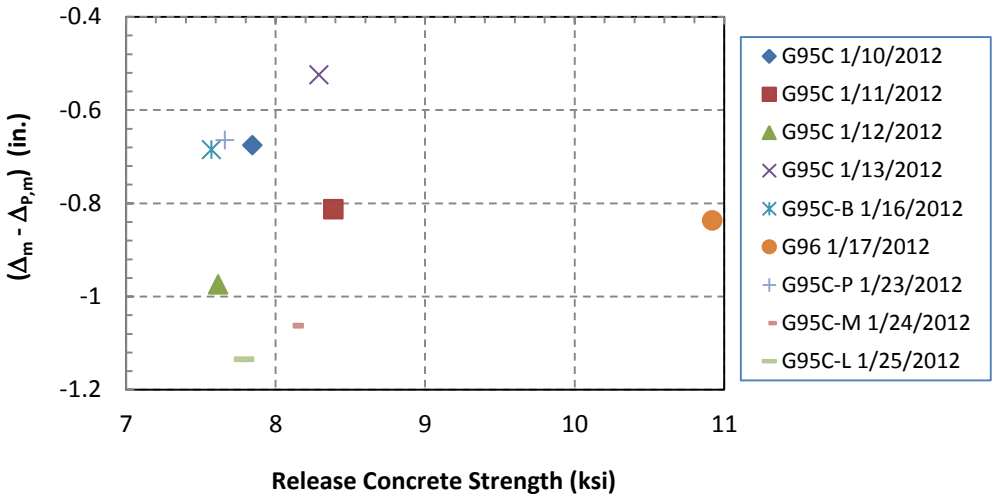

Figure 3-6. Alaska Way Viaduct Girders Release Camber Errors vs. Release Concrete Strength

The camber error varied from -0.53 in. to -1.14 in. with an average error of -0.82 in. This discrepancy is probably attributable to errors in measurements, thermal effects and models used to predict camber. However, thermal effects and predicted models would be primary factors since measurement errors should be less than ¼ in. Accelerated curing was used to achieve high early concrete strength, causing a non-uniform distribution of temperature in the girder. This thermal effect could cause upward or downward cambers depending on the temperature gradient at the time of bonding in each girder. Moreover, high temperature in girders can cause more prestress loss in the strands, causing downward deflection (Barr et al. (2005). Such thermal effects are not counted in currently available camber models. The effects of temperature effects on camber, both during curing and in service, will be examined in detail in Chapter 6 and Chapter 7 of this thesis.

3.5 Observed Long-Term Camber.

Long term cambers were measured were both by the UW researchers and CTC staff, as discussed earlier. From each of the two measured data sets, a logarithmic trendline was used to interpolate between measured points to provide a camber value for every day. The long-term

average camber was taken as the mean camber between the ages of 70 and 90 days, and the results are shown in Figure 3-7.

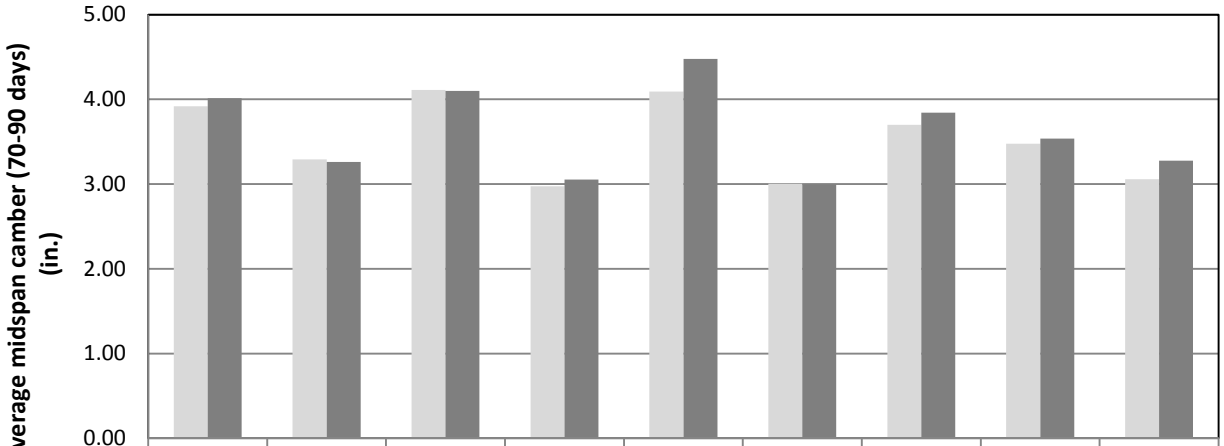

	G95C 1/10/2012	G95C 1/11/2012	G95C 1/12/2012	G95C 1/13/2012	G95C-B 1/16/2012	G96 1/17/2012	G95C-P 1/23/2012	G95C-M 1/24/2012	G95C-L 1/25/2012
CTC	3.92	3.29	4.11	2.97	4.09	3.00	3.70	3.48	3.06
UW	4.01	3.26	4.10	3.05	4.48	3.00	3.84	3.54	3.28

Figure 3-7. CTC and UW Average (70 to 90 days) Camber Measurements

The UW and CTC measurements are within 1/4 inch except for Girder G95C-B (0.4 in.). There are several possible reasons for this big discrepancy. One of them is the measurement methods. While UW recorded cambers on both sides of girders and took the average of two values as camber of the girder, CTC only measured the south face for this girder. UW records showed that there was a consistent difference in the camber measured on the two sides of Girder G96C-B, as shown in Figure 3-8. The long-term camber on the South face was usually about 0.2 inch smaller than that measured on the North face. This inconsistency was probably due to a discrepancy in the two sides of the formwork. Another possible reason is the times that the measurements were taken. Whereas, CTC took measurements in the early morning to avoid the effects of solar radiation, UW usually recorded camber readings around 2pm. Therefore, solar radiation could affect UW's camber readings and may have led to the discrepancy between the two measurements. However, the same effect should be expected to occur in all girders.

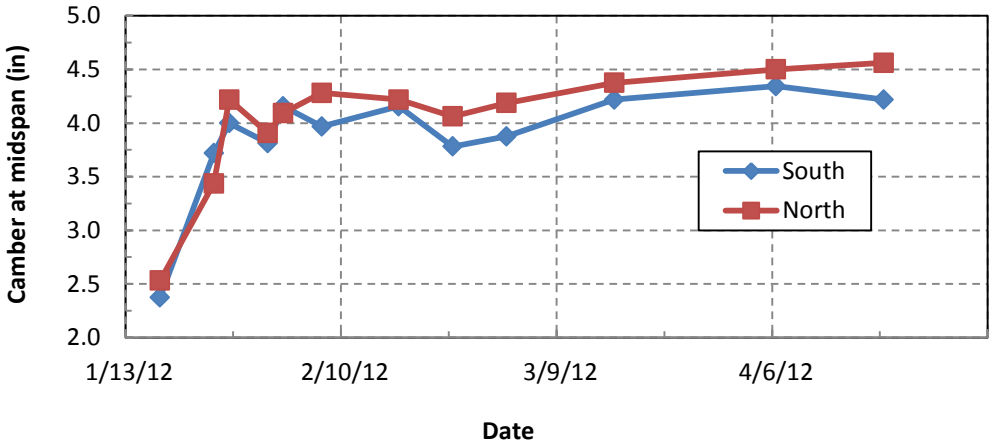

Figure 3-8. G95C-B Measured Camber at Both Sides

Initial camber and long-term camber of each girder were measured for different boundary conditions. Whereas release camber was measured when the girder was supported 19 ft. from each end, long-term cambers were taken when the girder was supported on the timbers, located 8 ft. from each end. Therefore, it does not make sense to compare the initial camber with the long-term cambers or evaluate one using the other one. Hence, the release camber was converted from supported at 19 ft. from the ends to supported 8 ft. from the ends. The converted release camber, Δ, was calculated as shown in Equation 3-1 and illustrated by Figure 3-9.

$$\Delta = \Delta_1 + \Delta_2 \qquad (3-1)$$

where:

Δ_1 = measured release camber taken by CTC,

Δ_2 = theoretical camber of the girder with boundary conditions and applied loads as shown in Figure 3-9,

Δ = converted release camber for the girder which is supported 8 ft. from each end.

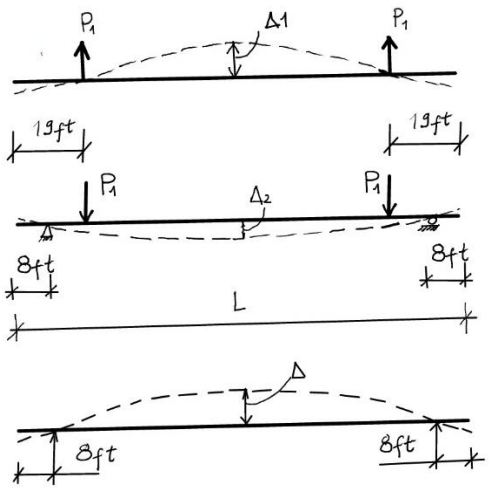

Figure 3-9. Model to Calculate Converted Release Camber

The calculations were made by using the assumption that deformations in the girder were small so Euler-Bernoulli Beam Theory can be used to compute the deflection of the girder (Δ_2). The calculations used the moment of inertia from the design cross section of the girder, and the concrete elastic modulus of the girder, calculated from the measured concrete strength using Tadros (2009)'s equation.

Figure 3-10 shows the camber histories recorded by the UW researchers for all nine girders. The release value plotted is the converted one, and the others are the average of the measurements from the two sides of the girders. The camber histories did not appear as smooth as expected. The variations with time might be due to two reasons. The first one is measurement accuracy. The second possibility is temperature variation. It was revealed that solar radiation could make the camber vary by more than one-half inch in the same day in summer. The investigation of that effect is reported in Chapter 6.

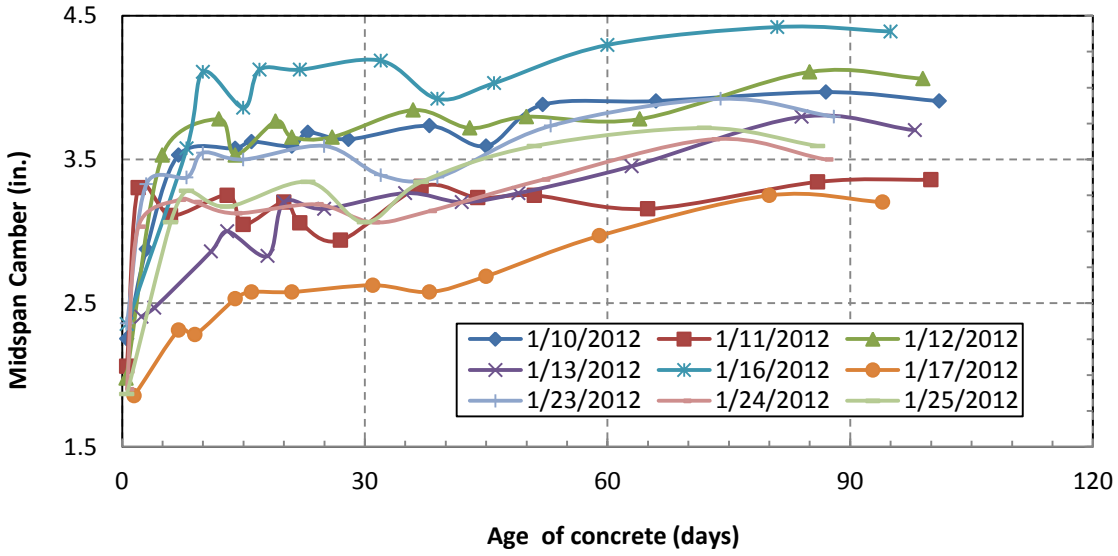

Figure 3-10. Alaska Way Viaduct UW Long-Term Camber Data with Converted Release Camber

The average measured camber based on UW measured data then were compared with the average predicted camber using measured concrete strength, the AASHTO 2005 models for the concrete elastic modulus and creep, and the AASHTO 2005 refined method for prestress loss. The long-term average camber error is defined as the measured value camber minus the predicted one (Δ_m - Δ_p), each averaged over the same period. Figure 3-11 and 3-12 represent the long-term average camber errors during the period of 71 days between ages 10 and 80 days vs. concrete strength at release and age of concrete at release.

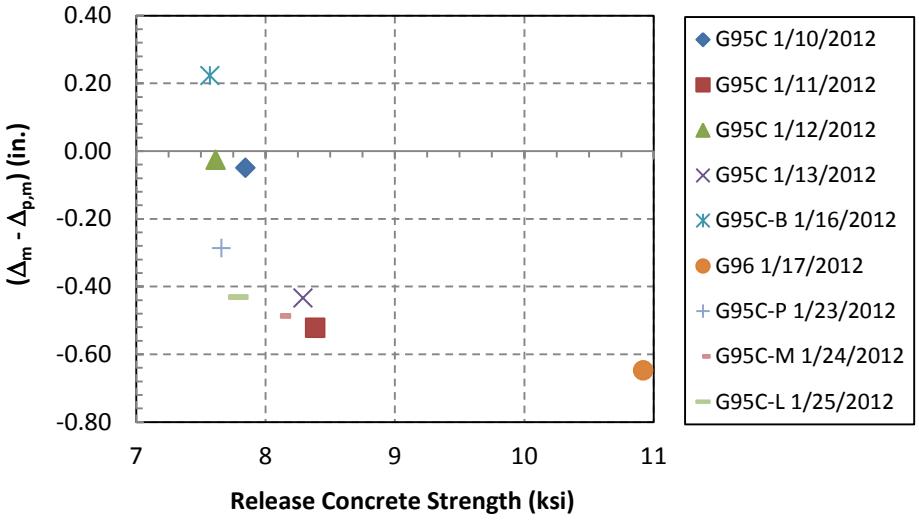

Figure 3-11. Long-Term Camber Errors vs. Release Concrete Strength

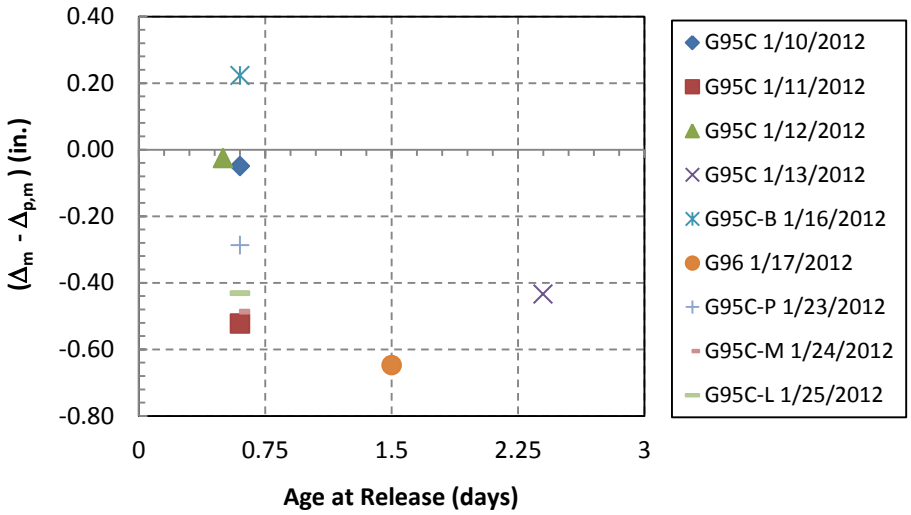

Figure 3-12. Long-Term Camber Errors vs. Age at Release

Figure 3-11 and 3-12 show that high concrete strength and high concrete maturity at release both led to higher camber errors (up to -0.65 in.). Because the measurement errors are just within ¼ in., it is believed the primary factors which contributed to those errors were the models used to calculate elastic modulus, creep and prestress loss for high strength and high concrete maturity girders. With the goal of improving camber predictions, some of those factors will be discussed in this study.

3.6 Summary

This chapter summarized the beam configuration and material properties used in the Alaska Way Viaduct girders. The procedures used for measuring camber and the observed behavior were also discussed. Discrepancies were found between the measured and predicted cambers. In an effort to improve predictions, chapters 4 to 7 will address some of the effects that might be expected to influence camber.

The average camber error for the Alaska Way Girders was -0.82 in. at release and -0.30 for long-term camber. The long-term camber error might be expected to be larger than the release camber error since estimates of camber at release rely only onelastic calculations, and they are not affected by creep. However, the measured data showed the opposite trend, which may be attributable to temperature effects during casting that are not included in existing camber models.

In particular, the accelerated curing needed to gain compressive strength rapidly is achieved by using high concrete curing temperatures. Due to the local differences in volume/surface ratio in different parts of the cross-section, the internal temperature varied and created a nonlinear temperature gradient over the height of the girder. This effect is discussed in Chapter 7 of this study.

4 EFFECT OF CONCRETE COMPRESSIVE STRENGTH ON CAMBER

The calculated camber is inversely related to the elastic modulus, which in turn is approximately proportional to the square root of the concrete compressive strength. Therefore, the concrete compressive strength is an important factor in predicting camber.

Because the actual concrete strength is unknown at the time of design, the design concrete strength is usually used in camber calculations. In fact, the actual concrete strength usually exceeds the design strength. This chapter investigates the effects on camber of differences between the actual and design concrete compressive strengths.

4.1 Design and Measured Concrete Strength

Rosa's database for 146 girders cast by Concrete Technology Corporation (CTC) and Central Premix Prestress Co. (CPM) shows that the measured concrete compressive strength at release and at 28 days was consistently higher than the design concrete strength. Table 4-1 shows the average ratio of the measured concrete compressive strength to the design concrete strength for the girders in his study. For example, Rosa's data shows that for the CTC girders, the compressive strength at release was on average 6% higher than the design value.

Table 4-1. Average Ratio of Measured to Design Concrete Compressive Strength

Measured/Design	No. of Girders	Release	28 Day
CTC's Girders in Rosa's database	103	1.06	1.12
CTC's Girders in Alaska Way Bridge	9	1.07	1.19
CPM's Girders in Rosa's database	43	1.14	1.30
All CTC's Girder	112	1.06	1.13
All girders	155	1.08	1.18

The strength data for the nine monitored Alaska Way Bridge girders had similar levels of overstrength. For these girders, the measured concrete compressive strength at release was 7% larger (on average) than the design strength.

The ratio at release was in all cases smaller than that at 28 days. This difference was expected, because typical practice is to monitor the concrete strength before release, using both maturity estimates and cylinder breaks and to release the strands as soon as the required strength is reached. Similar control does not exist at 28 days.

4.2 Alaska Way Viaduct Girders

Figure 4-1 compares the absolute camber errors, $|\Delta_m - \Delta_p|$ for the nine girders of Alaska Way Viaduct at release, using design concrete strength and measured concrete strength. All camber predictions were made by following the AASHTO 2005 models for the concrete elastic modulus and creep, and the AASHTO 2005 refined method for prestress loss. In all cases, the measured camber was smaller than the calculated camber. As shown in Figure 4-1, for all nine girders, the camber error was smaller when the camber was calculated using the actual concrete strength rather than the design strength. This result is reasonable, because increases in concrete strength lead to increases in the calculated elastic modulus, which in turn lead to estimates of camber that are lower and in this case, closer to the measure values.

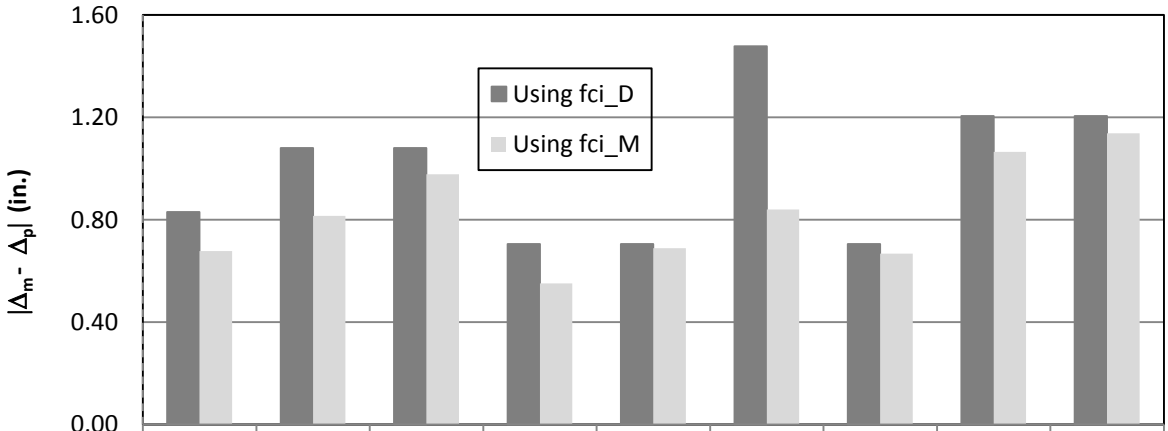

	G95C 1/10/2012	G95C 1/11/2012	G95C 1/12/2012	G95C 1/13/2012	G95C-B 1/16/2012	G96 1/17/2012	G95C-P 1/23/2012	G95C-M 1/24/2012	G95C-L 1/25/2012
Using fci_D	0.83	1.08	1.08	0.70	0.70	1.48	0.70	1.20	1.20
Using fci_M	0.68	0.82	0.98	0.55	0.69	0.84	0.67	1.07	1.14

Figure 4-1. Camber Errors at Release of Using Design Concrete Strength and Actual Concrete Strength.

Figure 4-2(a) plots the mid-span camber errors, (Δ_m - $\Delta_{p,d}$) versus the age at release. The lower case "d" in the notation $\Delta_{p,d}$ means camber prediction was made by using design concrete strength. Figure 4-2(b) is similar, but in this figure, the measured values of concrete strength were used to calculate camber, so the error is defined by (Δ_m - $\Delta_{p,m}$). The data does not show a consistent effect of the age of release on the errors.

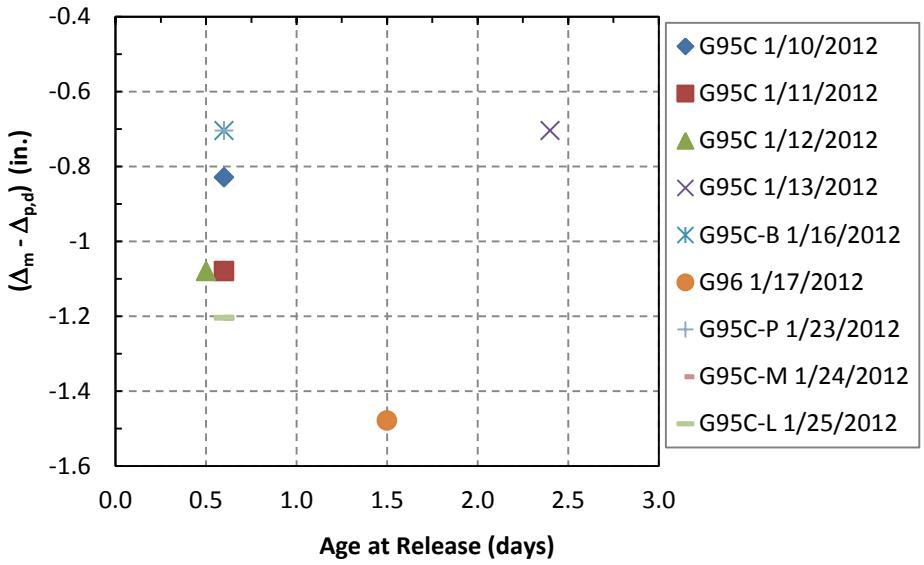

a) Using Design Compressive Concrete Strength

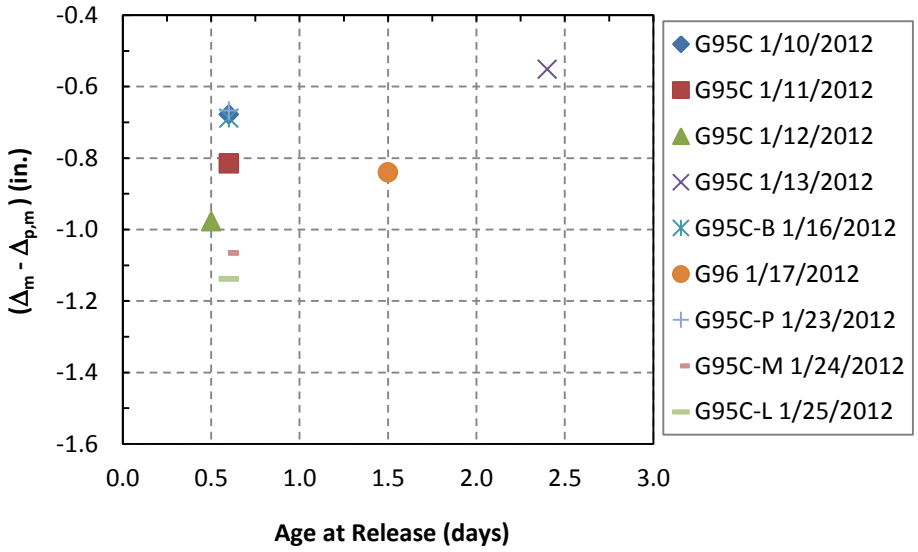

b) Using Measured Compressive Concrete Strength

Figure 4-2. Camber Prediction Error @ Release
a) Using Design Concrete Strength b) Using Measured Concrete Strength

Figure 4-3 shows the release camber error, (Δ_m - Δ_p) versus the release concrete compressive strength, using the design concrete strength and measured concrete strength. The figure indicates that the use of the measured concrete strength decreases camber errors.

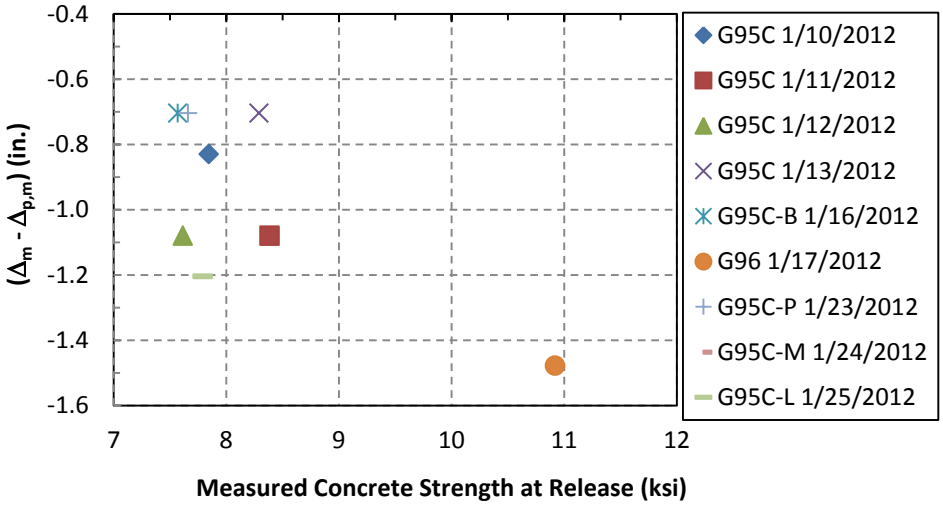

a) Using Design Concrete Strength

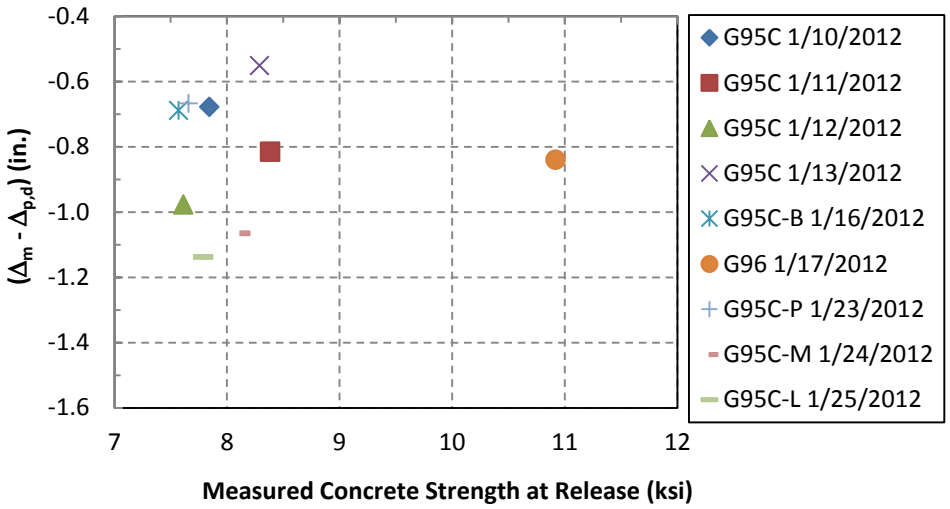

b) Using Measured Concrete Strength

Figure 4-3. Camber Prediction Errors @ Release
a) Using Design Concrete Strength b) Using Measured Concrete Strength

Figure 4-4 depicts the absolute camber errors, $|\Delta_m - \Delta_p|$ for the same girders at the 2nd comparisons, using design concrete strength and measured concrete strength. In this study, the 2nd comparisons refer to the second time at which the calculated and measured cambers were compared, rather than the second time that the camber was measured for those girders. For the Alaska Way Viaduct girders, the second comparison was made for cambers measured on Feb 17 2012. On that day, the age of girders varied from 23 to 38 days, depending on the casting date.

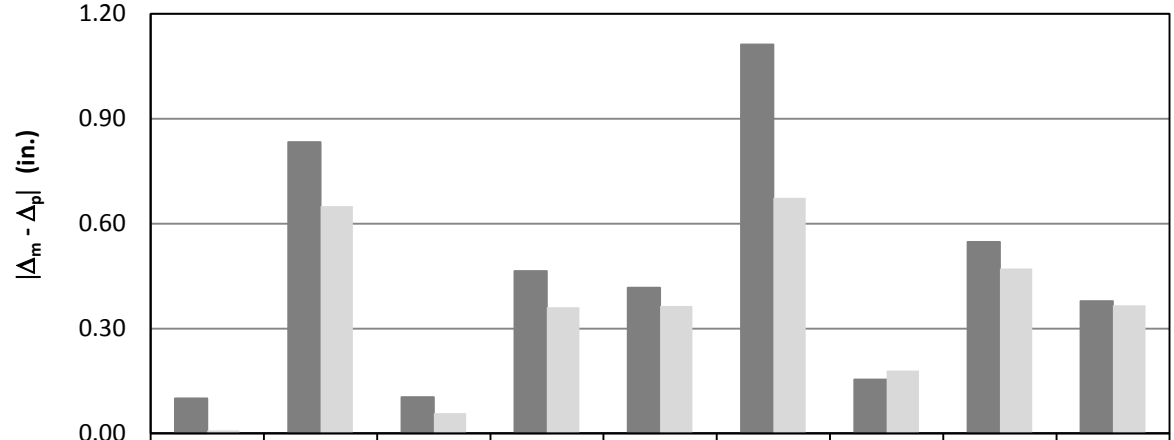

	G95C 1/10/2012	G95C 1/11/2012	G95C 1/12/2012	G95C 1/13/2012	G95C-B 1/16/2012	G96 1/17/2012	G95C-P 1/23/2012	G95C-M 1/24/2012	G95C-L 1/25/2012
Using fci_D	0.10	0.83	0.10	0.46	0.42	1.11	0.15	0.55	0.38
Using fci_M	0.01	0.65	0.06	0.36	0.36	0.67	0.18	0.47	0.37

Figure 4-4. Camber Errors at the 2nd Comparison of Using Design Concrete Strength and Measured Concrete Strength.

The measured concrete strength for the 2nd comparison was estimated based the measured release and 28-day compressive strengths as following equation (Naaman 2004).

$$f_c'(t) = f_c'(28)\frac{t_{str}}{b + ct_{str}}$$

where:

b = constant that changes the rate of increase

c = constant that changes the strength at infinite time

t_{str} = time after concrete starts to gain strength

$t_{release}$ = time from casting to release

t_{harden} = time from casting to time at which concrete starts to gain strength

$f'_c(28)$ = 28-day concrete compressive strength

$f'_c(t)$ = concrete compressive strength

$$b = (28 - t_{harden})(1 - c)$$

$$c = \frac{f_c'(28)(t_{release} - t_{harden}) - f_{ci}'(28 - t_{harden})}{f_{ci}'(t_{release} - t_{harden}) - f_{ci}'(28 - t_{harden})}$$

As was the case for the release measurements, the calculated cambers decreased and the accuracy increased when the measured concrete strength was used instead of the design value. This improvement was expected, because the higher measured concrete strength increased the calculated stiffness. Consequently, both the estimated cambers and the camber errors decreased.

Figure 4-5 shows the camber error, (Δ_m - Δ_p) at the second comparison versus the release concrete compressive strength. The data are plotted using the design strength and measured strength. The figure illustrates that the use of the actual concrete strength leads to smaller errors in prediction. It also demonstrates that the girders that had the highest concrete compressive strengths at release tended to have larger camber errors at the 2nd comparisons. However, it is not true at release as shown in Figure 4-3.

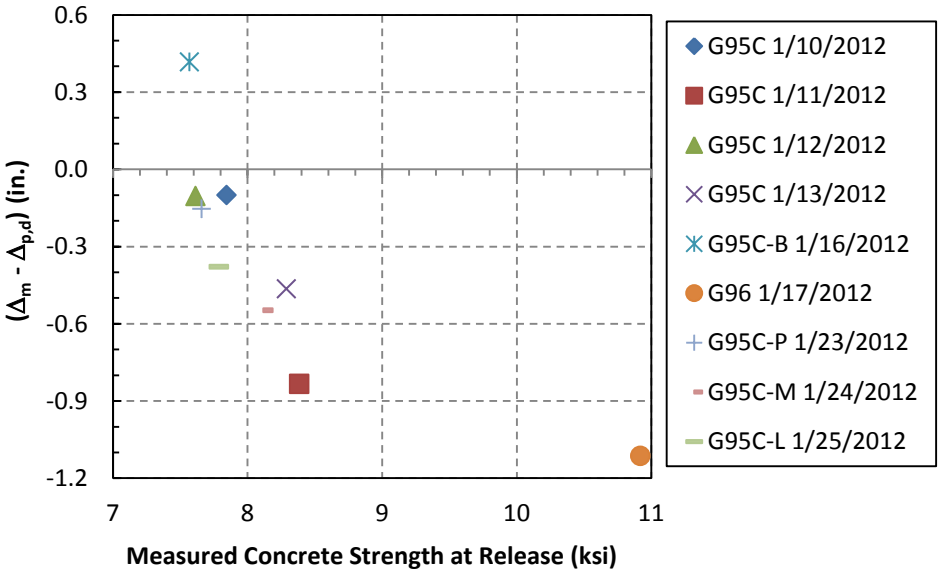

a) Using Design Compressive Concrete Strength

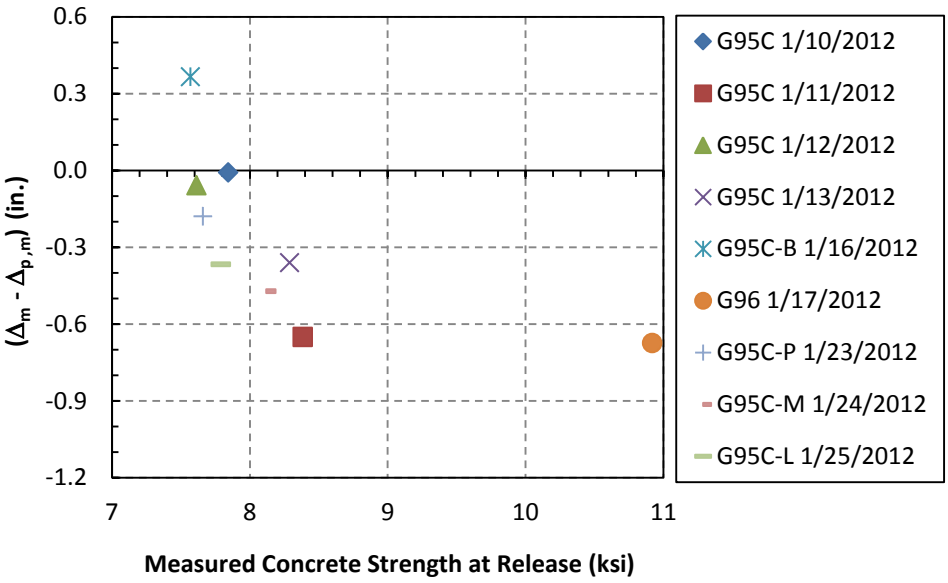

b) Using Measured Compressive Concrete Strength

Figure 4-5. Camber Prediction Errors @ the 2nd Comparison
a) Using Design Concrete Strength b) Using Measured Concrete Strength

Figure 4-6 shows camber errors at release and the 2nd comparison versus the difference between release measured and design concrete strengths at release. The predicted camber was taken as $\Delta_{p,d}$, for which the prediction was based on the design strength. The figure illustrates the trend that the bigger the difference between the measured concrete strength and design concrete strength, the higher the error in camber. This trend is more apparent for the 2nd comparison than at release. This difference may be attributable to the effect of fabrication temperature distributions on camber at release. Therefore, camber at release might vary depending on the actual thermal gradient in the girders.

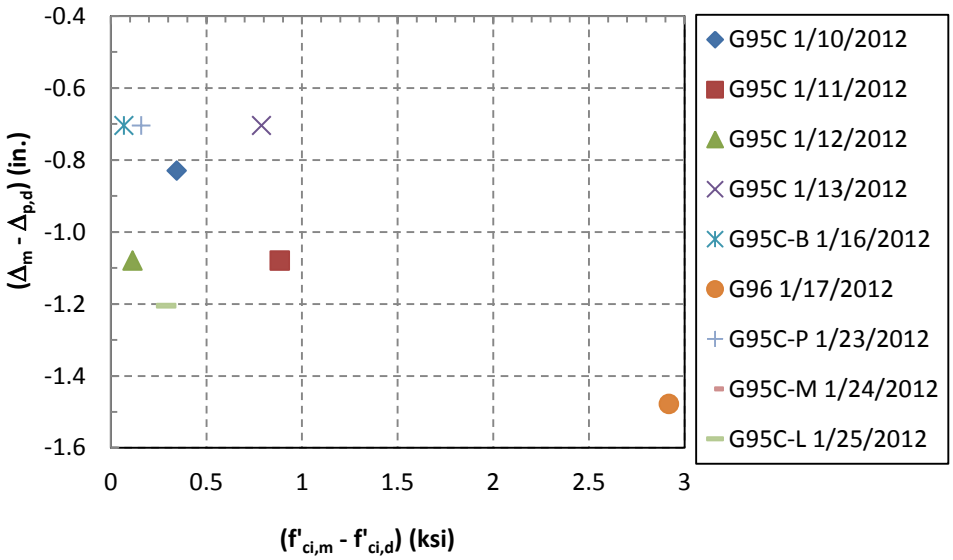

a) At Release

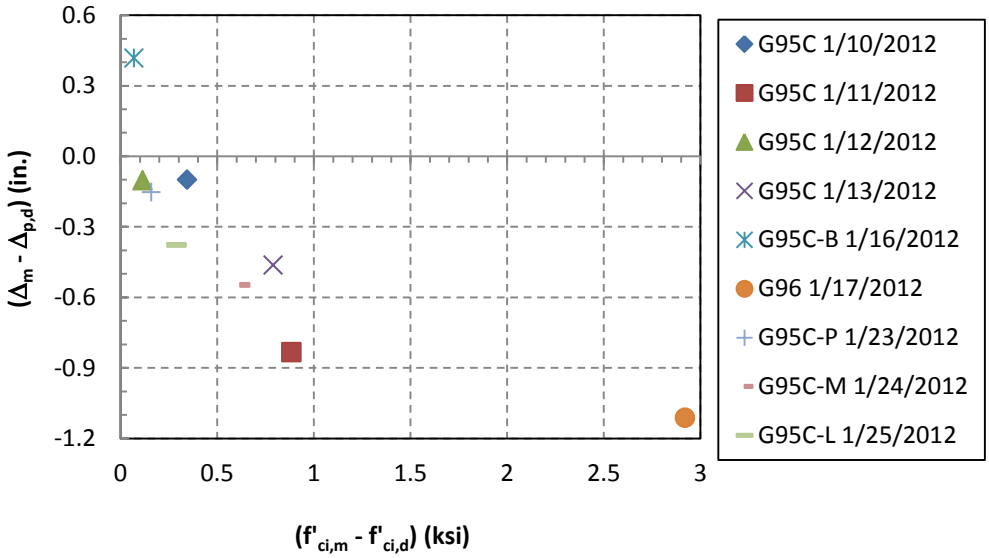

b) At the 2nd Comparison

Figure 4-6. Camber Errors vs. Differences between Actual Concrete Strength and Design Concrete Strength at Release a) At Release b) At the 2nd Comparison

The influence of concrete strength at release can be expressed another way. Figure 4-7 shows the ratio of the camber errors using the design concrete strength to the calculated camber

using design concrete strength on the vertical axis. The horizontal axis is the ratio of elastic modulus calculated using the design concrete strength over the elastic modulus calculated using the measured concrete strength at release. Values of elastic modulus were calculated using the AASHTO 2005 model.

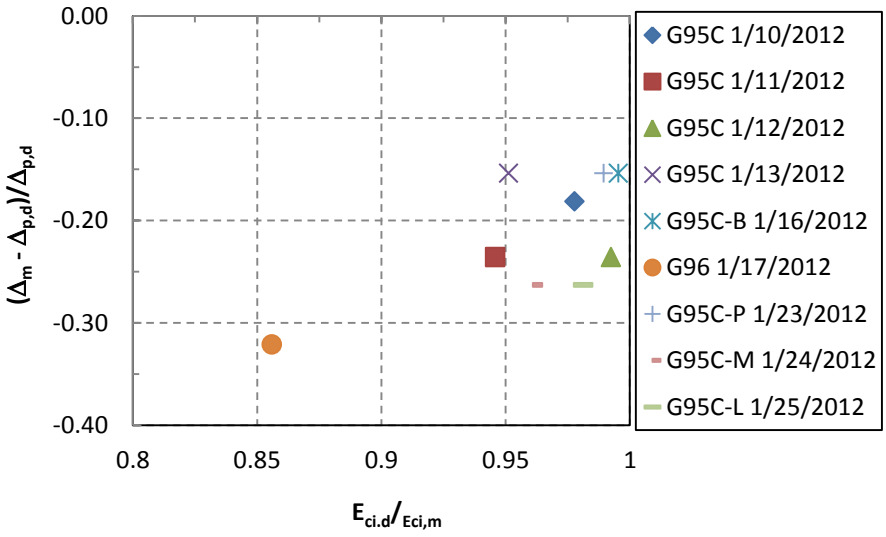

a) At Release

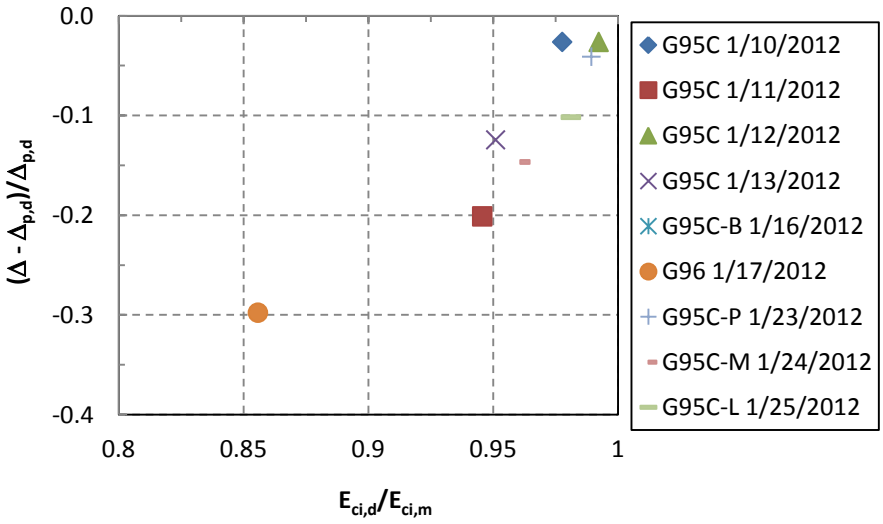

b) At the 2nd Comparison

Figure 4-7. Ratio of Camber Error vs. Ratio of Elastic Modulus For Alaska Way Viaduct a) At Release b) At the 2nd Comparison

The trends in Figure 4-7 are consistent with expectations in that the predictions improve as the calculate E_c value approaches the measured E_c. However, even at the ratio of $E_{ci,d}/E_{ci,m} = 1$, the errors were not equal to zero. Other effects must also be influencing the camber calculation errors, or the AASHTO 2005 equation for predicting E_c from f'c alone must be imperfect.

4.3 All Girders

As shown in the previous section, the use of the measured concrete strength improved the camber prediction accuracy for the Alaska Way Viaduct girders. This section evaluates the effect of using the measured concrete strength for all 155 girders, including the 146 girders in Rosa's database.

Figure 4-8 depicts the release camber errors resulting from the use of the design concrete strength and measured concrete strength for all 155 girders. The camber errors tended to be more negative (measured less than calculated) with increasing girder length in both Figure 4-8(a) and 4-8(b). Figure 4-9 shows similar plots for the 2nd comparison.

.

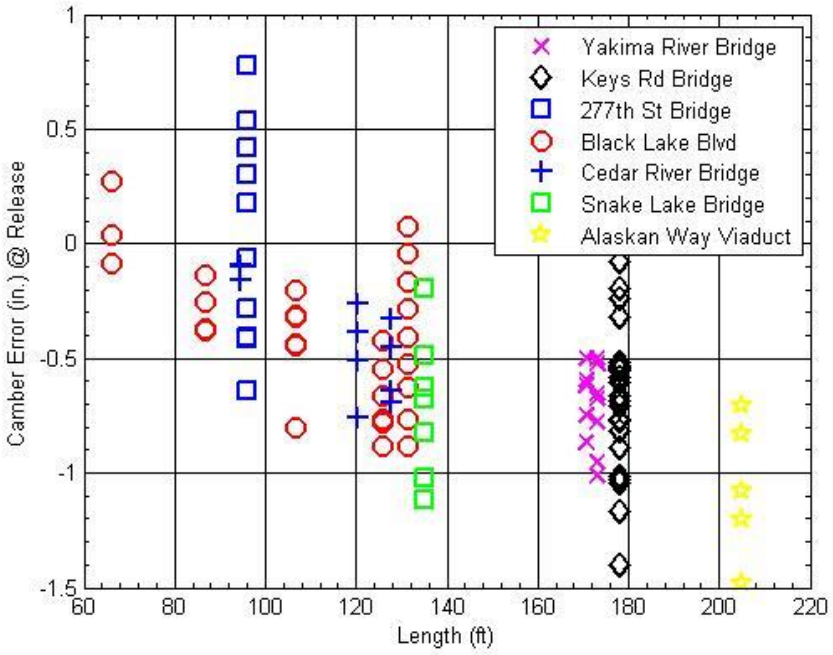

a) Using Design Concrete Strength

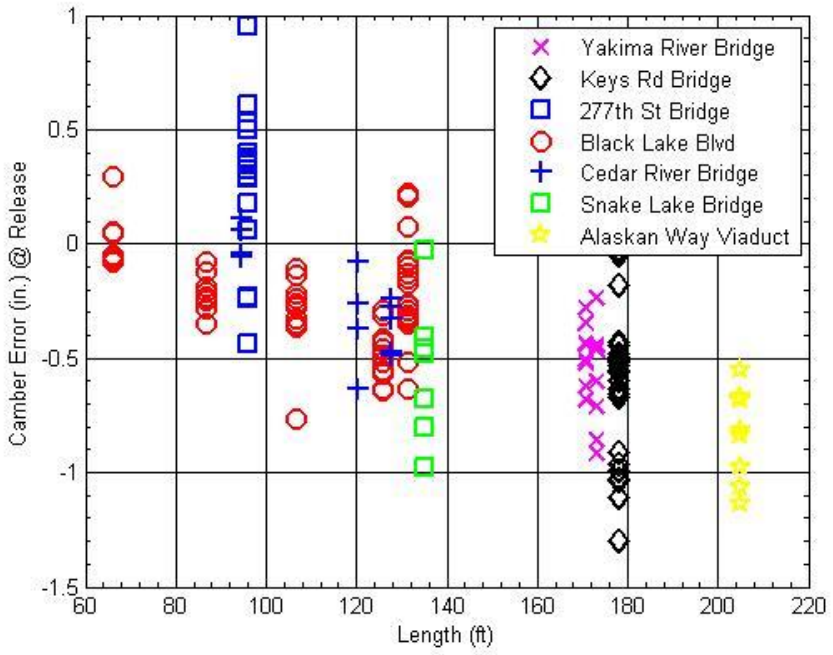

b) Using Measured Concrete Strength

Figure 4-8. Camber Prediction Errors at Release
a) Using Design Concrete Strength b) Using Measured Concrete Strength

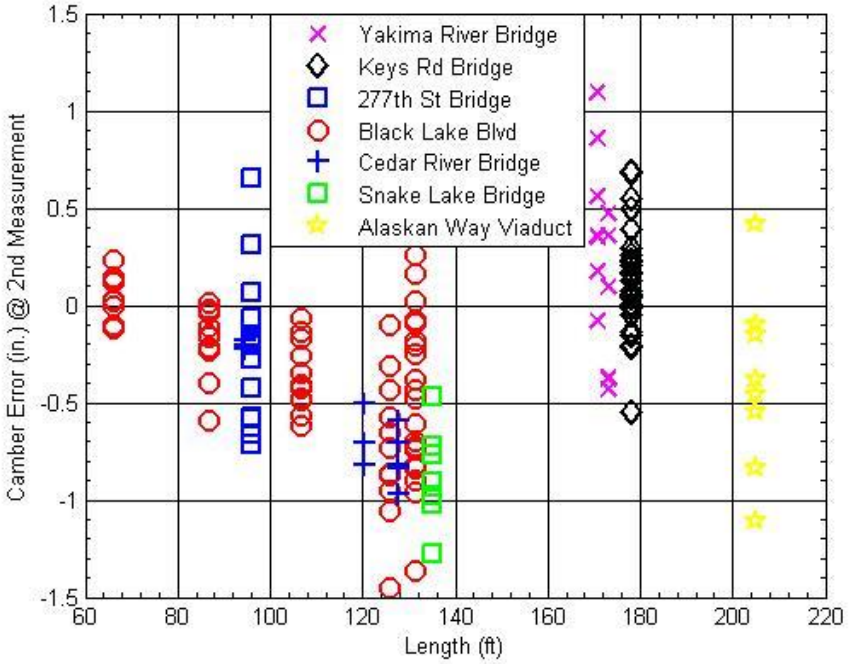

a) Using Design Concrete Strength

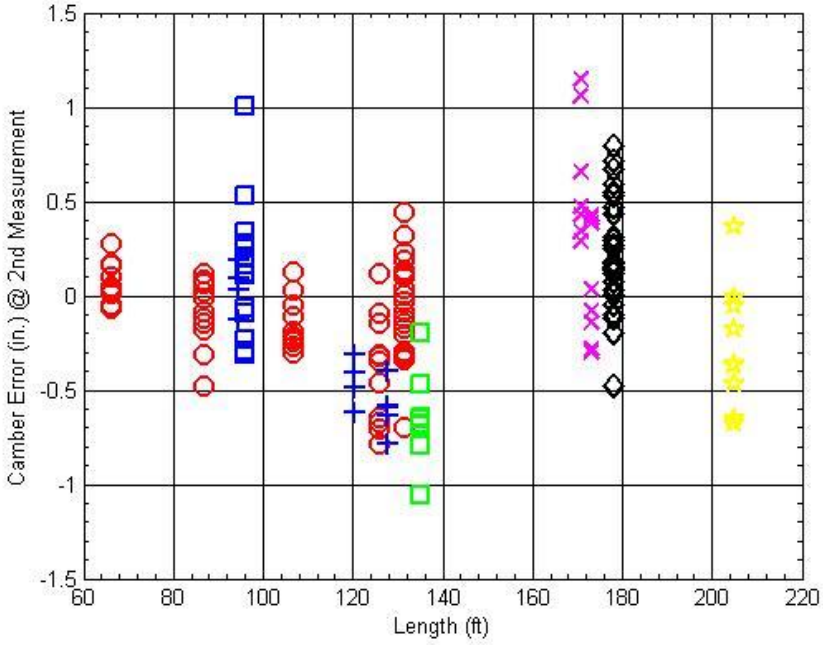

b) Using Measured Concrete Strength

Figure 4-9. Camber Prediction Errors at 2nd Comparison
b) Using Design Concrete Strength b) Using Measured Concrete Strength

These data suggest that use of actual strength does not make much difference at release, in terms of scatter (standard deviations). However, it makes a more noticeable difference at the 2nd comparison. It is believed that release camber was affected by other factors such as temperature during curing rather than models to calculate it as discussed in the Chapter 3. The effect of fabrication temperature during curing will be investigated more detail in Chapter 7 of this study.

Those camber errors are evaluated statistically in Table 4-2, using all 155 girders. Table 4-2 also gives statistics for subsets of the data.

Table 4-2. Summary of Camber Errors

Girders of	At Release			At the 2nd Comparison		
	Average Error	Average Absolute Error	Standard Deviation	Average Error	Average Absolute Error	Standard Deviation
Using Design Concrete Strength						
All Girders	-0.45	0.51	0.32	-0.71	0.78	0.50
CTC in Rosa's Database	-0.31	0.39	0.34	-0.81	0.89	0.53
CTC in Alaska Way Viaduct	-1.00	1.03	0.28	-0.36	0.56	0.45
CPM in Rosa's Database	-0.68	0.69	0.29	-0.55	0.58	0.45
Using Measured Concrete Strength						
All Girders	-0.32	0.41	0.31	-0.40	0.46	0.39
CTC in Rosa's Database	-0.18	0.30	0.32	-0.41	0.45	0.38
CTC in Alaska Way Viaduct	-0.82	0.84	0.20	-0.27	0.41	0.33
CPM in Rosa's Database	-0.56	0.57	0.30	-0.42	0.48	0.43

Figure 4-10 shows camber errors using design concrete strength versus differences between measured concrete strength and design concrete strength at release. It shows for all girders what Figure 4-6 showed for the nine girders. The figure also shows how the discrepancy between measured and design concrete strength affects camber errors. The trend was more apparent for the 2nd measurement. This difference may be attributable to the fact that fabrication temperature would affect the camber at release more than the 2nd measurement, especially when the readings for the 2nd measurement were taken in early morning, at which time the camber would contain almost no thermal component.

These data support the argument that something else (e.g., thermal effect) is happening at release. At the 2nd comparison, it looks as though error approaches zero as $f_{ci,m}$ approaches $f_{ci,d}$. However, at release the camber error is about -1/2 in. when $f_{ci,m}$ approachs $f_{ci,d}$. This is consistent with ½ in. downwards deflection due fabrication temperature as shown in Chapter 7.

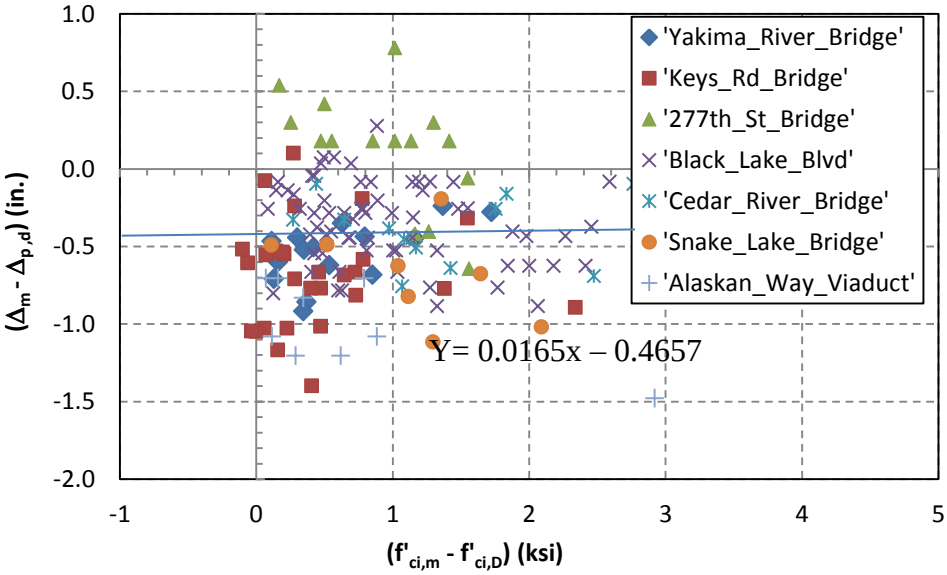

a) At Release

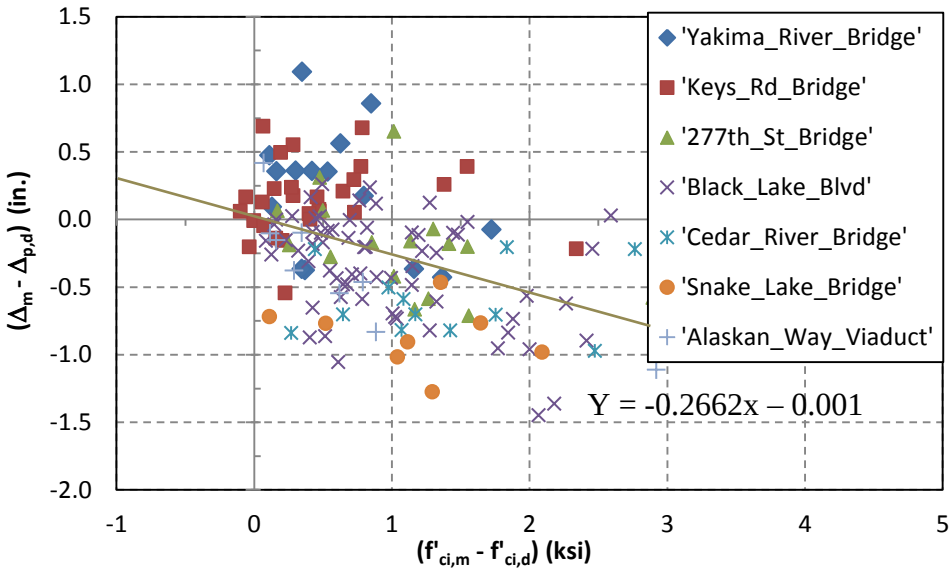

b) At the 2nd Comparison

Figure 4-10. Camber Errors vs Differences between Measured Concrete Strength and Design Concrete Strength at Release a) At Release; b) At 2nd Comparison

Figure 4-11 shows the effects of differences in concrete strength on camber error, for all 155 girders. The predictions improve as the calculate E_c value approaches the measured E_c at the 2nd comparison. However, the release camber errors seem to be poorly correlated with $E_{ci,d}/E_{ci,m}$.

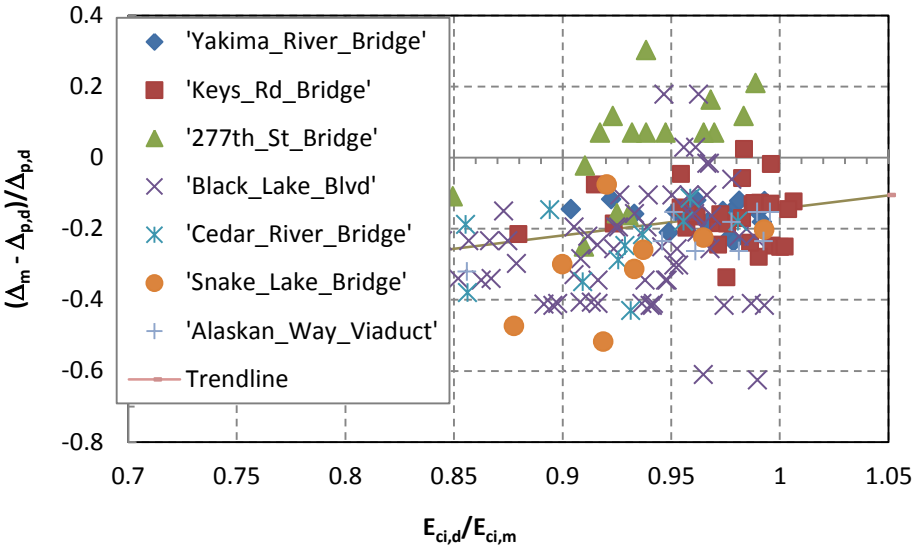

a) At release

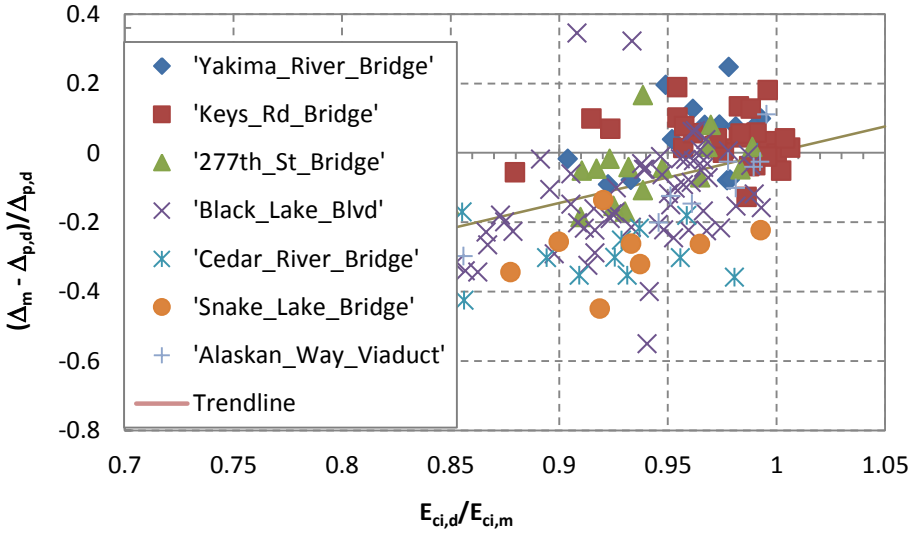

b) At the 2nd Comparison

Figure 4-11. Ratio of Camber Error vs Ratio of Elastic Modulus a) At Release; b) At the 2nd Comparison

4.4 Conclusions

Based on the measured cambers and compressive strengths for 155 girders, it appears that the use of the measured compressive strength improves camber predictions. However the measured the concrete strength is still unknown at the time of design. Based on the data presented in this study, the measured concrete strength can be estimated by multiplying the design concrete strengths by 1.08 at release and by 1.18 at 28 days (Table 4-1).

Using measured concrete strength improves the camber prediction at the 2nd comparison. However, the errors at release are affected only little (except for the weekend girders) because the precaster typically releases the strand as soon as the strength reaches the design concrete strength, so $f'_{ci,m} = f'_{ci,d}$.

Because camber is influenced by several other factors such as temperature, elastic modulus, creep, shrinkage…etc, the use of actual concrete strength instead of design concrete strength can only reduce camber errors, but it does not eliminate errors. The next chapter will discuss the effect of using various models of elastic modulus in predicting camber.

5 EFFECT OF ELASTIC MODULUS

5.1 Prediction of Elastic Modulus

It is often assumed that the concrete modulus of elasticity is proportional to the square root of compressive strength. Therefore, higher compressive strengths should be associated with higher modulus of elasticity and smaller deflections (Hinkle et al. 2006). There are many models that relate the elastic modulus to the concrete compressive strength. Since the concrete strength is a function of time, those equations for elastic modulus are implicitly time-dependent. This section will discuss three widely-used models for elastic modulus.

5.1.1 AASHTO LRFD (2006) Method

The AASHTO LRFD (2006) equation for the concrete elastic of modulus is:

$$E_c(t) = 33{,}000\gamma^{1.5}\sqrt{f_c'(t)}\ (ksi) \qquad 5\text{-}1$$

where :

$E_c(t)$ = concrete modulus of elasticity (ksi), as a function of time.

γ = unit weight of concrete (kcf).

$f_c'(t)$ = concrete compressive strength (ksi).

This equation is applicable for concrete with a unit weight of between 0.090 kcf and 0.155 kcf.

5.1.2 ACI Committee 363 Method (ACI 1992)

The equation recommended by ACI Committee 363 is specified for concrete that has a compressive strength higher than 6,000 psi. Similar to the AASHTO LRFD equation, the ACI Committee 363 equation is still a function of the unit weight of concrete and the concrete compressive strength.

$$E_c(t) = \left(\frac{\gamma}{0.145}\right)^{1.5} \left(1000 + 1265\sqrt{f_c'(t)}\right)(ksi) \qquad 5\text{-}2$$

5.1.3 NCHRP Report 496 Method (Eq. 48)

According to Tadros et al. (2003), one of the shortcomings in the AASHTO-LRFD Bridge Design Specifications and ACI-318 was the prediction of the elastic modulus of concrete, especially of high-strength concrete. The AASHTO-LRFD and ACI-318 formula only account for the unit weight and compressive strength, but do not account for other factors such as coarse aggregate content and properties of the aggregates that appear to affect the elastic modulus. Tadros et al. (2003) evaluated the effect of the coarse aggregate and proposed a formula for elastic modulus as shown in Equation 5-3. The proposed formula for modulus of elastic is recommended for concrete with a unit weight of less than 0.155 kcf.

$$E_c(t) = 33{,}000K_1K_2\left(0.140 + \frac{f_c'(t)}{1000}\right)^{1.5}\sqrt{f_c'(t)}\,(ksi) \qquad 5\text{-}3$$

where:

K_1 = factor representing the difference between national average and local average,

K_2 = factor representing whether an upper-bound or lower bound value is desired in the calculations.

For Washington State, Tadros et al. 2003 recommended using $K_1 = 1.154$ and $K_2 = 1.0$ as the mean values. However, K_2 can be adjusted to 1.182 or 0.817 to estimate respectively the 90th percentile upper-bound or 10th percentile lower-bound values. For the following sections, $K_1 = 1.154$ and $K_2 = 1.0$ will be used in calculations.

5.1.4 Rosa's Recommendation (2007) for Elastic Modulus Formulation

Base on calibrations for 146 Washington State girders, Rosa et al. (2007) proposed using the AASHTO 2006 equation for elastic modulus (Equation 5-1) with a correction factor of 1.15 for all girders cast in Washington State. Note that this recommendation was developed from back-calculating the elastic modulus from girder cambers, rather than from direct measurements

of the modulus. The constant K_1 = 1.15 was found by adjusting it so that the average error in predicting the release camber of 146 girders was minimized. In addition to using Eq. 5-3, the actual concrete strength, the AASHTO 2005 models for creep, shrinkage, and the AASHTO 2005 refined method for prestress loss were used to calculate the predicted cambers. The mean error dropped from 0.38 in. (using the raw AASHTO method) to 0.24 in. (using the corrected AASHTO method).

Rosa also made separate calibrations for girders fabricated at Concrete Technology Corporation (CTC) and girders fabricated at Central Premix Prestress Co. (CPM). The prediction errors were minimized by using a K1 factor 1.1 for CTC girders and 1.2 for CPM girders.

5.1.5 Comparison of Models

Figure 5-1 compares elastic modulus values calculated from the four models: AASHTO 2006, ACI 363, NCHRP 496 and Rosa's recommendation. For models including the unit weight of concrete, a value of 0.155 kcf was used. Measured modulus values from the field were not available for comparison. Figure 5-1 shows that the prediction equations given in the ACI 363 report and Rosa's recommendation respectively provide the lowest and highest modulus values for a given strength.

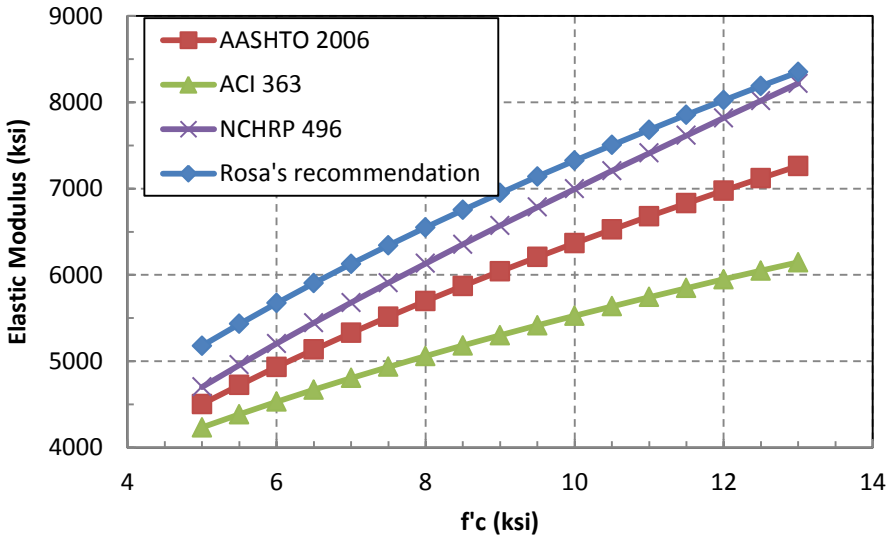

Figure 5-1. Comparison of Models to Calculate Elastic Modulus

To isolate the effects of elastic modulus on camber, this chapter uses the actual concrete strengths rather than the design concrete strength in all calculations. The following camber predictions in this chapter use the AASHTO 2005 models for creep, shrinkage, and the AASHTO 2005 refined method for prestress loss.

Because Rosa's recommendation (2007) developed modification factors from AASHTO 2006 model, so Rosa's recommendation was just one case of AASHTO 2006 when modification factors are applied. Therefore, the following calibrations will be only made for three the other models: AASHTO 2006, ACI 363, NCHRP 496.

5.2 Alaska Way Viaduct Girders

This section addresses optimizing factors that can be applied to the predicted elastic modulus to improve the camber predictions for nine girders in the Alaska Way Viaduct project. The goal is to minimize the root mean square (r.m.s.) camber error, which is defined as:

$$\text{error}_{\text{rms}} = \sqrt{\frac{\sum_{i=1}^{n} error_i^2}{N}} \qquad (5-1)$$

where:

error_i = difference between the measured and calculated cambers,

N = number of girders.

Figure 5-2 shows how the rms camber error in the Alaska Way Viaduct girders varies with the modifying factors for elastic modulus. Separate curves are shown for the three different methods for predicting elastic modulus from strength, namely the AASHTO 2006, ACI 363 and NCHRP 496 models. This step is necessary because the elastic modulus was not measured directly for these girders, and only strength measurements were available.

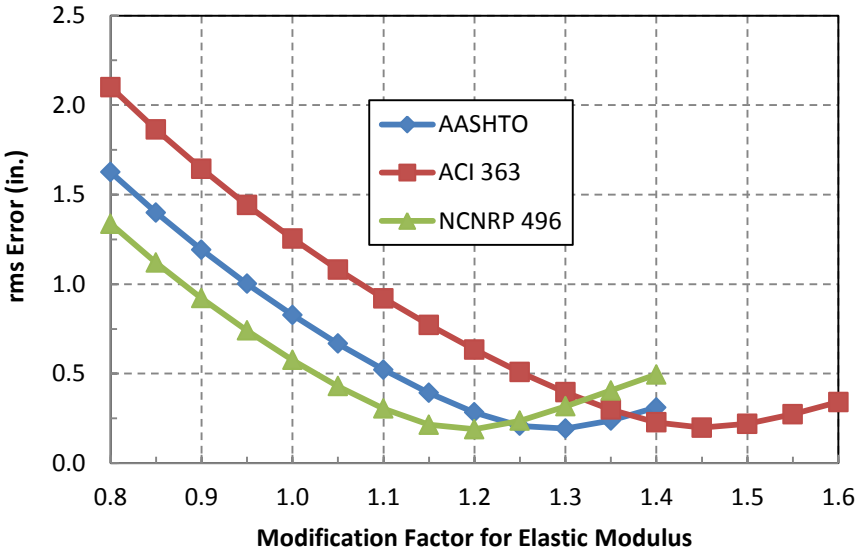

a) At Release

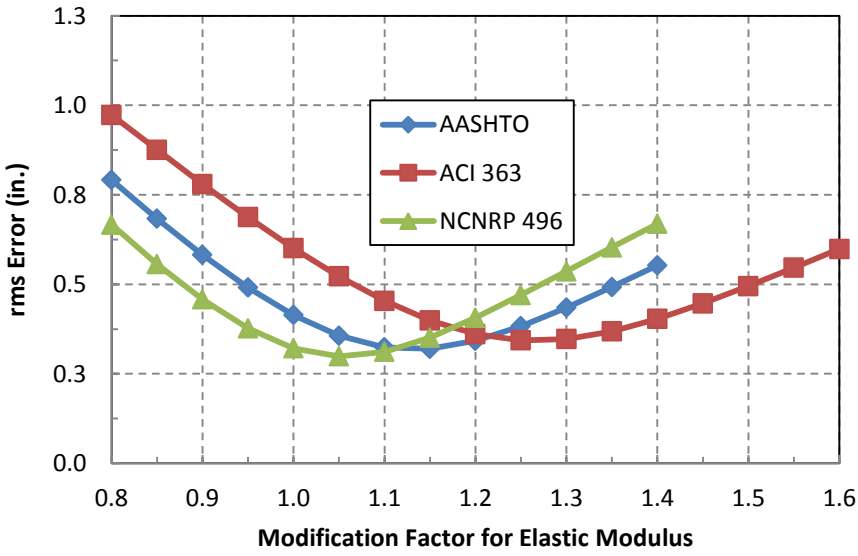

b) At 2nd Comparison

Figure 5-2. Calibration of Concrete Elastic Modulus – Alaska Way Viaduct

The factors that minimized the rms camber error at release and at the second comparison are shown in Table 5-1. For the Alaska Way Viaduct girders, the 2nd comparisons were made for cambers measured on Feb 17 2012.

Table 5-1 indicates that calibration factors for elastic modulus of the NCHRP 496 method are smallest and the factors in ACI 363 Model are biggest. This is consistent with Figure 5-1, in which the NCHRP 496 and ACI 363 methods predict the highest and lowest elastic modulus values when no modification factors were used.

Table 5-1. Optimized Elastic Modulus Factors for Alaska Way Viaduct Girders

	Release	2nd Comparison	Average
AASHTO 2006	1.30	1.15	1.25
ACI 363	1.45	1.25	1.40
NCHRP 496	1.20	1.05	1.15

Figure 5-2 presents the camber errors for the Alaska Way Viaduct girders without and with the use of the optimal modification factors given in Tale 5-1. As expected, the use of the modification factors reduced the camber errors. Most of the predicted cambers are within +/- 0.3 in. of the measured values.

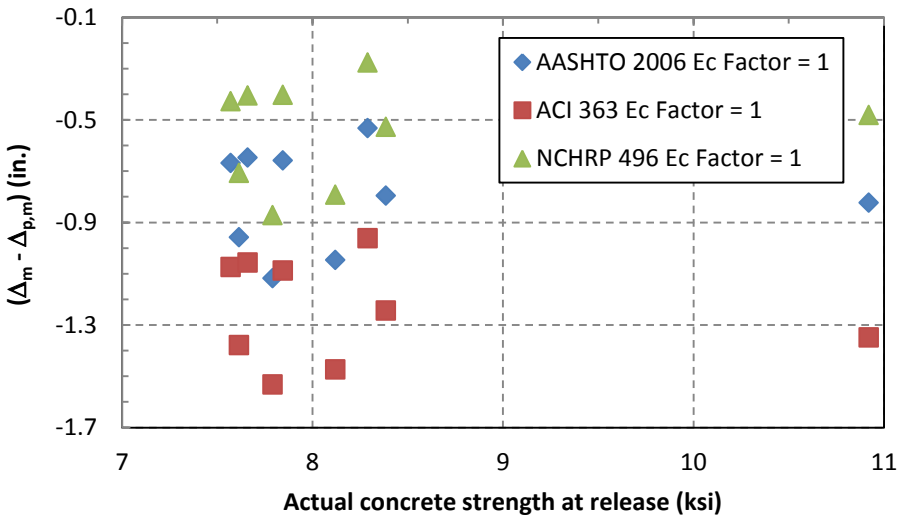

a) Release Camber Errors without Modification Factors

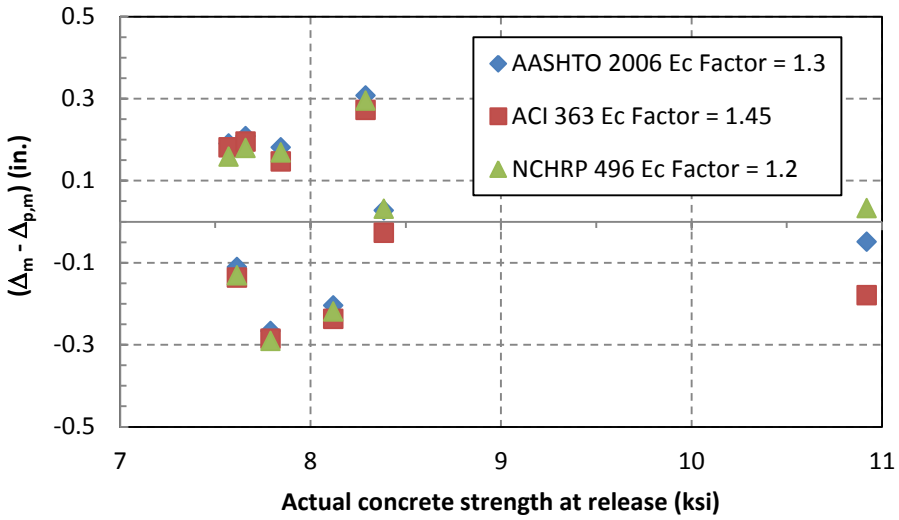

b) Release Camber Errors with Modification Factors

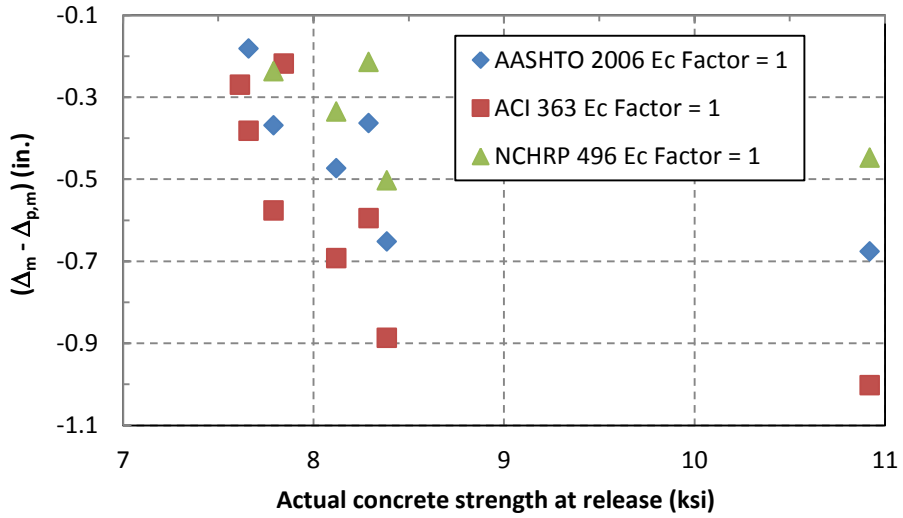

c) Camber Errors at the 2nd Comparison without Modification Factors

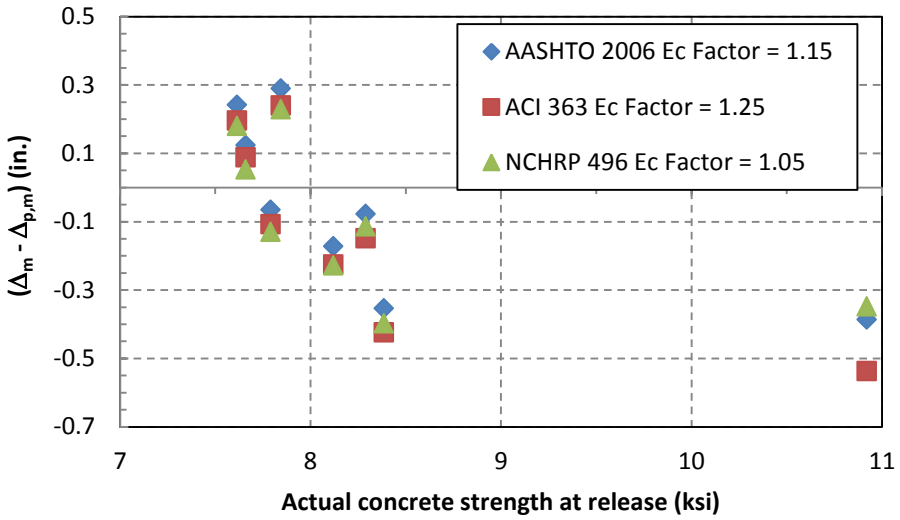

d) Camber Errors at the 2nd Comparison with Modification Factors

Figure 5-3. Error in Prediction of Camber Resulting from the Use of the Modified Elastic Modulus (E_c Factor)

5.3 All Girders

As shown in the previous section, the calibration factors for elastic modulus improved the camber prediction for the Alaska Way Viaduct girders. In this section, the modification factors for elastic modulus are optimized for the 155 available girders, including the 146 girders in Rosa's database and the 9 Alaska Way Viaduct girders. The 155 girders were separated into the 112 girders fabricated at Concrete Technology Corporation (CTC) and the 43 girders fabricated at Central Pre-Mix Prestress Co. (CPM) in order to account for the different aggregates used in the two plants.

Figure 5-4 shows the effect on the camber error of the elastic modulus factor for 112 CTC girders.

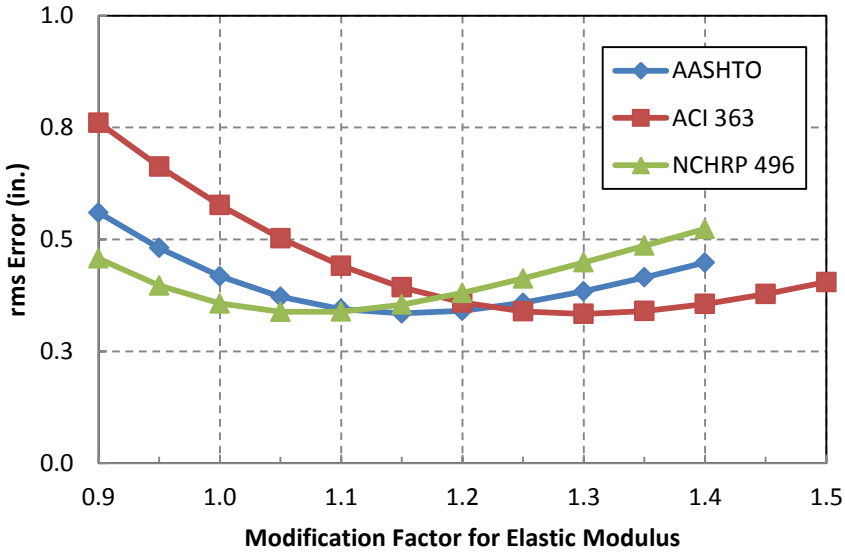

a) At Release

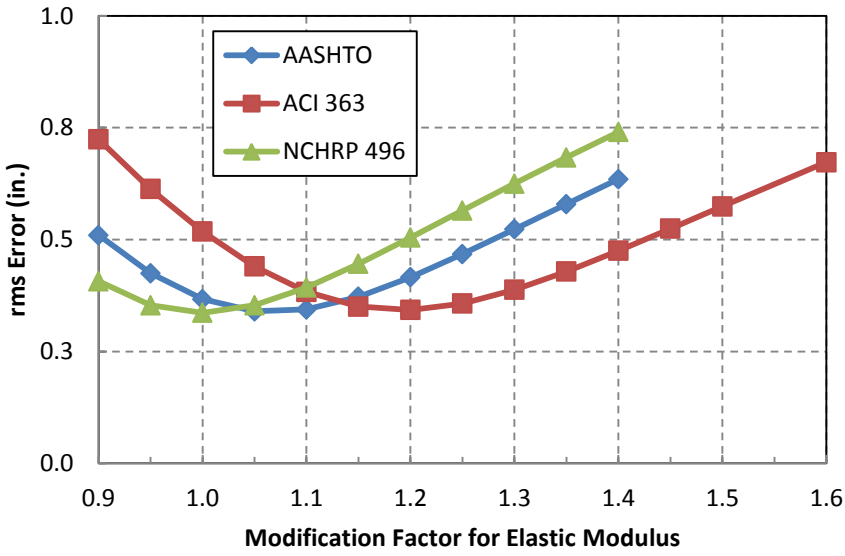

b) At the 2nd Comparison

Figure 5-4. Calibration of Elastic Modulus – CTC Girders

Table 5-2 shows the factors that minimized the rms camber errors at release and the second comparison for all girders. Calibration factors for elastic modulus in the NCHRP 496 model are the smallest and the factors in ACI 363 model are the largest. This result is the same as was found for Alaska Way Viaduct girders in Table 5-1.

Table 5-2. Optimized Elastic Modulus Modification Factors for the CTC Girders

	Release	2nd Comparison	Average
AASHTO 2006	1.15	1.05	1.10
ACI 363	1.35	1.20	1.28
NCHRP 496	1.05	1.00	1.03

Figure 5-5 shows calibrations of the concrete elastic modulus for 43 CPM girders.

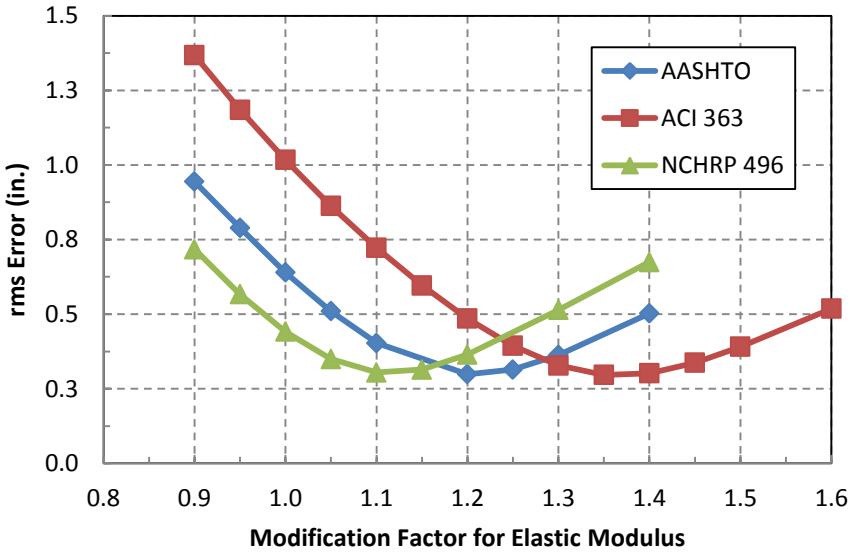

a) At Release

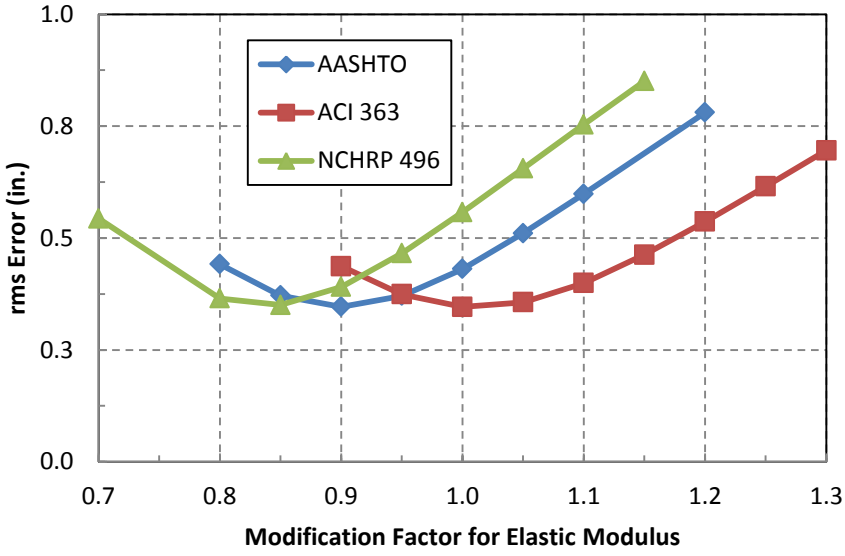

b) At the 2nd Comparison

Figure 5-5. Calibration of Elastic Modulus – CPM Girders

Table 5-3 and 5-4 summarize the factors that minimized the rms errors for all cases. They contain the same basic data but Table 5-3 classifies the modification factors according to fabricators (CTC and CPM). Table 5-4 organizes those factors according to times of comparison (at release and at the 2nd comparison).

Table 5-3. Optimized Modification Factors for All Girders

	CTC girders			**CPM girders**			
	Release	2nd Comparison	Average	Release	2nd Comparison	Average	All
AASHTO 2006	1.15	1.05	1.10	1.20	0.90	1.05	1.09
ACI 363	1.35	1.20	1.28	1.35	1.00	1.18	1.25
NCHRP 496	1.05	1.00	1.03	1.10	0.85	0.98	1.00

Table 5-4. Optimized Modification Factors for All Girders

	Release			**2nd Comparison**		
	CTC	CPM	All	CTC	CPM	All
AASHTO 2006	1.15	1.20	**1.18**	1.05	0.90	**0.98**
ACI 363	1.35	1.35	**1.35**	1.20	1.00	**1.10**
NCHRP 496	1.05	1.10	**1.08**	1.00	0.85	**0.93**

As shown in Table 5-3, at release, all modification factors are bigger than 1, so all the models underestimate the real E_c value. For the 2nd comparison, the three models gave better predictions for concrete elastic modulus when almost all factors were closer to 1.0 than the cases at release. In all cases, the NCHRP 496 model works the best for predicting the concrete elastic modulus.

It was also observed in Table 5-3 and 5-4 that at release, CPM girders were stiffer than CTC girders, but at the 2nd comparison, it is the other way round. There were two plausible explanations for this observation. The first one is CPM girders had high early elastic modulus than CTC girders. Because the CPM girders had probably lower water/concrete ratio to compensate for weaker aggregate than CTC girders, it leads to higher concrete strength (and higher elastic modulus) at release for CPM girders. However, eventually the CTC concrete will

catch up and stiffer at the 2nd comparison. The second explanation CPM girders have more creep than CTC girders. CPM is at East of Washington State where the weather is dryer than CTC (West of Washington). The dryer of weather is, the more creep we should expect.

Figure 5-6 shows a plot of the camber error, (Δ_m - $\Delta_{p,m}$), against the measured concrete strength at release, when the calculated elastic modulus using the NCHRP 496 model was multiplied by the optimal modification factors of 1.08 at release and 0.93 at the second comparison. The average absolute errors were -0.02 in. at release and -0.05 in. at the 2nd measurement.

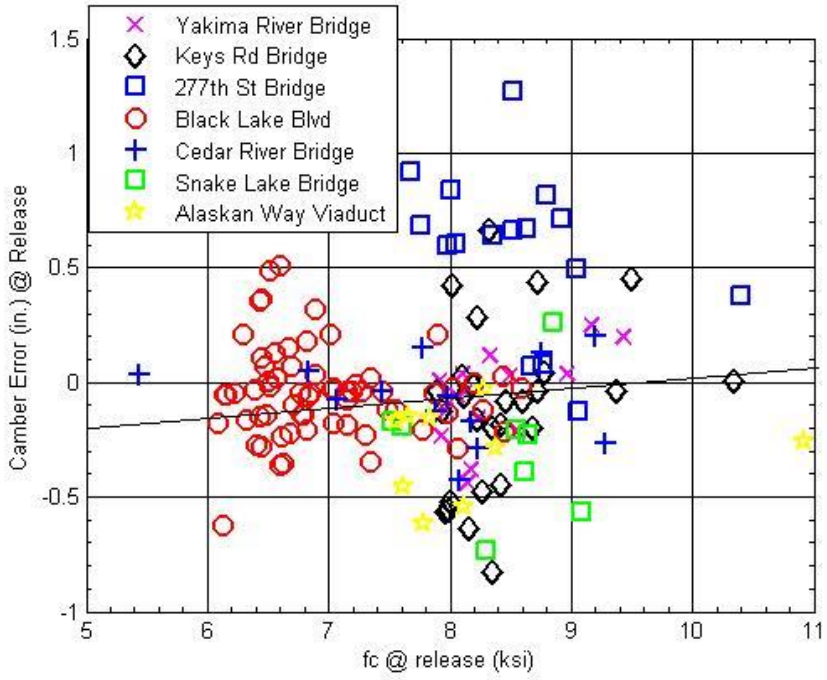

a) At Release, E_c Factor = 1.08

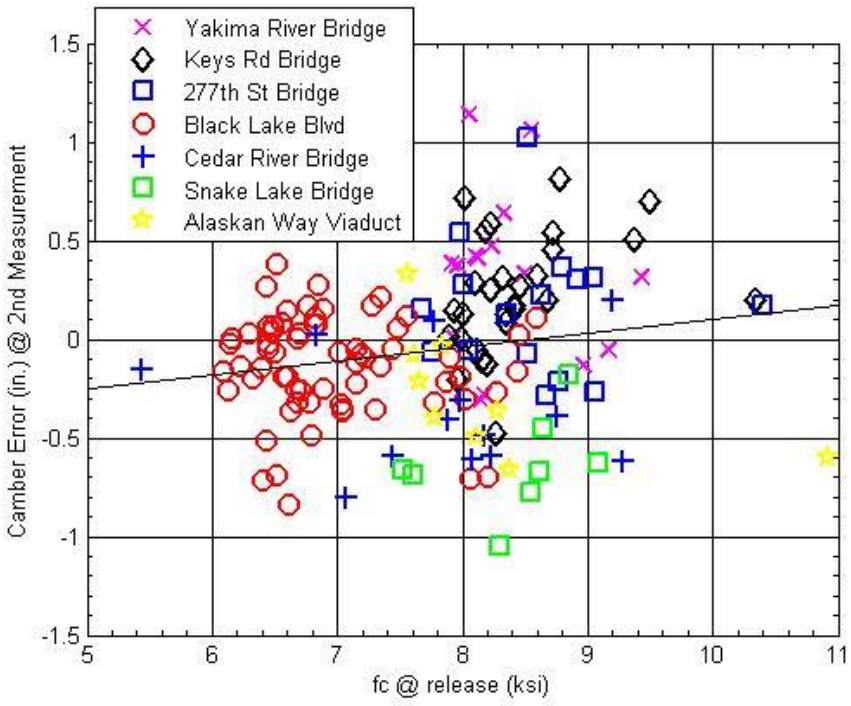

b) At the 2nd Comparison, E_c Factor = 0.93

Figure 5-6. Error in Prediction of Camber Resulting from Use the NCHRP 496 Model for the Concrete Elastic Modulus with Modification Factors

Figure 5-7 plots the camber error, (Δ_m - $\Delta_{p,m}$) from use of the NCHRP 496 model for the concrete Elastic Modulus with the optimized modification factors against a ratio of L/h. As shown in the figure, at the 2nd comparison, it appeared that the camber errors decreased as the L/h increased or the girder stiffness decreased. However, the trend was not obvious at release.

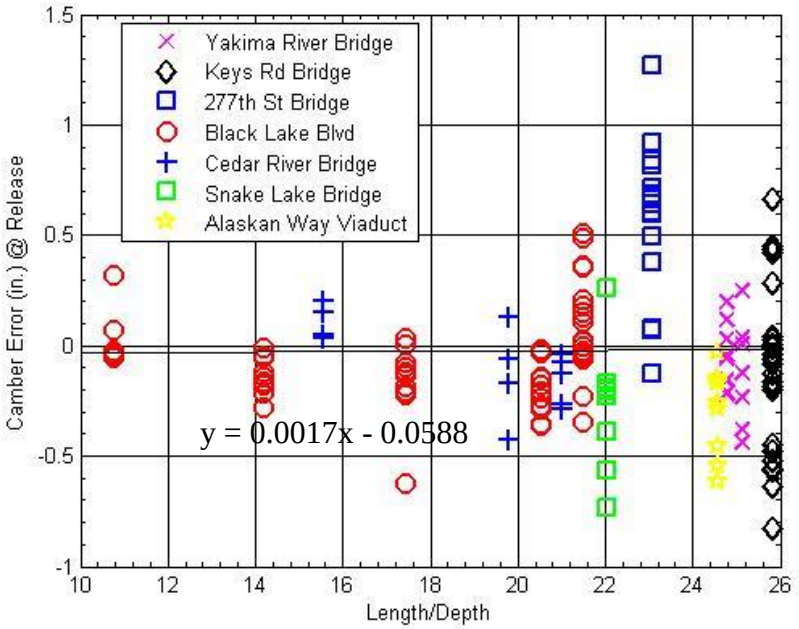

a) At Release, E_c Factor = 1.08

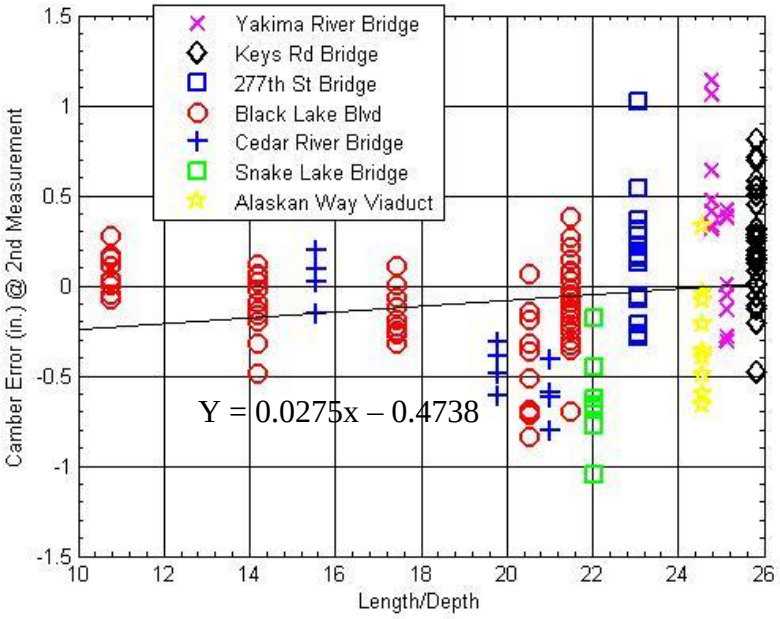

b) At the 2nd Comparison, E_c Factor = 0.93

Figure 5-7. Error in Prediction of Camber Resulting from Use the NCHRP 496 Model for the Concrete Elastic Modulus vs L/h

5.4 Conclusion

The modification factors for Elastic Modulus were calibrated by minimizing the rms error between the predicted and measured cambers for the set of 155 girders. That procedure leads to the following conclusions:

- The NCHRP 496 method predicts the best elastic modulus.
- In most cases, the AASHTO 2006 and ACI 363 formulations underestimated elastic modulus.
- The following modification factors are recommended for each model to calculate the concrete elastic modulus at release and long-term respectively:

Table 5-5. Optimized Modification Factors – All Girders

Model	Release	Long-term
AASHTO 2006	1.18	0.98
ACI 363	1.35	1.10
NCHRP 496	1.08	0.93

6 EFFECT OF DAILY TEMPERATURE VARIATIONS ON CAMBER

Girder camber is affected by daily variations in the girder temperature distribution. These effects must be evaluated to estimate the camber. This chapter examines the effect of daily temperature on camber by measuring internal temperatures of two WF100 girders on sunny days, then developing two practical, approximate methods for computing thermal camber variations when detailed information is not available on the internal temperature distributions.

Woolf at el. (1998) reported that during a day, 128ft 72M girders increased 1.5 in. in camber during the field study as the temperature at the top girders increased from 80 to 110 ^{o}F. Hinkle at el. (2006) observed that for the girders with average length of 128ft, the mid-span camber changed by up to 0.5 in. between 7.45 AM and 1:25 PM. Cullen at el. (2012) reported that cambers of. girders 119ft - 3 in. and 131ft - 6in long increased by 0.95 in. and 0.70 in. respectively during a day, which correspond to an overall camber increase of 16.1%.

Currently, there are several ways to estimate thermal camber:

- Measure the camber directly using a sensor. The measurements should be automated, electronic and continuous if possible. Potential drawbacks of this method lie in the need for equipment and power to run the system and a fixed point relative to which the camber can be measured.
- Measure the internal temperature over the height of the cross-section, compute the mechanical strains from them and integrate the resulting curvatures along the beam to give deflection. The data needed for this method are the internal temperature profile as a function of time, and the coefficient of thermal expansion.
- Use design temperature profiles provided by AASHTO LRFD (1994) Specifications or Priestley (1987) to calculate the internal strains, stress and external curvatures and deflections of the girders. This approach is necessarily more approximate than the others, but it requires little data.

6.1 Internal Temperature and Thermal Camber Measurement

To investigate the effect of daily temperature on camber, the second mentioned strategy was used in this study. A data logger was used to measure internal temperature of two WF100 girders. One girder had been cured over a weekend, and the other one had been cured during the work week. Table 6-1 shows some of the key girder properties.

Table 6-1. Girder Properties

	Mark Number	Cast Date	Measurement Date	Depth (in.)	Length (ft.)
Weekday Girder	H8A	5/29/2012	7/25&26/2012	100	163.96
Weekend Girder	H6B	5/18/2012	7/26/2012	100	172.71

Because the data logger had only 16 channels, only 16 thermocouples were installed to each of the two girders before casting. The cross sections were divided into three areas: the top flange, the web and the bottom flange. More thermocouples were placed in the flanges than in the web, because the flanges contained larger masses of concrete, and were expected to have big variations in temperature, than the web. The locations of the thermocouples for both the girders are depicted in the Figure 6-1.

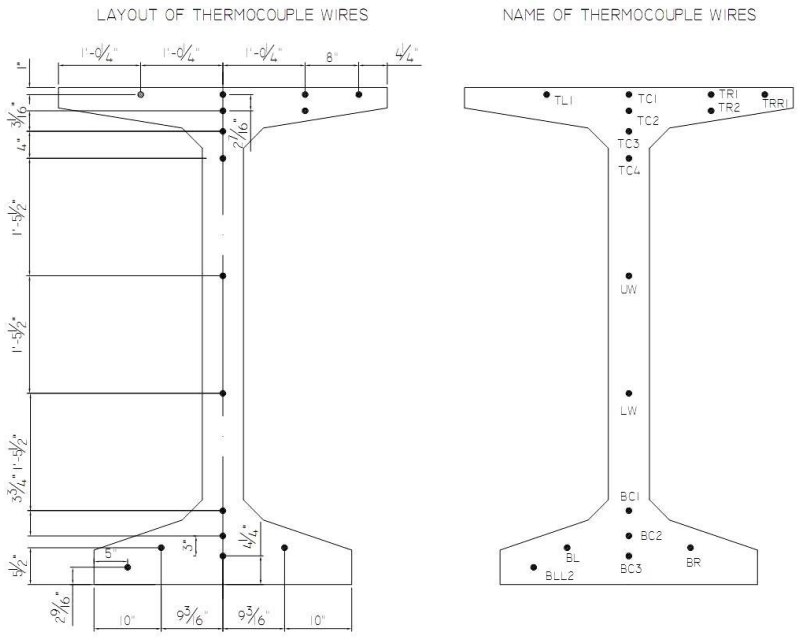

Figure 6-1. Thermocouple Locations

Figure 6-1 shows that the thermocouples were placed asymmetrically in the girder. This was done to optimize the information gained with a limited number of gages. The purpose of the Gage TRR1 and Gage TLL2 was to determine the distribution of temperature in the lateral direction. The measured internal temperature data was then used to calculate free thermal strains over the height of the cross section and then to compute the mechanical strains. The resulting curvatures along the beam were integrated to obtain the thermal camber. A sensor also was used to directly measure the daily camber change. The measured camber variations were compared to thermal camber calculated from internal temperature data.

Figure 6-2 shows the measured internal temperature distribution for the Girder H8A and Girder H6B.

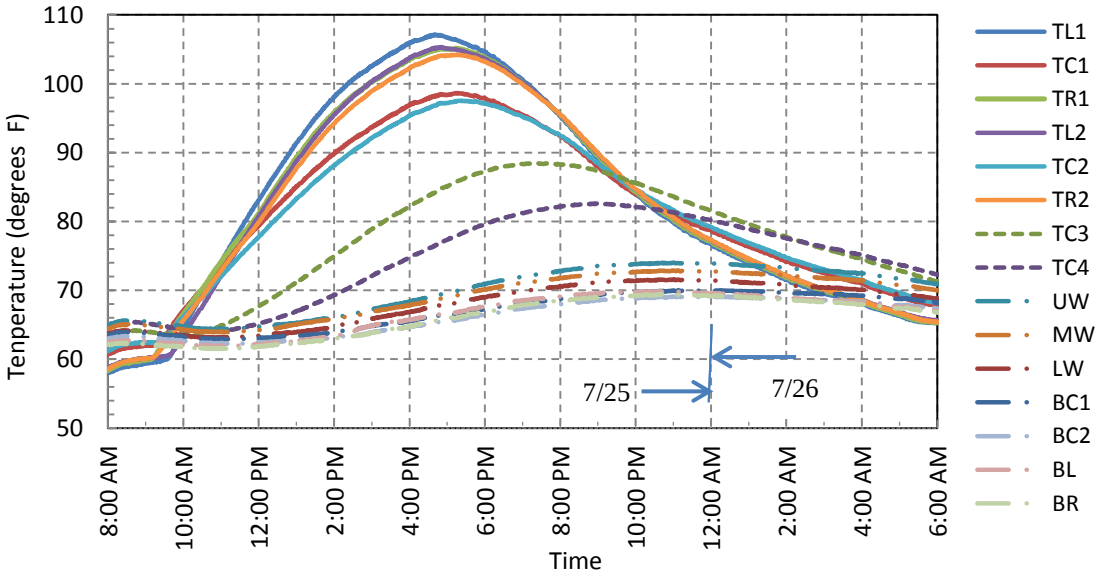

a) Girder H8A

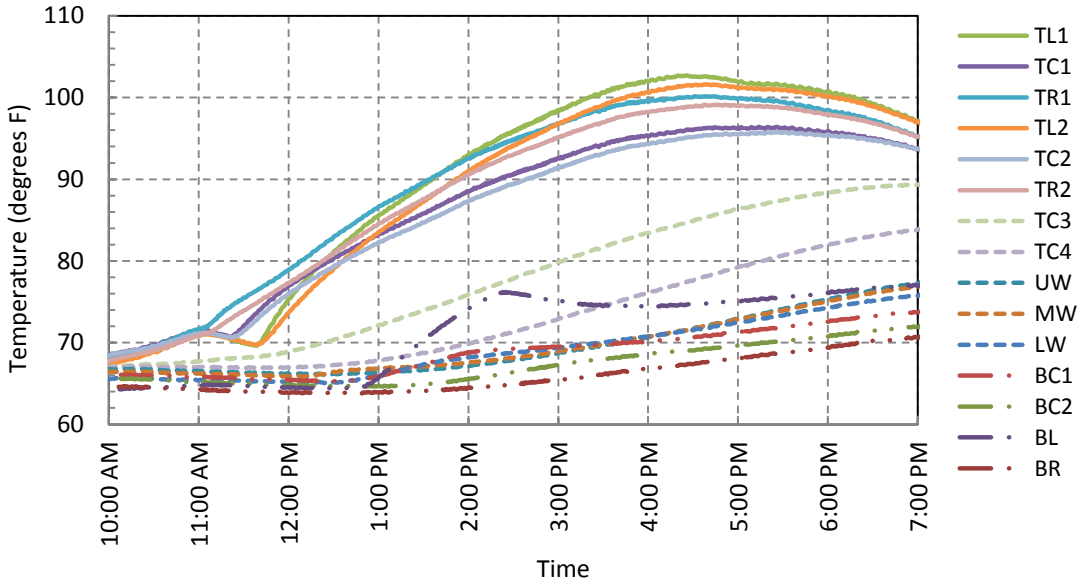

b) Girder H6B (Measured 7/26)

Figure 6-2. Internal Temperature Histories

The data follows expected trends. In the early morning, the temperature distribution over the height of girders is nearly uniform. However, when the accumulated solar radiation became stronger in the afternoon, the internal temperature in the top area that was exposed directly to sunlight increased rapidly. The web and bottom area experienced less temperature change under sunshine since they were shaded by the other girders. The left side of the Girder H6B was exposed to sunlight. That exposure is consistent with the data plotted in Figure 6-2(b), in which temperature at the bottom left position was higher than the bottom right or bottom center locations during day, when sunlight was strongest. In the late afternoon, the internal temperature at the top area dropped rapidly as the sunlight became weak and the air temperature decreased. However, in the web and bottom area in the girders, the rate of decrease was slower. This difference can be explained by the fact that the bottom area of girders was affected by heat from the ground and was less exposed to any cooling wind. During the day, the ground was heated by the sun. However, the rate of increase (or decrease) of temperature in the ground is slower than the air. Therefore, the ground heats or cools more slowly than the air temperature does. That is why, at night, the top of the girders cooled but the bottom continued to heat up.

Figure 6-3 and 6-4 show the vertical temperature profiles at different times. For each lateral section that had more than one thermocouple (in the flanges), the average value was taken. As shown in the Figs, in the early morning, the internal temperature was almost uniform over height of the girder. However when the sunlight came out, the top area were exposed to the sunlight and had the highest temperature in the girders.

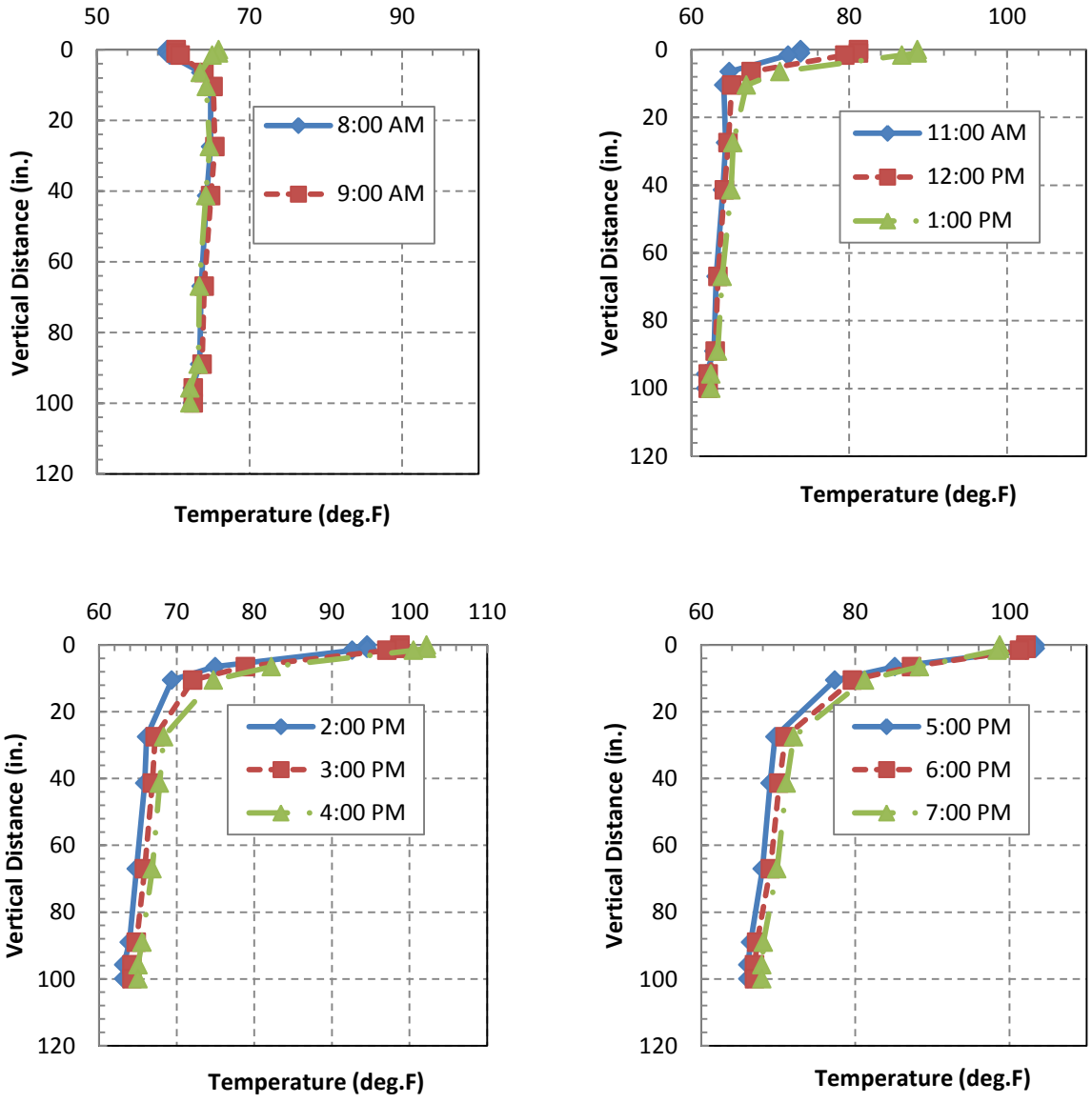

Figure 6-3(a). Temperature Distribution over Height of Girder H8A

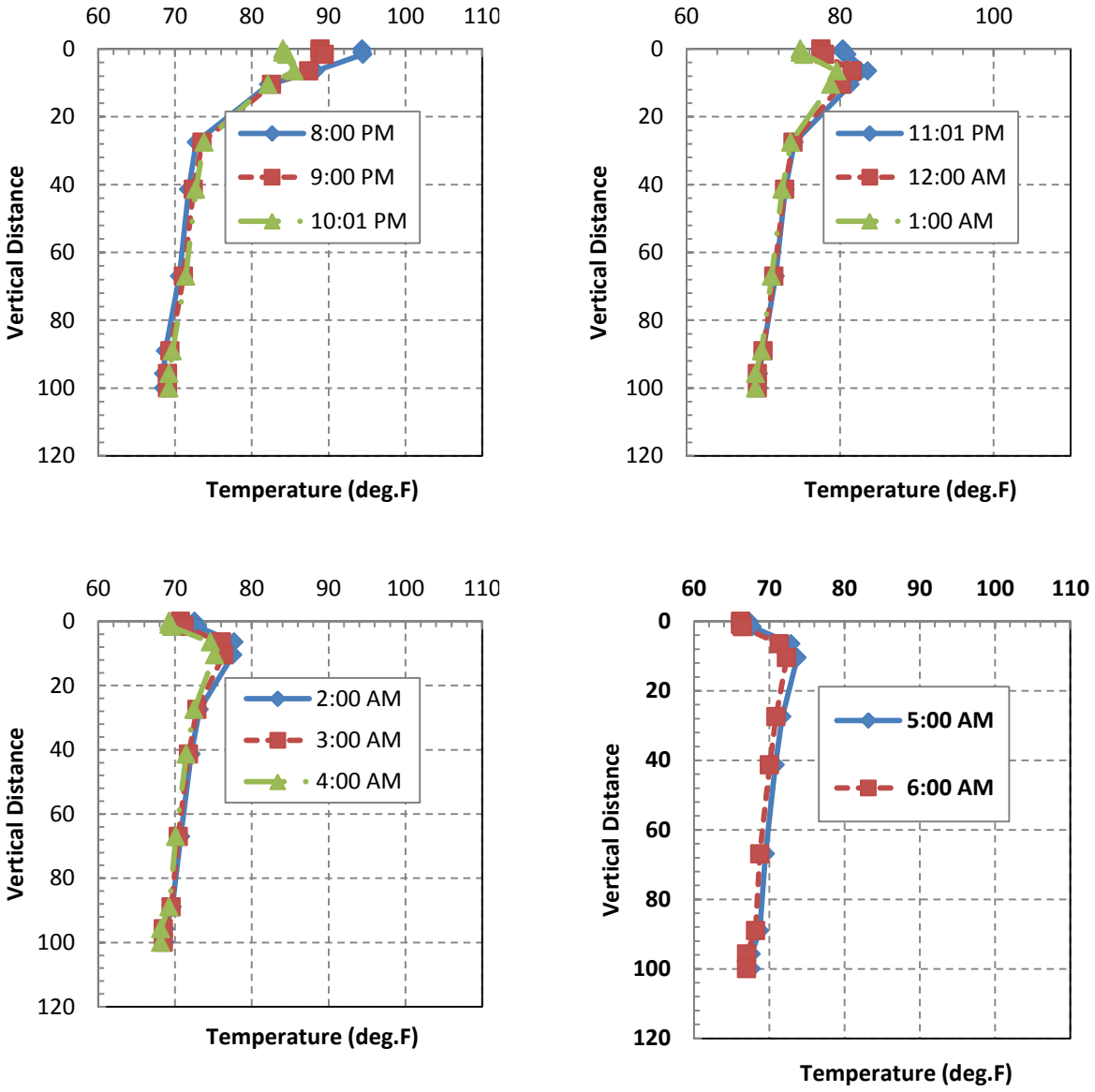

Figure 6-3(b). Temperature Distribution over Height of Girder H8A

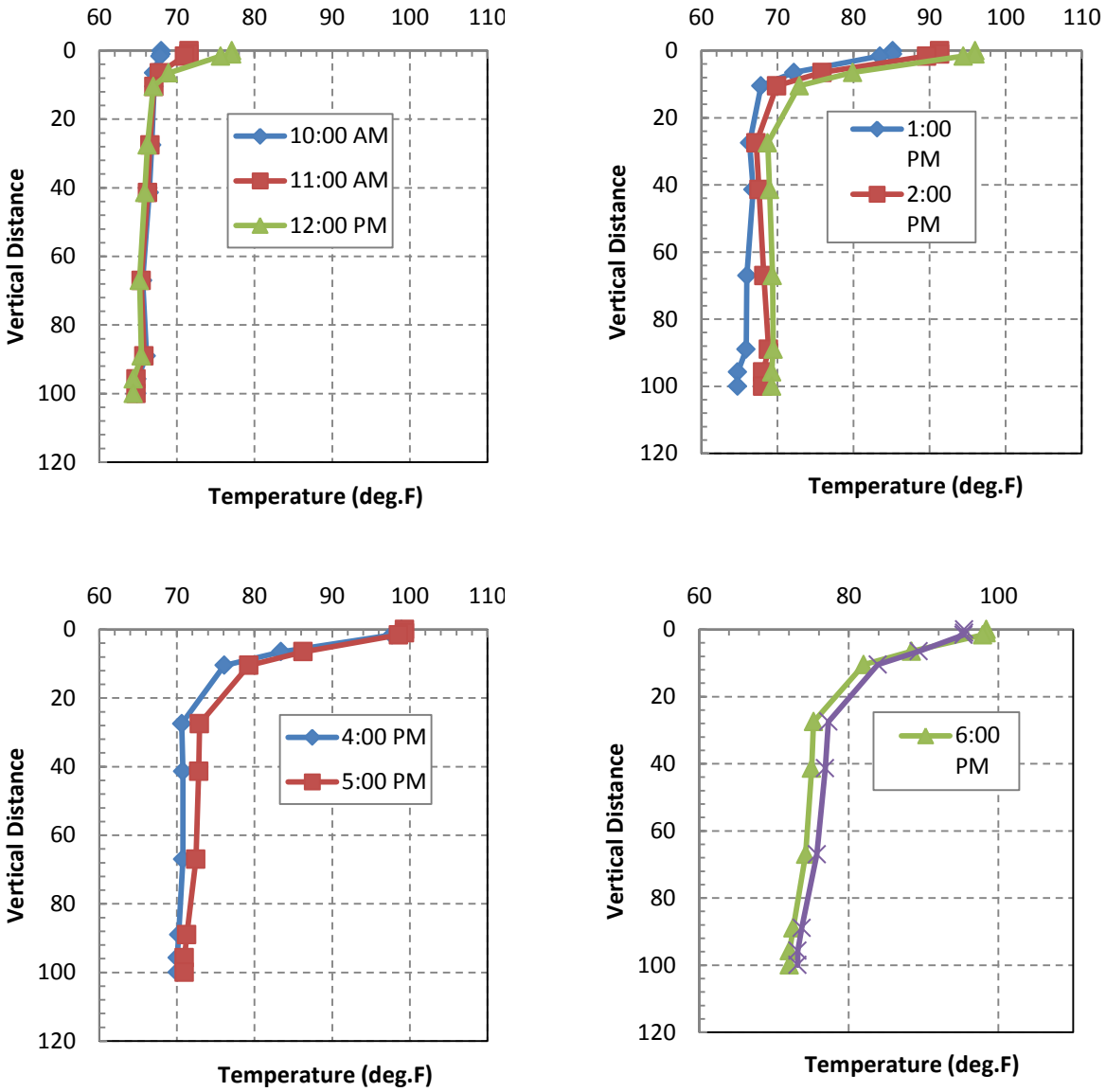

Figure 6-4. Temperature Distribution over Height of Girder H6B

From the vertical temperature distribution, the thermal strains over the height of the cross section and the curvature along the beam were computed to give the thermal camber. The calculation method is shown in Figure 6-5 and Equations from 6-1 to 6-8 (proposed by Barr at el. 2005):

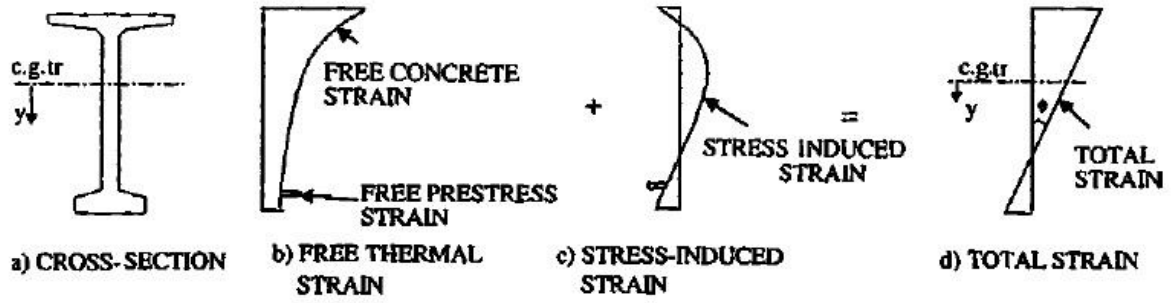

Figure 6-5. Strain Distribution in Simply Support Girder

Figure 6-5(a) shows a typical bridge girder in service. Heating the top of the bridge deck, as typically occurs during the day, causes the free thermal strain shown in Figure 6-5(b) which is calculated using Equation 6-1:

$$\varepsilon_{th}(y) = \alpha \Delta T(y) \qquad (6-1)$$

where $\varepsilon_{th}(y)$ = free thermal strain at any height, y, in the cross section, y = vertical coordinate measured downward from the girder centroid; α = coefficient of thermal expansion of the material; and $\Delta T(y)$ = temperature change at height y relative to temperature at construction.

The total strain field $\varepsilon_{tot}(y)$ is assumed to be linear [Fig. 6-5(d)] in accordance with the Bernoulli hypothesis, so mechanical (i.e., stress-induced) strains, shown in Fig.6-5(c), will be introduced. The total strain is then:

$$\varepsilon_{tot}(y) = \varepsilon_{th}(y) + \varepsilon_{mech}(y) \qquad (6-2)$$

where $\varepsilon_{tot}(y)$ is the total strain and $\varepsilon_{mech}(y)$ is the mechanical strain. The total linear strain field can be described by:

$$\varepsilon_{tot}(y) = \varepsilon_0 + y\phi_0 \qquad (6-3)$$

where $\varepsilon_0$is the strain at the centroid of the cross section and ϕ_0 is the curvature. Positive curvature is defined in the same sense, as is positive moment. The stress at height y is obtained from Eqs 6-2 and 6-3 as

$$\sigma(y) = E\varepsilon_{mech}(y) = E[\varepsilon_{tot}(y) - \alpha\Delta T(y)] \qquad (6-4)$$

Axial force equilibrium requires

$$0 = \int \sigma dA = E\int [\varepsilon_{tot}(y) - \alpha\Delta T(y)]dA \qquad (6-5)$$

Substituting for ε_{tot} in Eq. (6-4) leads to the centroidal strain

$$\varepsilon_0 = \frac{\alpha\int \Delta T(y)dA}{A} \qquad (6-6)$$

Similar logic for moment equilibrium leads to the following strain gradient or curvature:

$$\phi_0 = \frac{\alpha\int \Delta T(y)ydA}{I} \qquad (6-7)$$

If the temperature profile is known, the variables ε_0 and ϕ_0, which fully define the strain field, can be computed with Eqs. (6-6) and (6-7). The resulting stress induced at any level can then be computed with Eq. (6-4). The integrals in Eqs. (6-5) and (6-6) can easily be evaluated numerically.

Camber can be obtained by integrating the curvatures. For example, if the curvature is uniform over a simple span, the mid-span camber is given by

$$\delta = \frac{\phi_0 L^2}{8} \qquad (6-8)$$

Figure 6-6 compares the calculated and measured thermal cambers, assuming that the coefficient of the thermal expansion of concrete was $6.5*10^{-6}$ in.in./deg.F. In all cases, the thermal camber was arbitrarily assumed to be zero when the measurements were started.

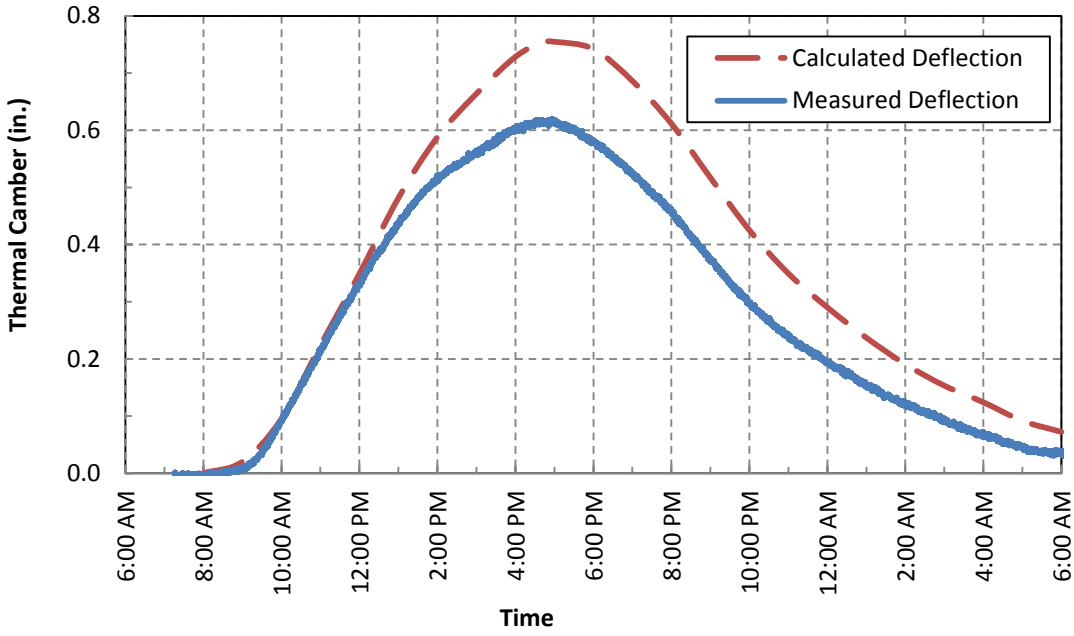

a) Girder H8A

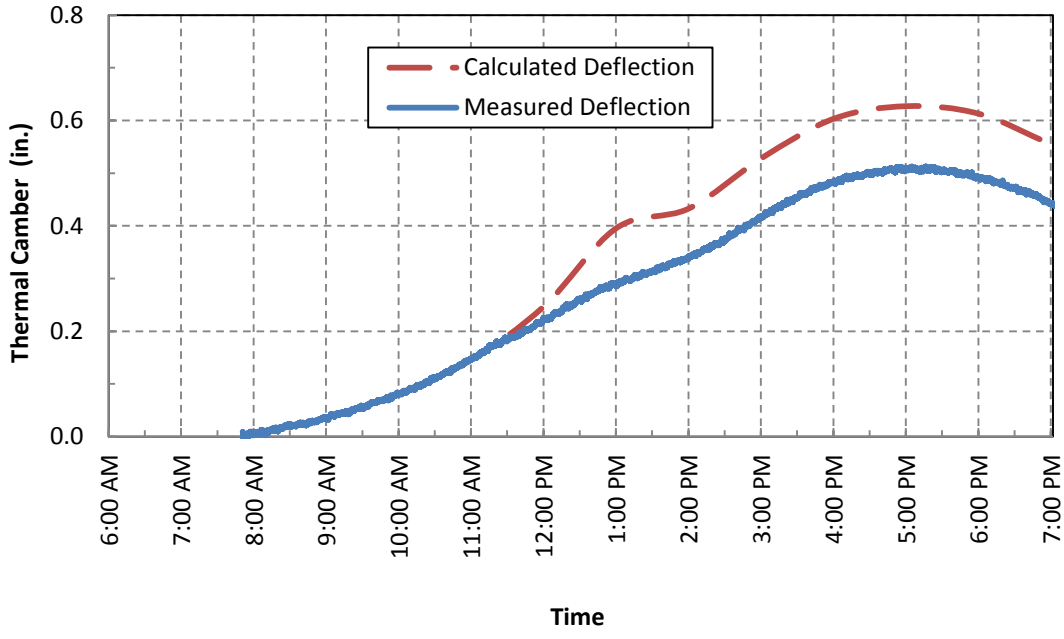

b) Girder H6B

Figure 6-6. Comparison between the Measured and Calculated Thermal Cambers

Figure 6-6 shows a consistent difference of about 0.15 in. between the measured and calculated cambers in the afternoon. This discrepancy may due to the error in taking measurement or in assumptions of calculations or the thermal expansion of concrete was not equal $6.5*10^{-6}$ in.in./deg.F. The author tried several thermal expansions of concrete and α equal $5.5*10^{-6}$ in.in./deg.F brought the best fit.

Measuring internal temperature distributions is a potential way to predict the thermal camber, but it requires internal temperature data. Therefore, two ways were developed to predict the thermal camber that are more approximate but require knowledge of the air temperature alone. These methods are discussed in Sections 6.2 and 6.3 of this chapter.

6.2 Temperature History Model

6.2.1 Proposed Model

The Temperature History Model is based on the assumption that the temperature difference between the top and bottom of the girders is related to the ambient temperature. Ambient temperatures are available on meteorological websites.

Although the measured temperature data showed that the temperature distribution in the girders is highly nonlinear, in the Temperature History Model, the total strain profile over the height of the girder is still assumed to be linear, in accordance with the Bernoulli hypothesis and to make the model as simple as possible. For the sake of convenience, it is represented here by a fictitious thermal strain gradient that varies from zero at the bottom to ε_{TH} at the top, as shown in Figure 6-7.

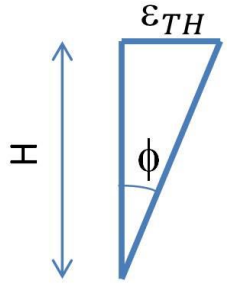

Figure 6-7. Assumed thermal strain distribution in girder

The thermal curvature is then:

$$\phi\,(t) = \frac{\varepsilon_{TH}}{H} \qquad (6-9)$$

Here:

ε_{TH} = the free thermal strain and equal to $\alpha\Delta T$,

α = the coefficient of thermal expansion,

ΔT = temperature difference between the top and bottom of the girder, and

H = depth of the girder

The corresponding camber at mid-span, for a girder simply supported at its ends, is

$$\Delta\,(t) = \phi(t) * \frac{L^2}{8} \qquad (6-10)$$

Here:

L = length of the girder

To calculate the camber at any time during the day, ε_{TH} (t) is needed. In the Temperature History Model, the girder temperature difference is approximated by a multiple, A_0, of the difference between the ambient temperature at time t and the minimum temperature of that day, as shown in Equation 6-11:

$$\Delta T\,(t) = A_0(T(t) - T_{min}) \qquad (6-11)$$

Here:

A_0 is a calibration factor that will be selected in Section 6.2.2.

Therefore:

$$\varepsilon_{TH} = A_0\,\alpha(T(t) - T_{min}) \qquad (6-12)$$

Combining equations 6-9 through 6-12 results in a calculated thermal camber of:

$$\Delta(t) = \frac{\alpha A_0}{H}\,(T(t) - T_{min}) * \frac{L^2}{8} \qquad (6-13)$$

As shown in Equation 6-13, camber at time t is related directly to air temperature at that time. Therefore, the calculated camber is sensitive to rapid changes in ambient temperature. However, it is not true in practice because the rate of change of temperature in the girders is not as fast as in the air because of the thermal mass of the girder. To solve this issue, the Moving Average Method was selected. The component T(t) in the Equations 6-11 to 6-13 was taken as an average of the current temperature and air temperature data during the two preceding hours. T(t) was taken as:

$$T(t) = \frac{T(t) + T(t - 1hour) + T(t - 2hour)}{3} \qquad (6-14)$$

The constant A_0 accounts for:

- the difference between the ambient and girder temperatures
- the difference between the true concrete temperature and the fictitious one that leads to a linear strain gradient
- the difference between the true (but unknown) α value and the standard value of 6.5×10^{-6} in.in./deg.F that was used here.

6.2.2 Calibration of Temperature History Model

Data from 24 girders from three states including data from the two monitored girders, 5 girder data from Barr et al. (2000), 14 girder data from Cullen at el. (2012) and 3 girder data from Hinkle at el. (2006) were used to calibrate the Temperature History Model. Those girders had a variety of depths, lengths, times of casting and times of measurement. Table 6-2 summarizes their key properties.

Table 6-2. Girder Properties

Girders	Location	Measurement Date	Depth (in.)	Length (ft.)	Length/Depth
1A	Washington	2/4/1997	74	80.0	12.98
1C	Washington	2/4/1997	74	80.0	12.98
2A	Washington	3/6/1997	74	137.1	22.24
2B	Washington	3/10/1997	74	137.1	22.24
2C	Washington	3/12/1997	74	137.1	22.24
H6B	Washington	7/26/2012	100	172.5	20.70
H8A	Washington	7/25/2012	100	163.7	19.65
MN54 - Beam 1	Minnesota	9/28/2010	54	122.0	27.11
MN54 - Beam 2	Minnesota	9/28/2010	54	122.0	27.11
MN54 - Beam 3	Minnesota	9/28/2010	54	122.0	27.11
MN54 - Beam 4	Minnesota	9/28/2010	54	122.0	27.11
MN63 - Beam 1	Minnesota	5/17/2011	63	132.0	25.14
MN63 - Beam 2	Minnesota	5/17/2011	63	132.0	25.14
MN63 - Beam 3	Minnesota	5/17/2011	63	132.0	25.14
MN63 - Beam 4	Minnesota	5/17/2011	63	132.0	25.14
MN45 - Beam 1	Minnesota	5/17/2011	45	119.0	31.73
MN45 - Beam 2	Minnesota	5/17/2011	45	119.0	31.73
MN45 - Beam 3	Minnesota	5/17/2011	45	119.0	31.73
MN45 - Beam 1	Minnesota	6/30/2011	45	119.0	31.73
MN45 - Beam 2	Minnesota	6/30/2011	45	119.0	31.73
MN45 - Beam 3	Minnesota	6/30/2011	45	119.0	31.73
W45 - 6	Georgia	8/31/2003	79	129.3	19.64
W45 - 7	Georgia	8/31/2003	79	128.1	19.45
W45 - 8	Georgia	8/31/2003	79	127.3	19.34

For each girder, camber readings were recorded throughout the course of a day. The measured camber values (M) were compared to the calculated values (C) using Equation 6-13. The average error was defined as:

$$Average\ Error = \sqrt{\sum_{i=1}^{n} \frac{(M_i - C_i)^2}{n}} \qquad (6-15)$$

Table 6-3 lists the errors between calculated and measured values for all girders.

Table 6-3. Errors between Measurement and Calculation using different A_0

		Optimum A_0 and error		A_0 = 1.25
Girders	Numbers of Observation	A_0	Error	Error
1A	7	1.15	0.014	0.016
1C	7	1.46	0.023	0.027
2A	7	1.51	0.042	0.050
2B	7	1.34	0.037	0.038
2C	7	1.56	0.031	0.074
H6B	18	0.73	0.063	0.224
H8A	18	1.00	0.064	0.130
MN54 - Beam 1	7	1.40	0.010	0.027
MN54 - Beam 2	7	1.21	0.027	0.028
MN54 - Beam 3	7	0.20	0.015	0.018
MN54 - Beam 4	7	1.23	0.012	0.012
MN63 - Beam 1	5	1.35	0.036	0.054
MN63 - Beam 2	5	1.24	0.073	0.074
MN63 - Beam 3	5	1.53	0.091	0.142
MN63 - Beam 4	5	1.11	0.052	0.075
MN45 - Beam 1	5	1.45	0.031	0.113
MN45 - Beam 2	5	1.33	0.051	0.065
MN45 - Beam 3	5	1.12	0.045	0.084
MN45 - Beam 1	7	1.57	0.102	0.184
MN45 - Beam 2	7	1.27	0.079	0.079
MN45 - Beam 3	7	1.07	0.062	0.106
W45 - 6	3	1.59	0.110	0.133
W45 - 7	3	1.03	0.070	0.085
W45 - 8	3	1.45	0.104	0.113
Average		**1.25**	**0.05**	**0.08**

The parameter A_0 was varied to optimize the fit between the predicted and measured values. In all cases the standard value of coefficient of thermal expansion, α, was assumed to be $6.5*10^{-6}$ in./in./deg. F because no measured value was available. Thus, the value of the parameter A_0 covered errors in both the assumed temperature distribution and the coefficient of thermal expansion. The Solver function in Excel was used to optimize the model. The target was to minimize the average errors by changing A_0. The optimum fit was obtained for a value of A_0 = 1.25.

Table 6-3 gave an average error of 0.08 in. using the Temperature History Model with the optimal value of A_0 = 1.25. Figure 6-8 shows the optimized A_0 for each girder and the corresponding error value.

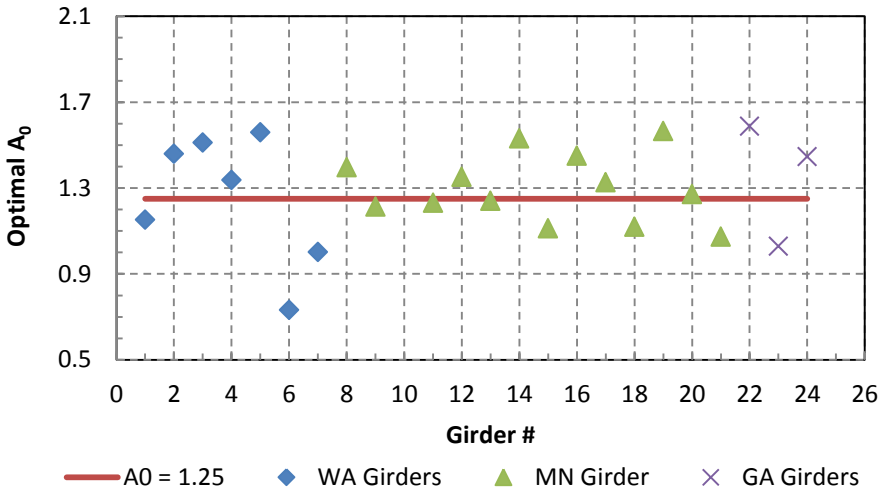

Figure 6-8. Optimized values of A_0 for all girder

Figure 6-9 and 6-10 compare the measured and the calculated thermal camber histories using the Temperature History Model with A_0 = 1.25 for Washington and Minnesota State girders, respectively. In those Figures, the prefix "Meas" means measured camber. The measured thermal cambers represent the changes in measured camber over time.

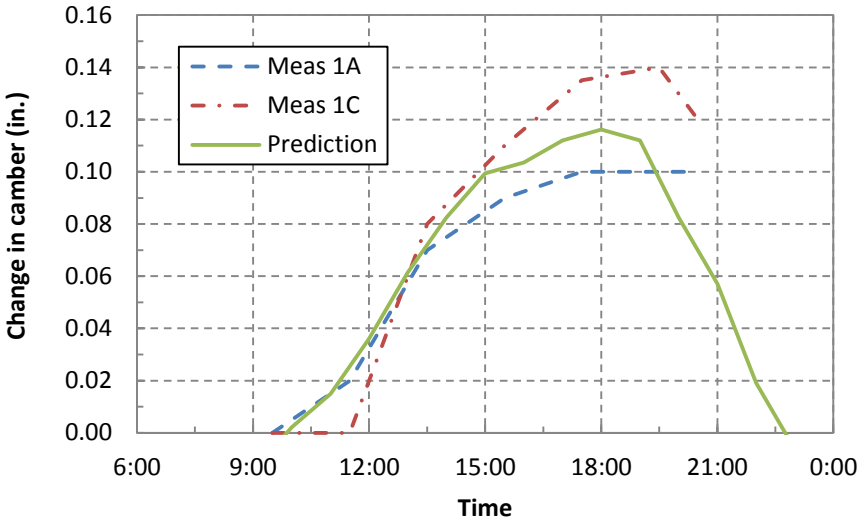

a) Girder 1"X"

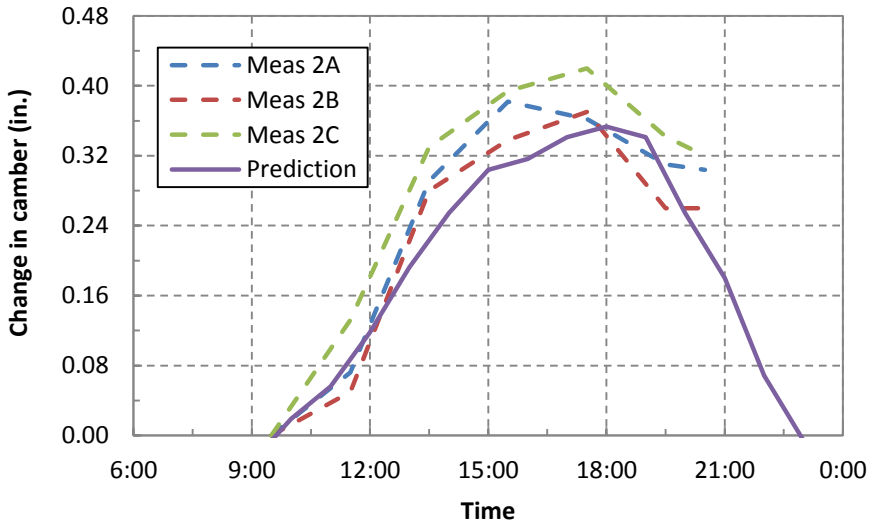

b) Girder 2"X"

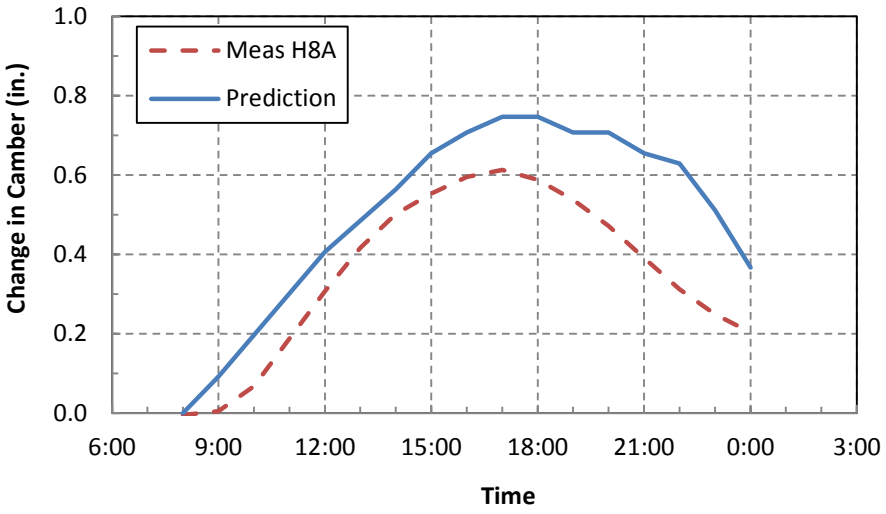

c) Girder H8A

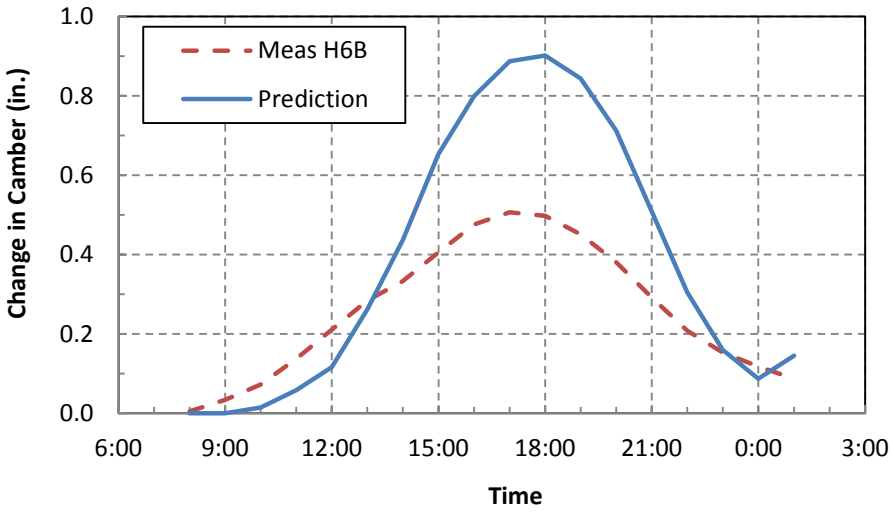

d) Girder H6B

Figure 6-9. Comparison between Measured and Calculated Thermal Camber Changes – WA Girders

It appeared in Figure 6-9 that the Temperature History Model works quite well for 1A, 1C, 2A, 2B, 2C girders that were cast in Central Pre-Mix Concrete Co (CPM) when the modified prediction and measurement curves were similar and the error was about 0.05 in. at peak time. However, for the two girders cast in Concrete Technology Corporation, the errors were 0.20 in.

for Girder H8A and 0.40 in. for Girder H6B. One possible explanation for the big error between measurements and predictions of Girder H6B is that the left side of the Girder H6B was exposed to sunlight. Therefore, the girder was heated over its whole height, while the other girders were subjected to solar radiation primarily on the top flange. Also, the Girder H6B was cast on Friday and, because of the longer curing time over the weekend; a different thermal profile was used during curing and resulted in concrete that was more mature than usual at release. There is no reason to believe that this factor should affect the daily thermal camber, because the measurements were taken about three months after casting. However, the weekend curing was the primary difference between this and the typical girder. Another possible reason can explain for the big errors of Girder H8A and Girder H6B is that the CTC girders were WF100 whereas 5 girders from Barr at el. (2000) were F74G. The WF series have bigger top flanges and that would mean that they probably heat up more slowly in the same ambient temperature, so the camber would be smaller than expected.

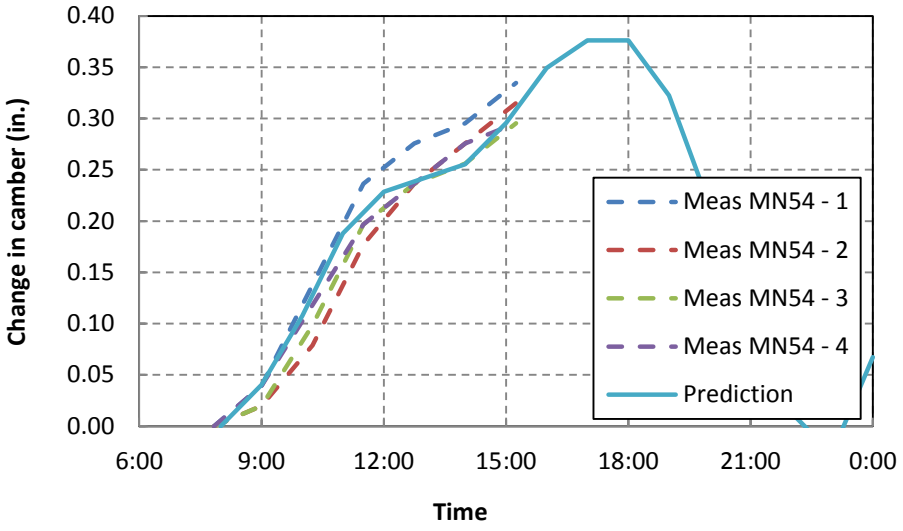

a) Girder MN54

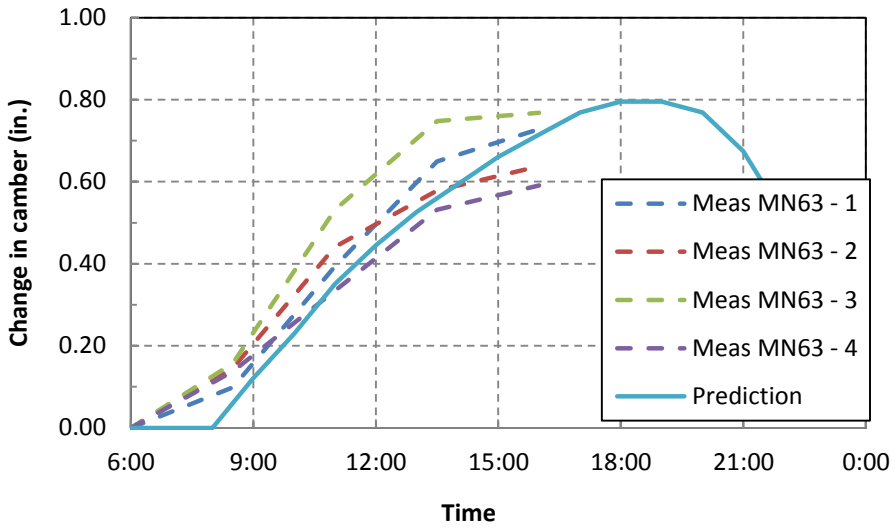

b) Girder MN63

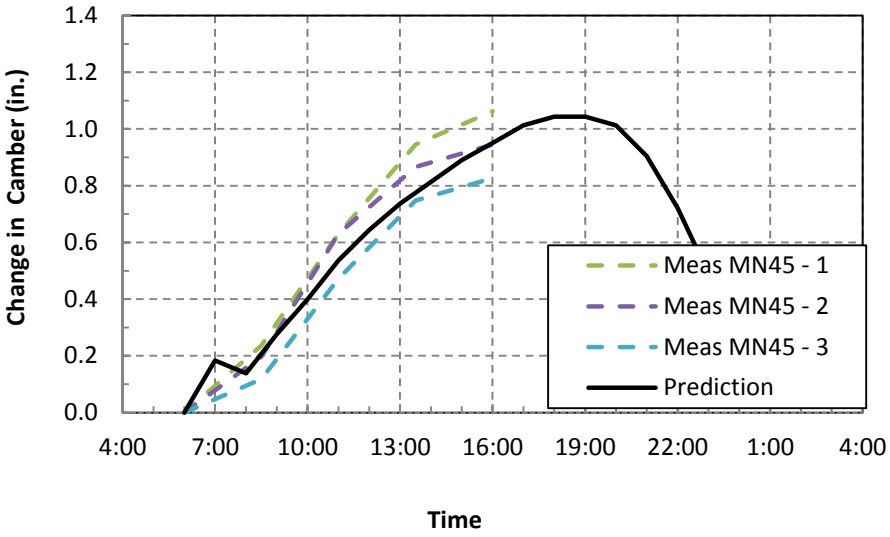

c) Girder MN45 (Measured on 05/17/2011)

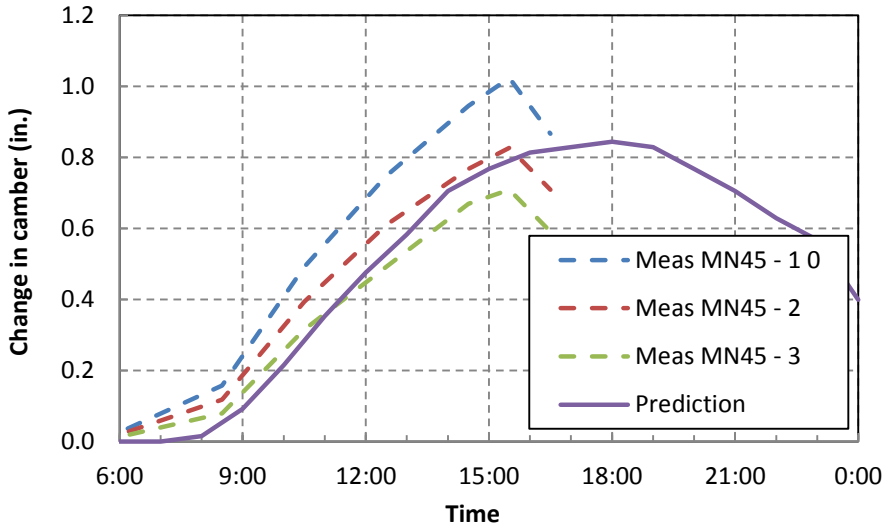

d) Girder MN45 (Measured on 06/30/2011)

Figure 6-10. Comparison between Measured and Calculated Thermal Camber Changes – MN Girders

Figure 6-10 shows that cambers predicted by the Temperature History Model were close to the measurements for all Minnesota girders.

Figure 6-11 compares the measured thermal camber and the calculated thermal camber using Temperature History Model with $A_0 = 1.25$ for Georgia girders.

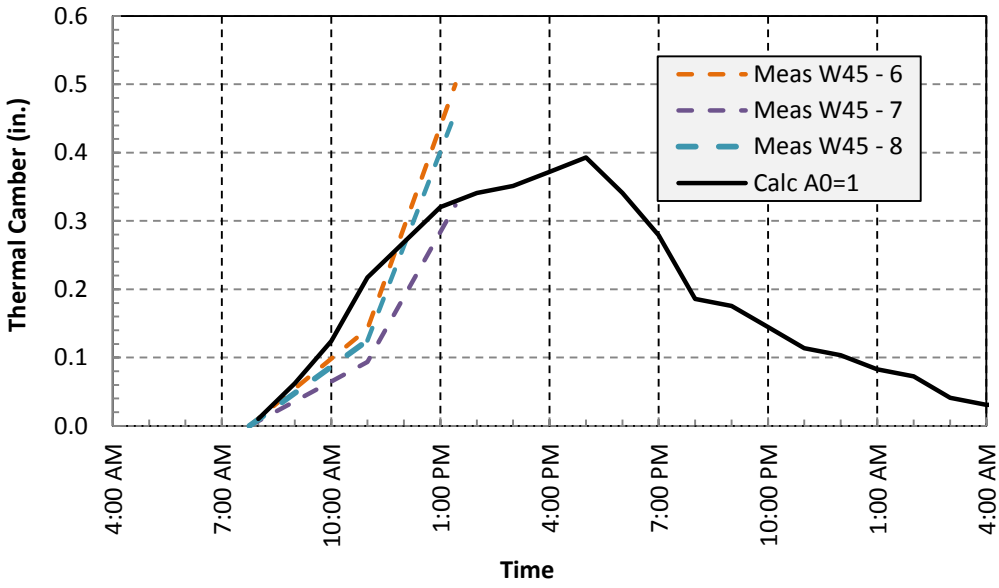

Figure 6-11. Comparison between Measured and Calculated Thermal Camber Changes – GA Girders

For the GA girders, the predictions did not match the measured values well. This may be partially explained by the fact that only three data points were taken for each girder. This set of girders was also measured in Georgia, where the temperature, humidity, length of day etc. differ from those in Washington and Minnesota.

6.3 Peak Temperature Model

6.3.1 Proposed Model

The Peak Temperature Model is based on the assumption that the temperature difference between the girder top and bottom (ΔT) is related to the daytime high temperature and the low (night-time) temperature for that 24-hour period. These two values are available on meteorological websites when the time and location are defined.

Equations for the thermal curvature and the corresponding camber were given in equations 6-9 and 6-10. To estimate the camber at any time during the day, an instantaneous value of $\Delta T(t)$

is needed. In the Peak Temperature Model, that temperature is approximated from the maximum and minimum temperatures of that day using a cosine function, as shown in Equation 6-16

$$\Delta T\ (t) = (T_{max} - T_{min}) \frac{\left(1 - \cos\left(\frac{(t - t_0)}{24} 2\pi\right)\right)}{2} \qquad (6-16)$$

where: t_0 = is the reference time for counting the thermal camber during that day. The ΔT has the value 0.0 when $t = t_0$ or t_0+24 hours, and reaches its maximum of T_{max} and T_{min} at $t = t_0$ + 12 hours.

Therefore, the assumed thermal strain is:

$$\varepsilon_{TH} = A_1 \alpha (T_{max} - T_{min}) \frac{\left(1 - \cos\left(\frac{(t - t_0)}{24} 2\pi\right)\right)}{2} \qquad (6-17)$$

Combining equations 6-9, 6-10, 6-16 and 6-17 results in a thermal camber of:

$$\Delta(t) = \frac{\alpha A_1}{H} \frac{(T_{max} - T_{min}) \left(1 - \cos\left(\frac{(t - t_0)}{24} 2\pi\right)\right)}{2} * \frac{L^2}{8} \qquad (6-18)$$

where A_1 is a calibration factor that will be selected in Section 6.3.2.

6.3.2 Calibration of Peak Temperature Camber Model

The Peak Temperature Camber Model was calibrated by matching its prediction against the measured values for the girders as considered in Section 6.2.2. Table 6-4 shows the errors between the calculated and measured thermal camber changes for all investigated girders.

Table 6-4. Errors between measured and calculated thermal camber changes using different A_1 and t_0

Girders	Peak of measured thermal camber (in.)	Optimum A_1 and t_0			Optimum A_1 with t_0 = 5		A_1= 1.24; t_0 = 5
		A_1	t_1	Error	A_1	Error	Error
1A	0.100	0.96	6.36	0.010	1.17	0.014	0.015
1C	0.140	1.16	6.98	0.010	1.47	0.027	0.031
2A	0.382	1.53	4.99	0.039	1.53	0.039	0.054
2B	0.370	1.36	4.97	0.040	1.35	0.040	0.042
2C	0.420	1.57	5.00	0.018	1.57	0.019	0.077
H6B	0.507	0.66	4.51	0.045	0.61	0.052	0.277
H8A	0.613	1.02	5.53	0.040	1.08	0.057	0.086
MN54 - Beam 1	0.335	1.48	3.35	0.019	1.39	0.030	0.040
MN54 - Beam 2	0.315	1.22	5.13	0.020	1.22	0.020	0.020
MN54 - Beam 3	0.295	1.21	4.04	0.021	1.19	0.024	0.026
MN54 - Beam 4	0.295	1.28	3.64	0.011	1.23	0.020	0.020
MN63 - Beam 1	0.728	1.05	4.90	0.032	1.05	0.032	0.099
MN63 - Beam 2	0.638	0.95	3.68	0.025	0.97	0.056	0.147
MN63 - Beam 3	0.768	1.17	3.70	0.041	1.20	0.073	0.076
MN63 - Beam 4	0.591	0.85	4.30	0.009	0.87	0.026	0.188
MN45 - Beam 1	1.063	1.34	4.23	0.016	1.37	0.050	0.092
MN45 - Beam 2	0.945	1.22	3.88	0.038	1.26	0.073	0.074
MN45 - Beam 3	0.827	1.44	2.23	0.077	1.06	0.042	0.109
MN45 - Beam 1	1.024	1.41	3.14	0.136	1.48	0.072	0.142
MN45 - Beam 2	0.827	1.18	4.32	0.048	1.20	0.057	0.061
MN45 - Beam 3	0.709	1.00	4.62	0.052	1.01	0.053	0.130
W45 - 6	0.500	3.83	8.23	0.000	1.77	0.092	0.141
W45 - 7	0.323	2.44	8.19	0.000	1.15	0.058	0.061
W45 - 8	0.458	3.59	8.28	0.000	1.61	0.087	0.115
Average	**0.55**	**1.45**	**4.92**	**0.03**	**1.24**	**0.05**	**0.09**

The average measured camber change at peak was 0.55 in.

The parameters A_1 and t_0 were varied to optimize the fit between the predicted and measured values. The Solver function in Excel was again used to optimize the model. The optimum fit was obtained with A_1 = 1.45 and t_0 = 4.92. However, in order to make the model as simple as possible, t_0 was rounded to 5.0. Figure 6-12 shows the optimized t_0 for all girders.

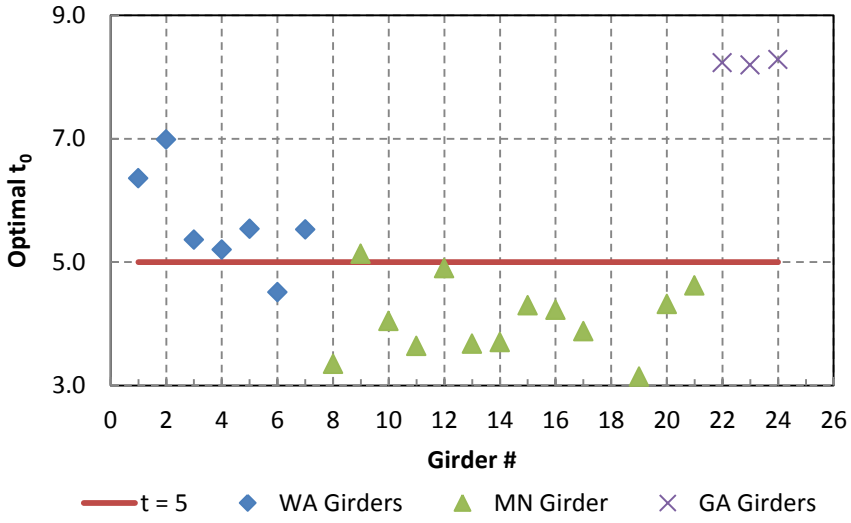

Figure 6-12. Optimized values of t_0 for all girders.

Figure 6-12 shows that with the use of the Peak Temperature Model, the maximum thermal cambers of Washington girders occurred around 6pm. The Minnesota girders had maximum of thermal camber at about 4pm. The Georgia girders had maximum thermal cambers at 8pm that is unlikely to be true because the air temperature cannot be maximum at 8pm. For the Washington and Minnesota girders, the values of t_0 reflect the expected field behavior, for which air temperature reached their maximum values from about 3pm to 5pm in the summer and it took a little time for the sun to transfer heat into girders.

The Solver function was again used to minimize the errors by adjusting A1 while t_0 was held constant at 5.0. The value of $A_1 = 1.24$ was found. Figure 6-13 depicts the optimized values of A_1 for the 24 girders, with $t_0 = 5$ for all case.

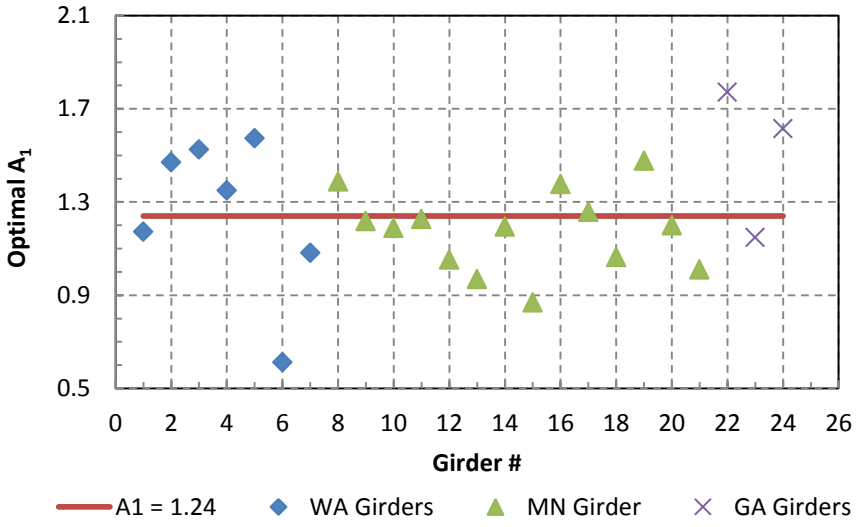

Figure 6-13. Optimized values of A_1 for all girders, using t_0 = 5am

The last step was calculate the thermal camber change with A_1 = 1.24 and t_0 = 5 and then compare to measured values. Table 6-4 gave an average error of 0.09 in. using the Peak Temperature Model with A_1 = 1.24 and t_0 = 5.

Figure 6-14, 6-15 and 6-16 compare the measured and the calculated thermal camber changes using the Peak Temperature Model with A_1 = 1.24 and t_0 = 5 for the Washington, Minnesota and Georgia girders, respectively. As shown in Figure 6-14, the biggest error occurred in Girder H6B of Washington State with an error of 0.28 in.. It is believed that the exposure of the left side of Girder H6B created a lower value of thermal camber for this girder than the ones of normally shaded girders. Neither the Temperature History Model nor Peak Temperature Model considered this factor in their calculations, which led to large errors.

The Peak Temperature Model works well for Minnesota girders when shapes of measurement and calculation curves were similar and the average error was just about 0.08 in..

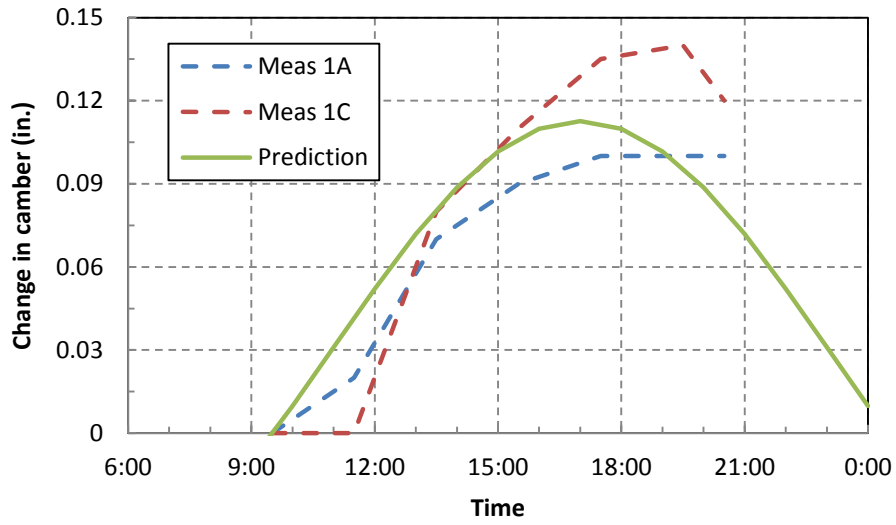

a) Girder 1"X"

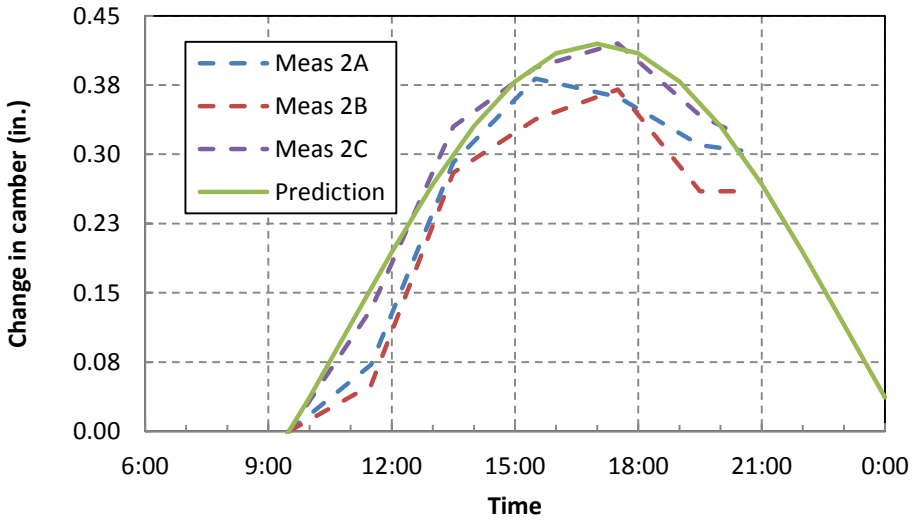

b) Girder 2"X"

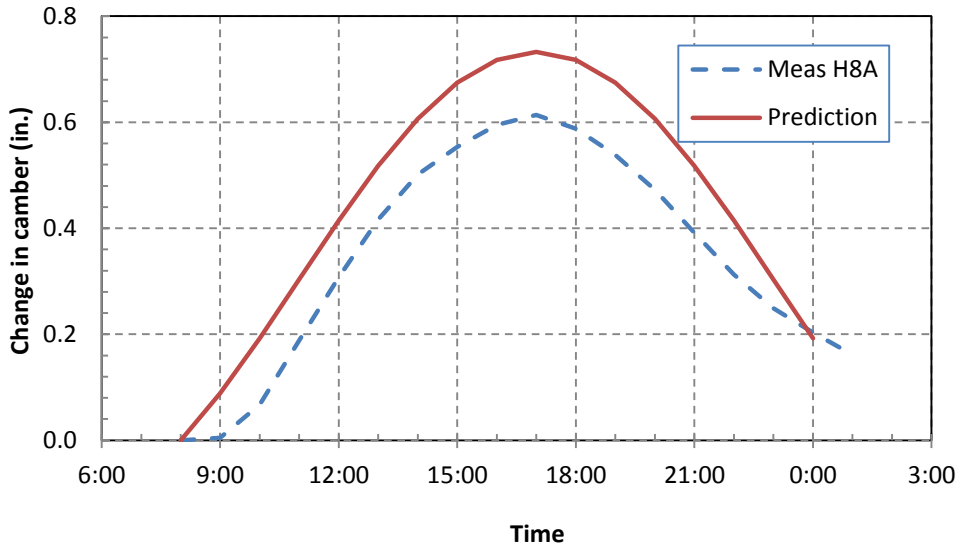

c) Girder H8A

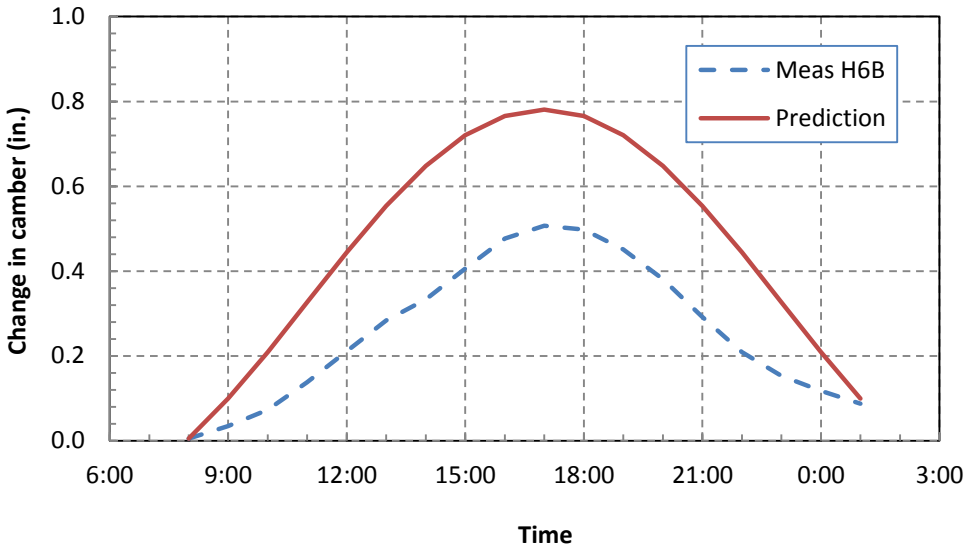

d) Girder H6B

Figure 6-14. Comparison between Measured and Calculated Thermal Camber Changes – WA Girders

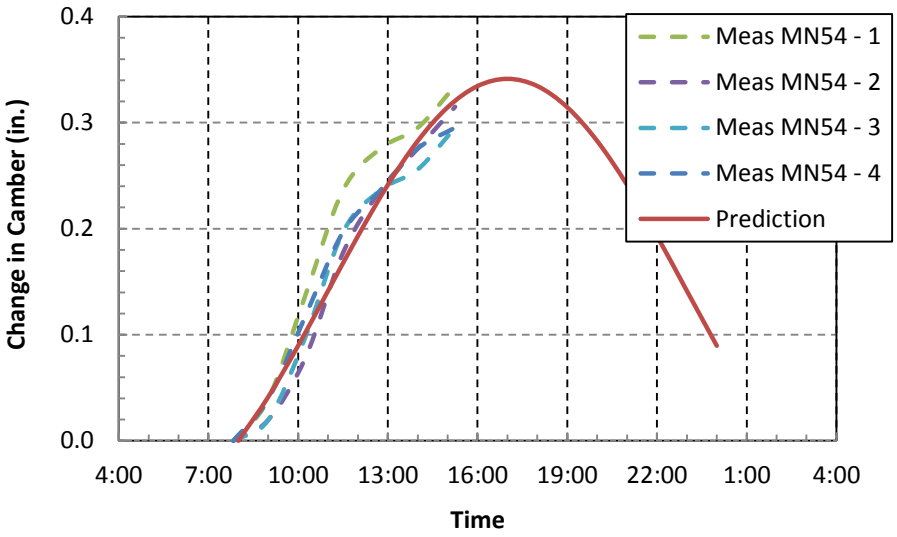

a) Girder MN54

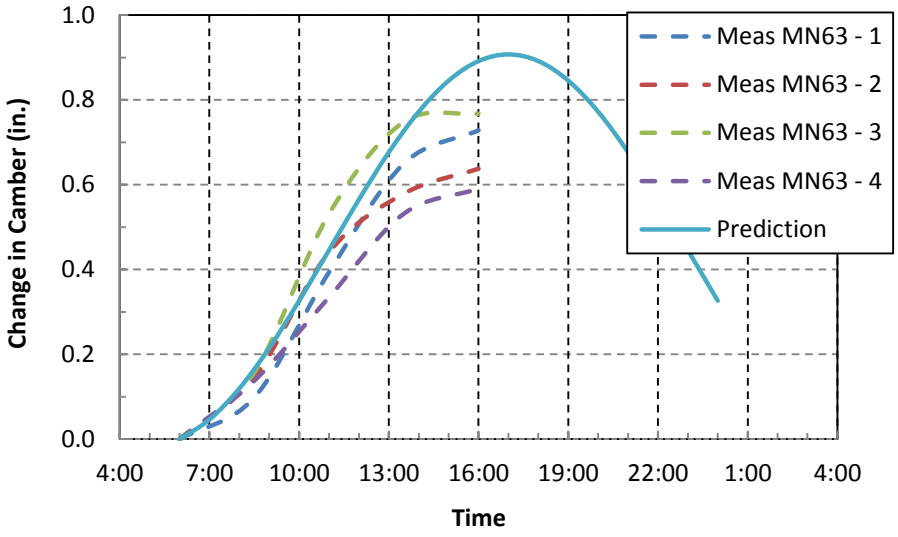

b) Girder MN63

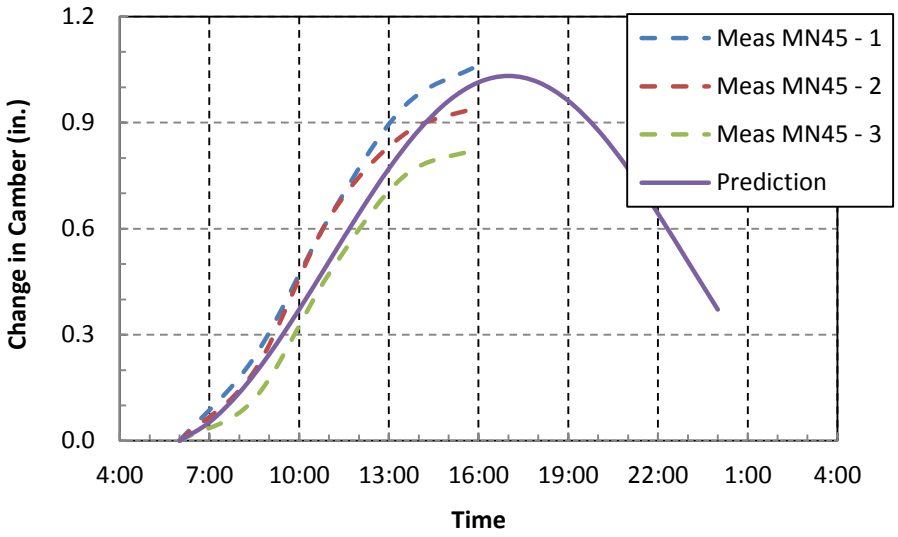

c) Girder MN45 (Measured on 05/17/2011)

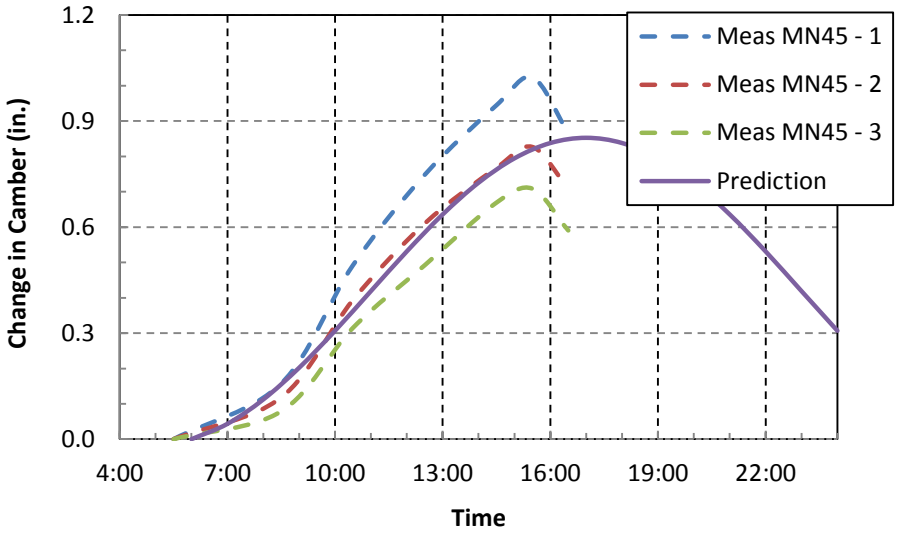

d) Girder MN45 (Measured on 06/30/2011)

Figure 6-15. Comparison between Measured and Calculated Thermal Camber Changes – MN Girders

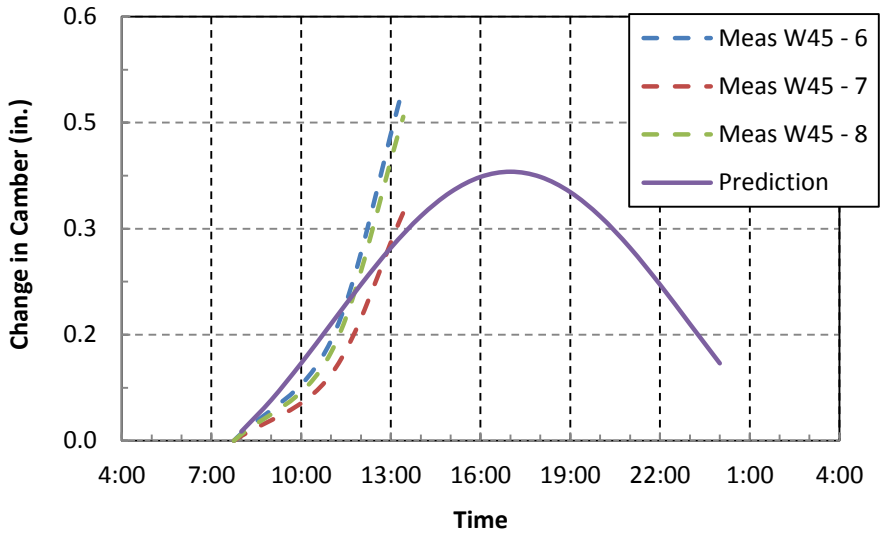

Figure 6-16. Comparison between Measured and Calculated Thermal Camber Changes – GA Girders

Figure 6-16 compares the measurements and calculations for the Georgia girders. As same with the Temperature History Model, the shapes of measured and predicted curves were different.

6.4 Summary

The Temperature History Model and Peak Temperature Model provide simple ways to estimate the camber change due to daily variations in temperature. They require knowledge of air temperature during a 24-hour period, which are typically available from meteorological records.

The governing equation of the Temperature History Model is:

$$\phi(t) = A_0 \frac{\alpha}{H} (T(t) - T_{min}) \qquad (6-19)$$

The governing equation for the Peak Temperature Model is:

$$\phi(t) = A_1 \frac{\alpha}{H} \frac{(T_{max} - T_{min})\left(1 - \cos\left(\frac{(t-t_0)}{24} 2\pi\right)\right)}{2} \qquad (6-20)$$

For a simply supported girder, the predicted camber history is:

$$\Delta\,(t) = \phi(t) * \frac{L^2}{8}$$

In these equations, the coefficient of thermal expansion is taken as 6.5*10-6 in./in./deg. F. For Washington State and Minnesota State Girders, A_0 = 1.25, A_1 = 1.24 and t_0 = 5 were recommended to apply.

The Temperature History Model had an average error over time of 0.08 in. whereas this number in the Peak Temperature Model was 0.09 in. Both models offered good predictions on thermal camber under daily temperature. Therefore, both two models are recommended for practical uses.

Neither model works as well for the Georgia girders, which were located in a different state than the Washington girders and Minnesota girders. The geographic difference may have led to differences in temperature, humidity or solar radiation, any of which could affect the girder camber. The other possible reason for the discrepancy was that the available data was not enough to calibrate the models for Georgia girders. The two models also did not work well for Washington State Girder H6B, which had one side exposed to sunlight. In such cases, a more sophisticated model, with more detailed thermal input data, would be needed for successful prediction of thermal camber.

7 EFFECT OF CURING TEMPERATURE ON RELEASE CAMBER

In the current AASHTO Specification (AASHTO 2012), the release camber is estimated as the sum of the deflections due to self-weight and prestress at release. This approach seems reasonable, because the girders are assumed to be linearly elastic and uncracked at release, and because creep and shrinkage are assumed to be negligible at this time. However, during curing, fabricators usually heat the concrete to reduce the total time needed to achieve the desired release strength. This method affects the concrete properties and camber at release. High curing temperatures leads to prestressing loss and a resulting change in camber. Moreover, the curing process can create a significant gradient over height of the girder, causing another change in camber. This effect is neglected in current calculations.

Culen at el. (2011) reported that for 1076 girders in Minnesota, at release, the average measured camber was only approximately 74% of the predicted value (using the MnDOT (2012) Specifications). The UW researchers used the actual concrete strength and followed the AASHTO 2005 models for creep, shrinkage, and the AASHTO 2005 refined method for prestress loss to predict release cambers and observed an average error of 0.82 in. (23% of the average measured camber) between predicted and measured cambers at release of nine girders in Alaska Way Viaduct (as shown in Chapter 3). This chapter addresses the effect of temperature due to curing on the change in camber at release by monitoring internal temperature of three girders cast by CTC on different days.

7.1 Internal Temperature Measurements

To investigate the effect of curing heat on release camber, UW researchers monitored internal temperature and camber of two WF74 and one WF83 girders from Concrete Technology Corporation (CTC). One of them (Girder WF74_2) was cured over a weekend and the other two girders were cured during weekdays. In additionally, data of temperature and camber from three other W74G girders from Barr et al. (2000) were used. Those girders were cast at Central Premix Corporation (CPM). Table 7-1 presents some of the key girder properties.

Table 7-1. Girder Properties

Mark Number	Cast Date	Destressing Date	Depth (in.)	Length (ft.)	Fabricator
WF74_1	12/11/2012	12/12/2012	74	147.50	CTC
WF74_2	12/14/2012	12/17/2012	74	147.50	CTC
WF83	2/14/2013	2/15/2013	83	161.75	CTC
2A	3/6/1997	3/7/1997	74	137.00	CPM
2B	3/10/1997	3/11/1997	74	137.00	CPM
2C	3/12/1997	3/13/1997	74	137.00	CPM

The data logger used to measure internal temperature of girders in the service condition (Chapter 6) was also used to monitor internal temperature during fabrication for the three CTC girders. As mentioned in Chapter 6, the number of channels in the data logger was limited to a maximum of 16; therefore only 16 thermocouples were installed in each of the three girders before casting. The locations of the thermocouples in the top and bottom flanges are the same for all three girders. This was possible because all girders in the WF series have the same flange dimensions. Because Girder WF83 had a taller web, the spacing of the thermocouples in its web were larger than in Girder WF74_1 and Girder WF74_2. The locations of the sensors are presented in Figure 7-1. Although 16 thermocouples were embedded to Girder WF83, two of them (TC3 and LW) were damaged during casting. Therefore, only 14 histories were recorded for Girder WF83.

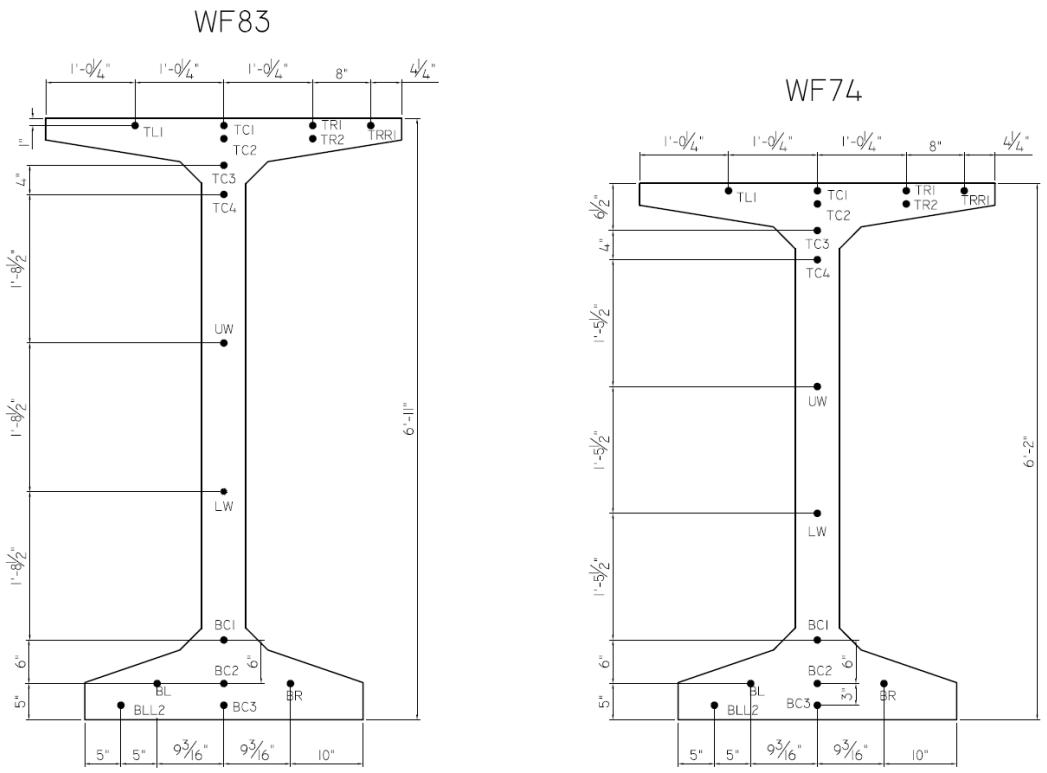

Figure 7-1. Layout of Thermocouples

The readings were taken continuously at 1-minute intervals from casting to destressing. After that, the girders were lifted out of the form and transported to a storage location. During transportation, the data logger was turned off to avoid damage, but it was reconnected within an hour of destressing after the girders were placed in the storage yard.

The recorded internal temperature data were used to predict changes in strand stress and camber due to high fabrication temperatures.

Figure 7-2 shows the temperature histories recorded for each thermocouple embedded 18ft east of mid-span (to avoid the vertical joint in the form) for three CTC girders.

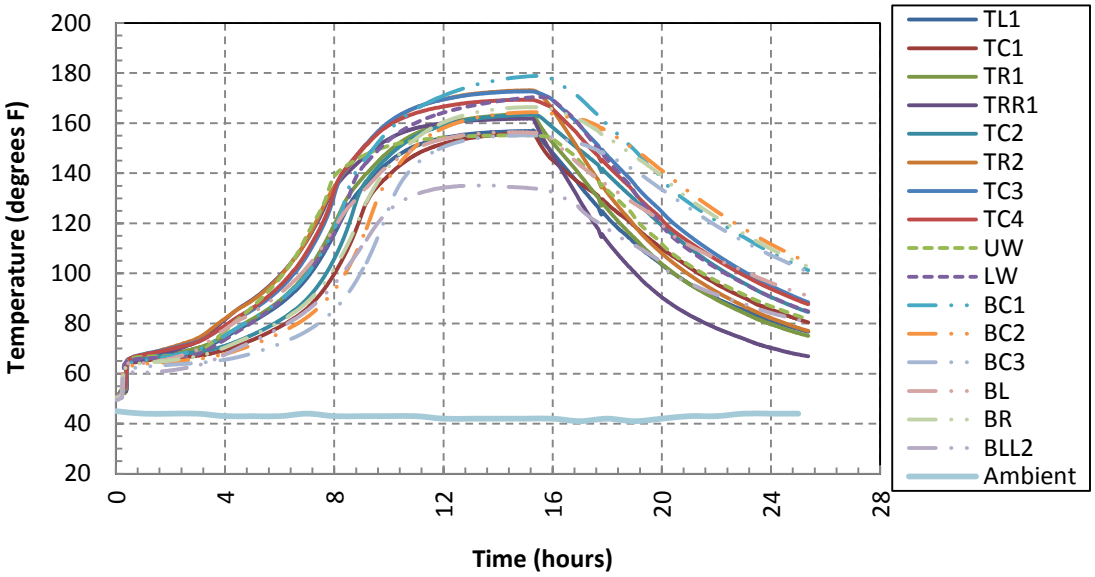

a) Girder WF74_1

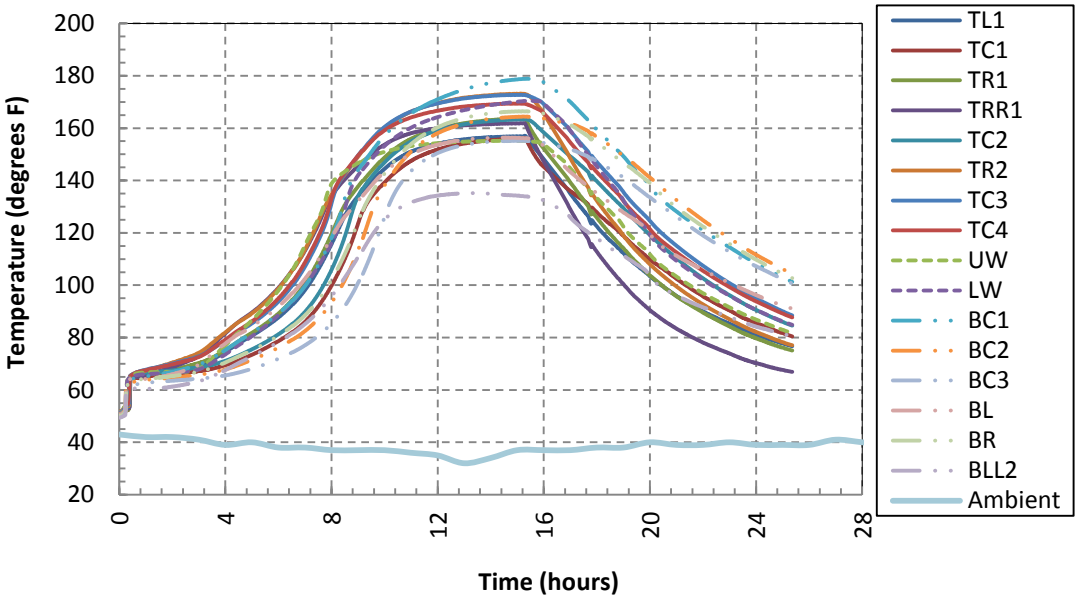

b) Girder WF74_2

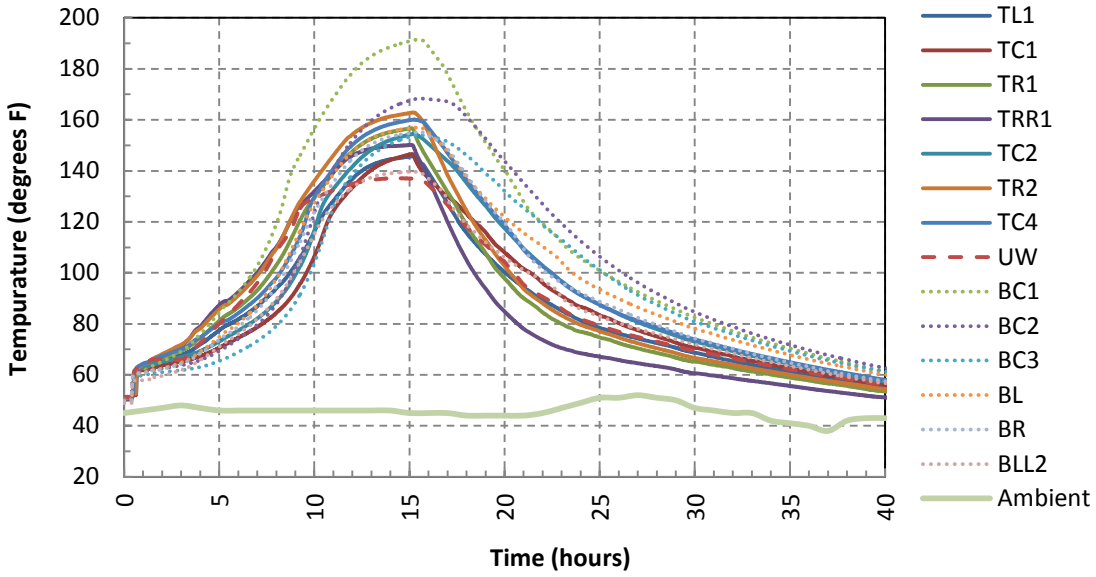

c) Girder WF83

Figure 7-2. Internal Temperature Histories during Curing – CTC Girders

The temperature data shown in Figure 7-2 follow expected trends. As shown in the figure, all the thermocouples measured the same ambient temperature before casting. After that, the temperature inside the forms jumped upward from the ambient temperature to the concrete temperature. Heat from the hydration of the cement and from the external heating source caused the concrete temperature to increase until the curing system deactivated and the blanket and form were removed, at which time the girders started to cool rapidly. The concrete temperature reached its peak around 15 hours after casting in all the temperature histories, including the Girder WF74_2 which was cast on Friday and followed a different thermal profile during curing.

The strands were assumed to be bonded to the concrete between 6 and 10 hours after casting. This assumption is consistent with the assumptions made by Barr at el. (2005). Figure 7-3 shows the vertical temperature profiles of the three girders at 6 hours, 10 hours form casting, at release and at 9 hours after release for the three CTC girders. For each level that had more than one record (more than one thermocouple), the shown value was an average.

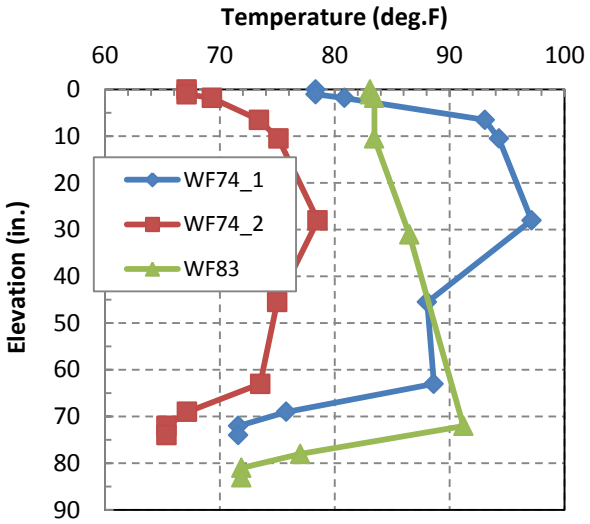

a) 6 hours from casting

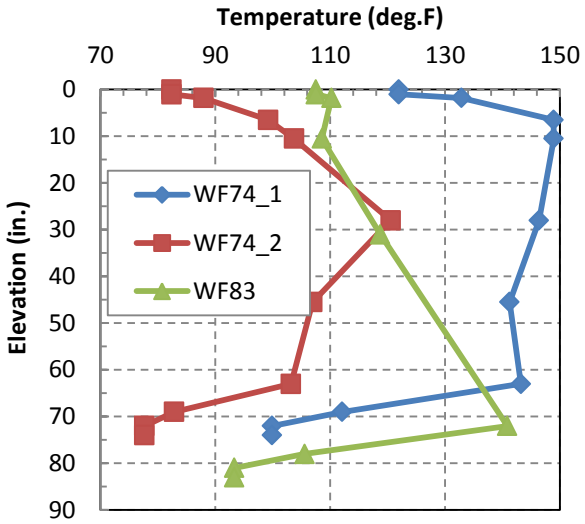

b) 10 hours from casting

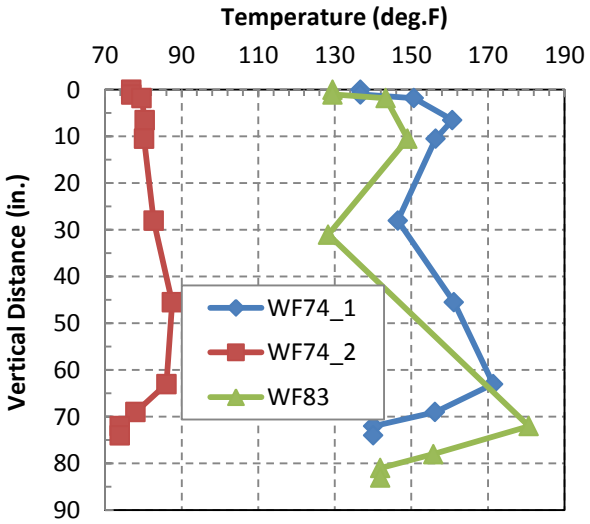

c) Release

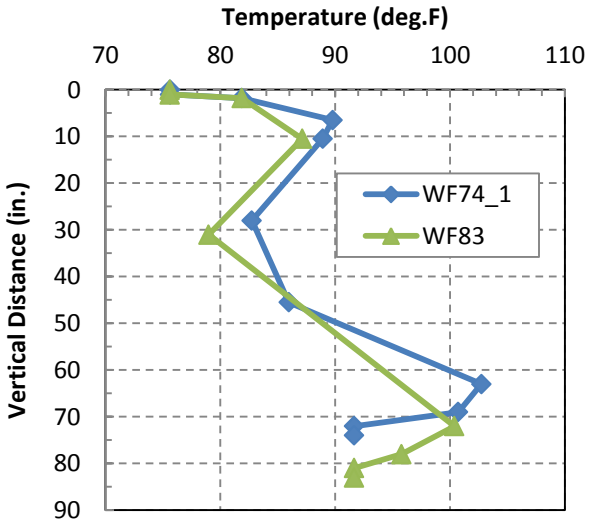

d) 9 hours after release

Figure 7-3. Vertical Temperature Distributions

During curing, gage BC1 of Girder WF83 shown in Figure 7-3(a) and 7-3(b) recorded the highest temperature. This was different to the other girders in which some locations near the top showed the highest temperature at those times. There are two potential causes for this difference. One was that gage BC1 was located within the biggest mass of concrete in the girder, so

hydration of cement could make it very hot during curing. The other possibility is that gage BC1 of Girder WF83 could have been near the heating unit of the form so it might have made the BC1 location hotter than it would been otherwise. The latter possibility is probably more likely since the first case was not shown in the other girders even they have the same geometrical dimension of the bottom flange.

In almost all cases shown in Figure 7-3(a) and 7-3(b), the temperature was lowest at the bottom of the girders, which means that in all three girders the camber was expected to decrease as the concrete cooled to a more uniform temperature.

Figures 7-3(c) and 7-3(d) indicated that at times of release and 9 hours later, the bottom of the girders was hotter than the top. That trend was expected. After removing the form, the concrete was exposed to the ambient temperatures and lost heat. The top regions of the girders, which contained less concrete mass and had more contact with ambient conditions, were expected to lose heat more quickly than the bottom regions.

The locations of the thermal sensors used by Barr et al. (2000) to record internal temperature histories for the three girders cast by CPM are shown in Figure 7-4. Those sensors were thermistors, rather than thermocouples, and were built integrally into vibrating wire strain gages. However, their function, namely to record temperature, was the same. Figure 7-5 shows the variations of concrete temperature with time for the girders. Figure 7-5 illustrated that for Barr's girders, during the curing period, the top of all the girders was consistently hotter than the bottom.

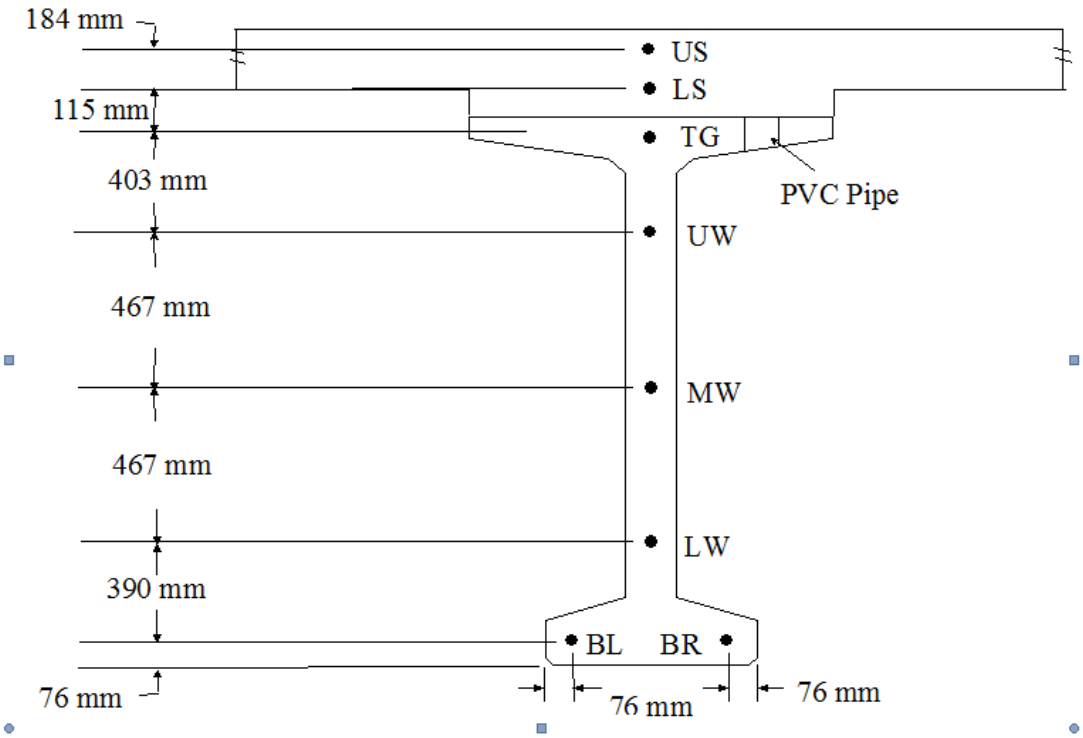

Figure 7-4. Locations of Instrumentation

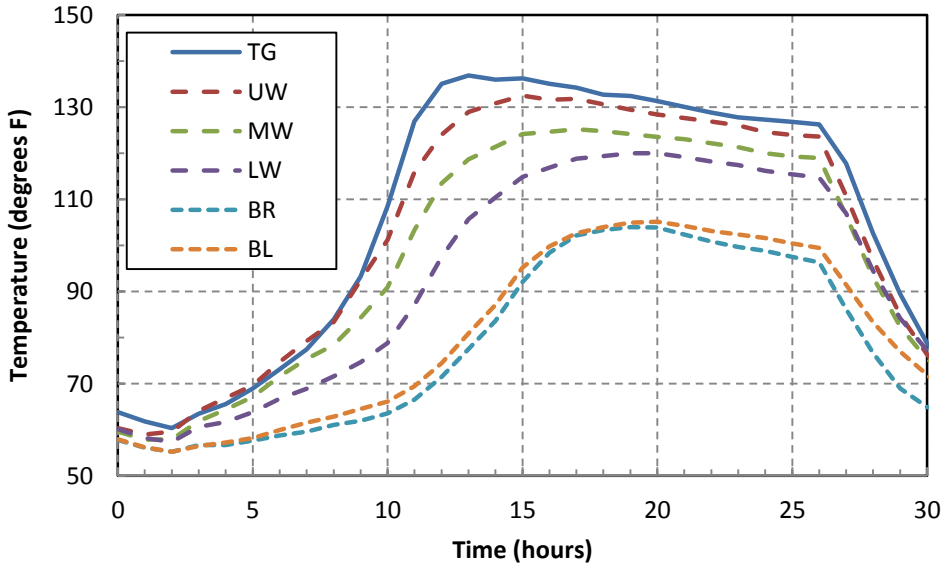

a) Girder 2A

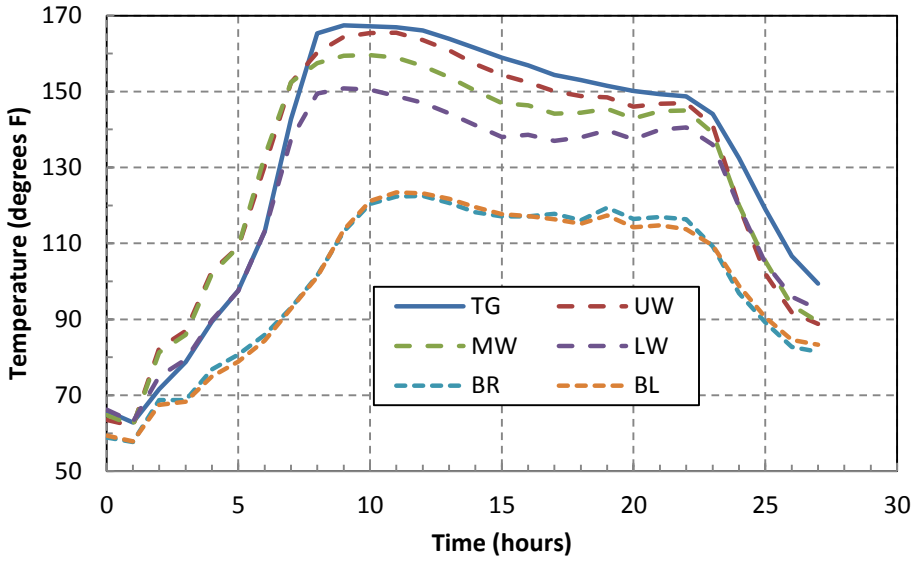

b) Girder 2B

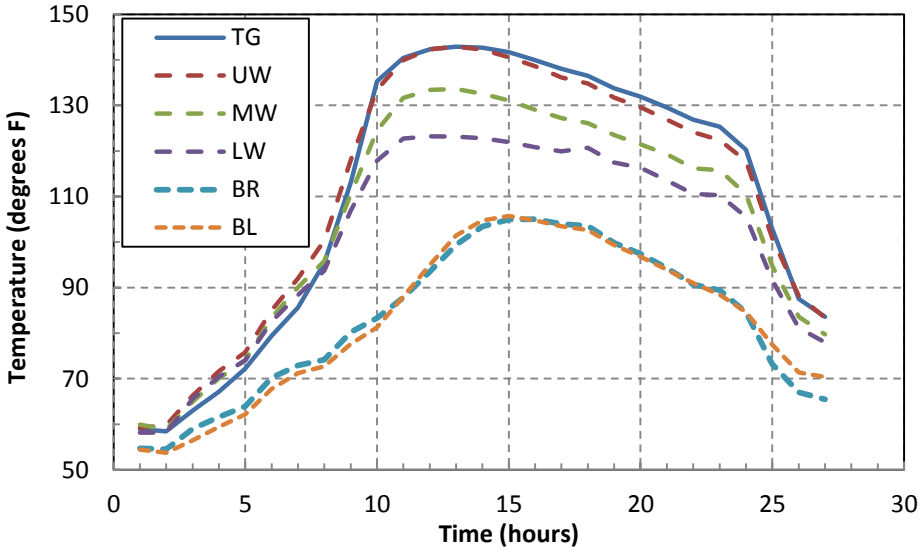

c) Girder 2C

Figure 7-5. Concrete Temperature Histories during Curing – CPM Girders

7.2 Response to Temperature Variations

Barr et al. (2005) showed that high curing temperatures could affect prestress forces and cambers in at least three ways. The first way is by heating the prestressing strands. The strands

are stressed at ambient temperature but gradually they are heated by the surrounding concrete. This leads to a loss of prestress Δf_{P1}, and resulting change in camber, δ_1.

Second, if the coefficient of thermal expansion of the concrete is higher than that of prestressing steel, the stress in the prestressing steel decreases (Δf_{P2}), leading to a decrease of camber ($\delta 2$) as the beam cools. [More information on this effect can be found in Barr et al. (2005)]

Finally, if the girder undergoes a thermal gradient when the concrete hardens, values of prestressing and camber will change (Δf_{P3} and $\delta 3$). As showed in Barr et al. (2005), the difference between coefficients of thermal expansion for the concrete and steel had the smallest effect on camber. Therefore, this section will only discuss the effects of the first and the last factors on the changes in prestressing and camber. In this chapter, they will be named as Effect of Bonding Strands and Effect of Temperature Gradient, respectively.

7.2.1 Effect of Heating Strand before It Bonds to Concrete

If there is any difference between the temperature at the stressing time and the bonding time, the stress in strands will change. In general, strands are stressed at ambient temperature. However, after 6 hours or 10 hours from casting, which was considered as the bonding time of the concrete, the concrete temperature increases as the result of curing heat and cement hydration. The temperature of the strands increased, but they could not expand because they were fixed at two ends. So the strands lost stress. The prestress loss Δf_{P1} was estimated by Barr at el. (2005) as follows:

$$\Delta f_{p1} = -\frac{\alpha_p E_p}{L_{bed}}\{(T_{out} - T_j)L_{out} - (T_{in} - T_j)L_{in} - (T_g - T_j)L_g\} \qquad (7-1)$$

where:

α_p = coefficient of thermal expansion of prestressing strand,

E_p = elastic modulus of prestressing strand,

L_{bed} = length of strand between the abutments,

L_{out}, T_{out} = length and temperature of strand outside the blanket,

L_{in}, T_{in} = length and temperature of strand inside the blanket,

L_g, T_g = length and temperature of strand through the girder.

The variables used here were necessary because some of the girders were cast in a long bed out of doors, during winter. Heating was conducted by placing a thermal blanket over the forms and injecting steam under it. However, the blanket was longer than the form. Thus three regions were considered. Outside the blanket, the strand remained cold, at the ambient temperature. Inside the end of the blanket, but outside the form, the bare strand was heated by the steam. Inside the form (and under the blanket) the concrete and strand were both heated by the steam and the hydration reaction. For girders cast indoors, with heated forms rather than a heating blanket, L_{out} is 0.0.

The resulting camber change due to prestressing loss can be calculated as:

$$\Delta\delta = -\frac{\Delta f_p A_p L_g^2}{8E_{ci}I}\left[e_{mid} + (e_{end} - e_{mid})\frac{4a^2}{3L_g^2}\right] \qquad (7-2)$$

here:

$\Delta\delta$ = change in midspan camber due to thermal stress loss, Δf_p,

E_{ci} = concrete elastic modulus at release,

I = moment of inertia of beam,

A_p = cross-sectional area of prestressing strand,

e_{mid}, e_{end} = eccentricities of prestressing strand at midspan and end of the girder,

a = distance from the harped point to the end of the girder.

Table 7-2 shows some key characteristics of the strands to calculate prestressing loss and camber changes due to thermal change.

Table 7-2. Strand Configurations

Girder	L_{bed} (ft.)	L_g (ft.)	L_{out} (ft.)	T_j (^{0}F)	A_p (in.^{2})	e_{mid} (in.)	e_{end} (in.)	a (in.)
WF74_1	395	147.5	247.5	44	12.80	31.82	15.18	708.0
WF74_2	395	147.5	247.5	40	12.80	31.82	15.18	708.0
WF83	395	161.75	233.3	43	12.59	31.13	16.76	799.5
2A	200	137	63	39	8.68	34.82	20.46	657.6
2B	200	137	63	46	8.68	34.82	20.46	657.6
2C	200	137	63	40	8.68	34.82	20.46	657.6

The estimated prestressing losses and changes in camber due to heating the strand before it bonded to the concrete were calculated using equations 7-1 and 7-2, with parameters shown in Table 7-2. The resulting changes are plotted in Figure 7-6 and 7-7 as a function of the assumed bonding/hardening time. The ambient temperature during curing, T_{out}, was taken from a meteorological website for the specific location (Spokane).

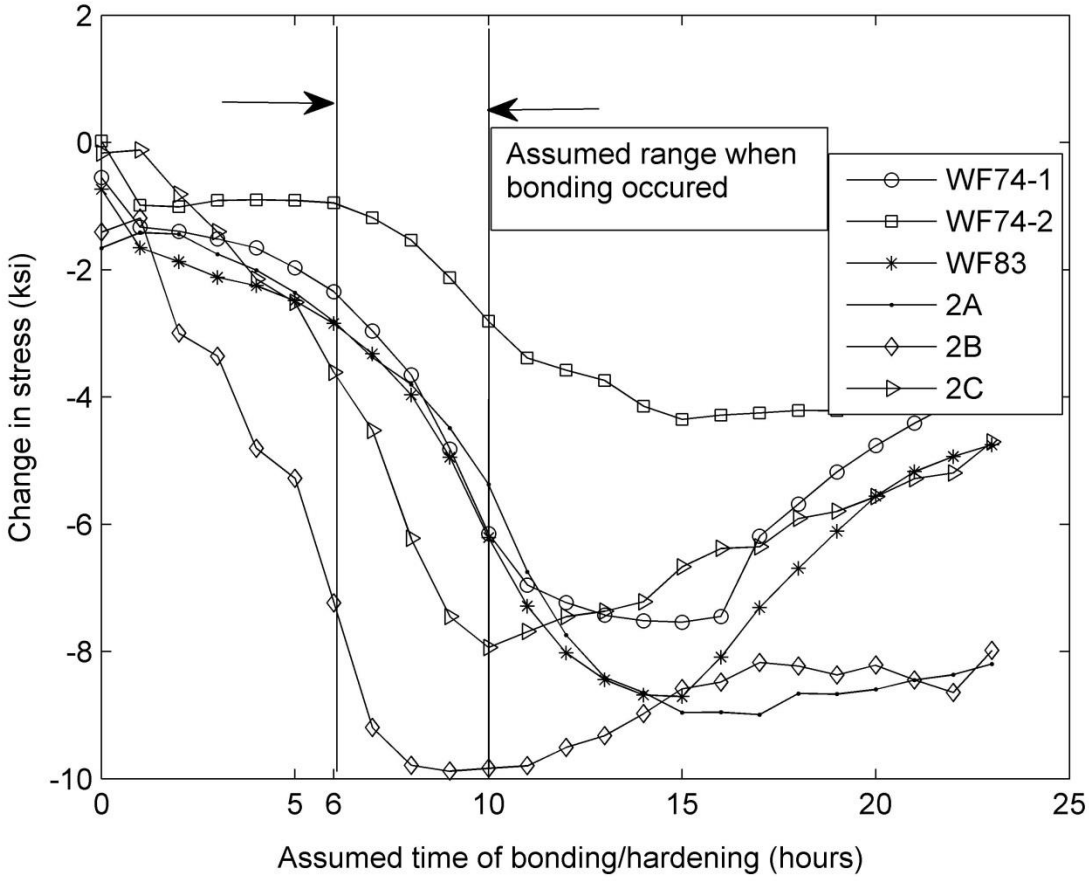

Figure 7-6. Prestressing Loss Caused by Curing Temperature

As expected, because the curing temperature in the girders at the bonding time (6 hours to 10 hours from casting) was higher than the ambient temperature at stressing time, the strands lost stress. The magnitude of this loss is fixed and unrecoverable as soon as the strand bonds to the concrete. Figure 7-6 shows that if the bonding occurred between 6 to 10 hours from casting, the predicted change in stress varied from -1 ksi (Girder WF74_2) to about -10 ksi (Girder 2B). The difference is caused by the fact that Girder WF74_2 was cast on Friday and cured during the

weekend using a different curing schedule. For it, less heat was applied, which leads to concrete temperatures cooler than those in the weekday girders. For the weekday girders, the average stress change was about -2.7 ksi if bonding occurred 6 hours after casting and about -6.5 ksi if bonding occurred 10 hours after casting. The negative sign indicates a loss in prestress.

The camber change associated with this loss in prestress is calculated using Equation 7-2 and plotted in Figure 7-7.

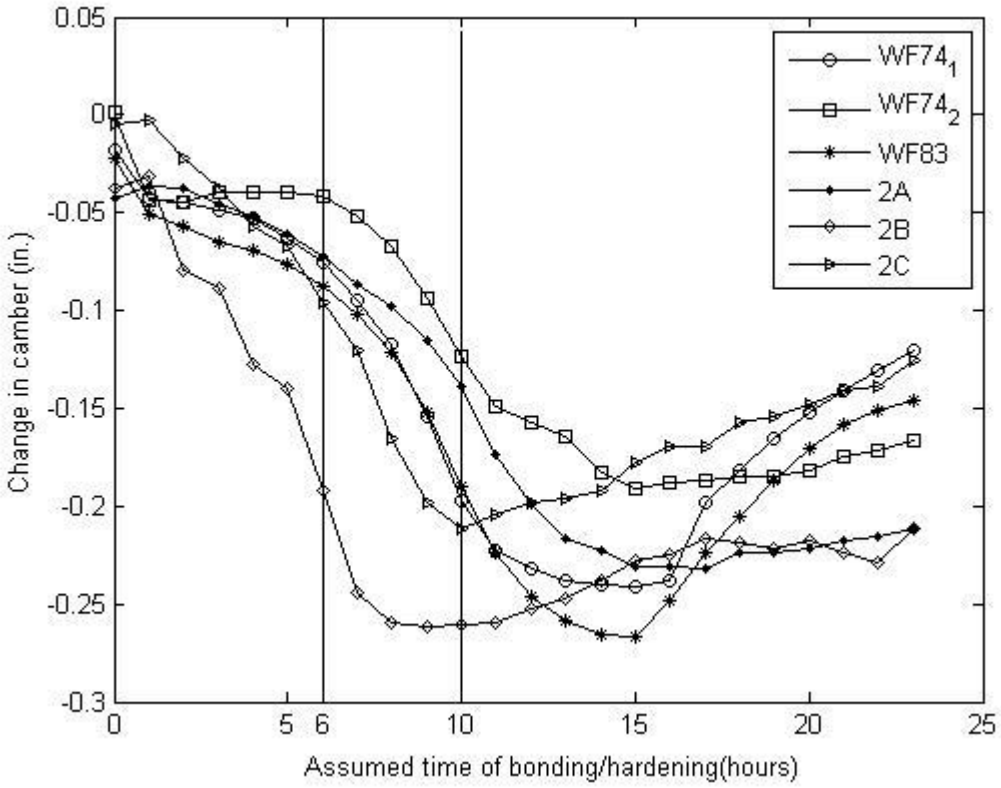

Figure 7-7. Camber Change Caused by Prestressing Loss

In Figure 7-7, it was observed that Girder WF74_2 and Girder 2B experienced less and more change, respectively, in strand stress and camber than the others did.

7.2.2 Effects of Temperature Gradient at Hardening of Concrete

If a thermal gradient is present when the concrete hardens, thermal and mechanical strains are introduced into the cross section. When the concrete eventually cools to a

uniform temperature, a change in temperature in temperature gradient will occur that is equal and opposite to the gradient induced when the concrete hardened (Barr et al. (2005)). For all monitored girders, the girders were hotter at the top when the concrete hardened as shown in the Figure 7-3 and 7-5. Therefore, cooling to uniform temperature decreased the upward camber. The changes in camber due to thermal gradient were estimated using Equations 6-3 to 6-6, and are shown in Figure 7-8.

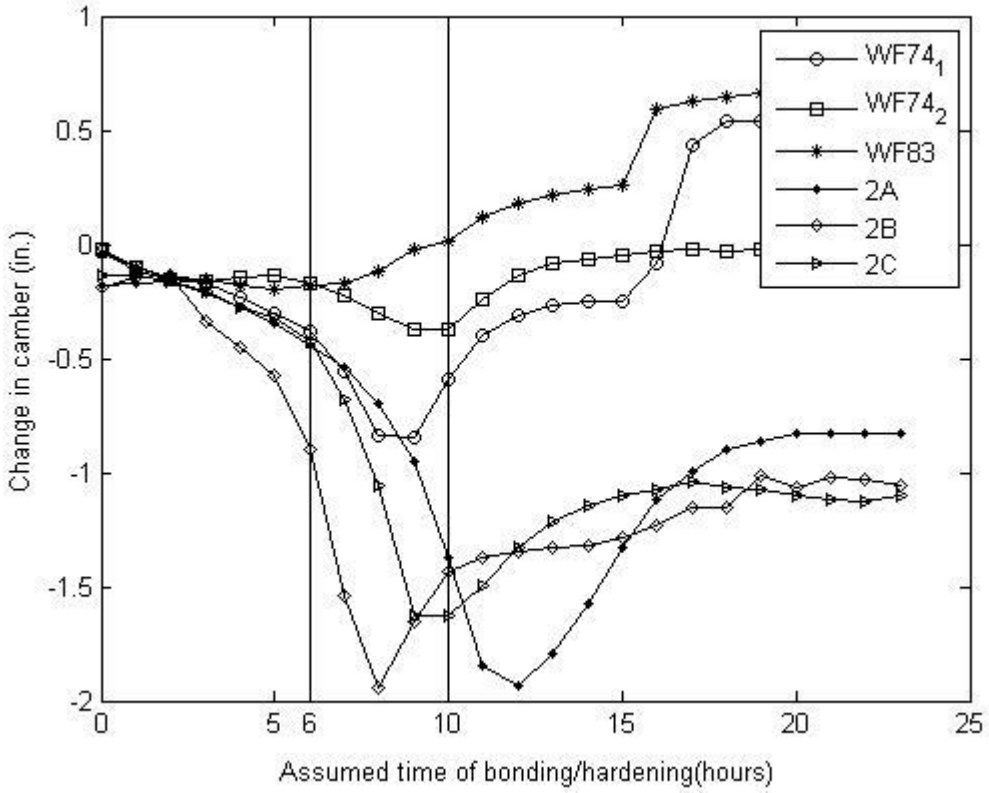

Figure 7-8. Camber Change Caused by Temperature Gradient

The camber changes in the CPM girders (2A, 2B and 2C) are much larger than those for the CTC girders (WF74_1, WF74_2, and WF83). This occurred because of the different curing procedures used at the two plants, and the fact that the CPM girders were cast out-of doors in winter using steam heat and a blanket, whereas the CTC girders were cast indoors using heated forms. The result was that the CPM girder experienced a much larger thermal gradient, with the

lowest temperatures at the bottom, at the assumed time of bonding. The largest camber decrease 1.97 in., occurred in Girder 2B.

Figure 7-9 shows the changes in stress due to temperature gradient for six investigated girders. These stress changes will occur at the time of release.

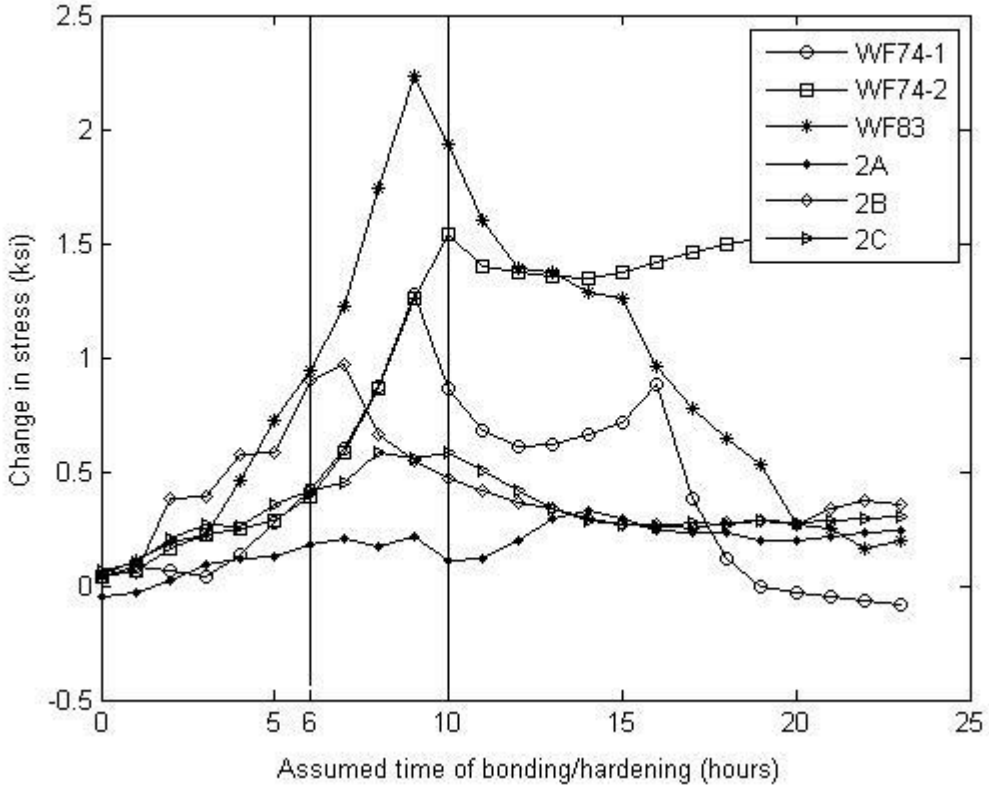

Figure 7-9. Prestressing Stress Change Caused by Temperature Gradient

7.2.3 Total Effect of High Fabrication Temperature

Figures 7-10 and 7-11 summarize the estimated prestressing losses and camber change, caused by the two thermal components caused by the high fabrication temperature.

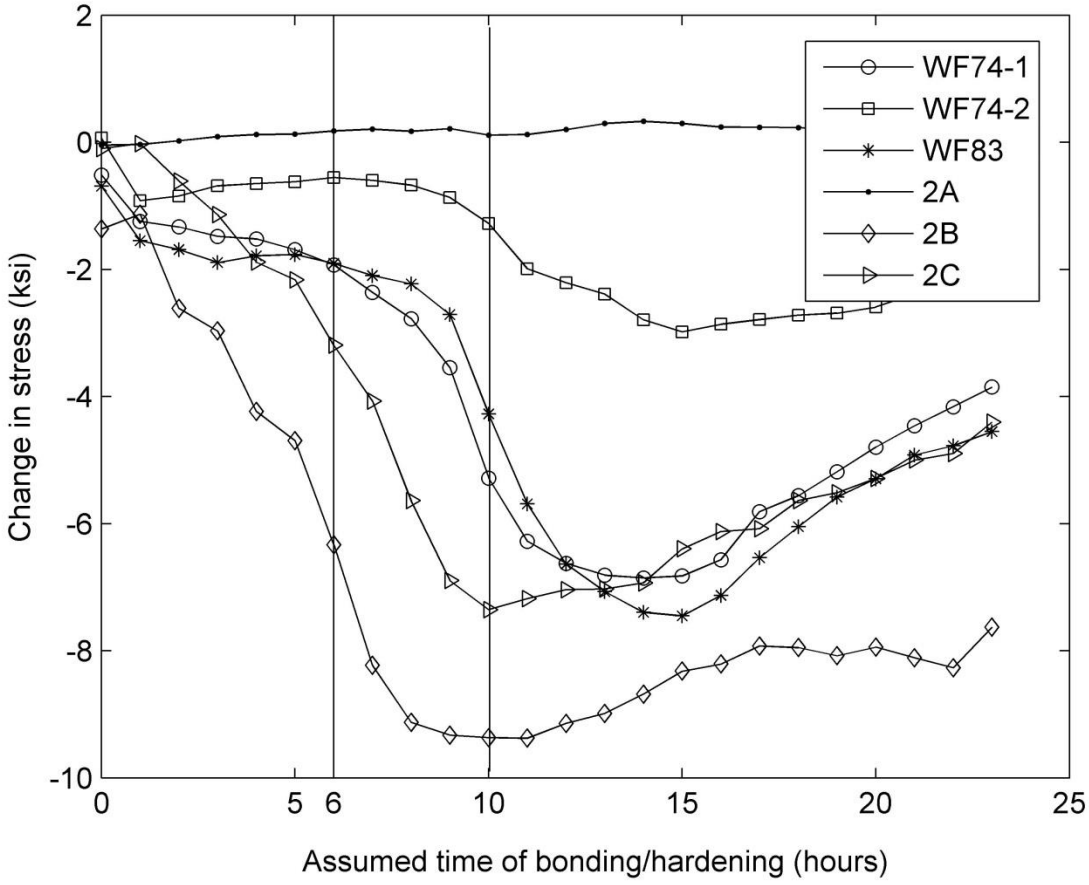

Figure 7-10. Total Change in Stress due to Curing Temperature

Girder 2B had the biggest change in both camber and strand stress. The combination of the effect of heating the strand before bonding and the effect of temperature gradient at hardening of concrete changed the upward camber by -1.70 in (63% of the calculated initial camber) and caused a stress loss of 9.4 ksi, if bonding occurred 10 hours after casting. This stress loss is about 4.5 times the one caused by relaxation, but it is not accounted for in the AASHTO Specifications, whereas the relaxation loss is.

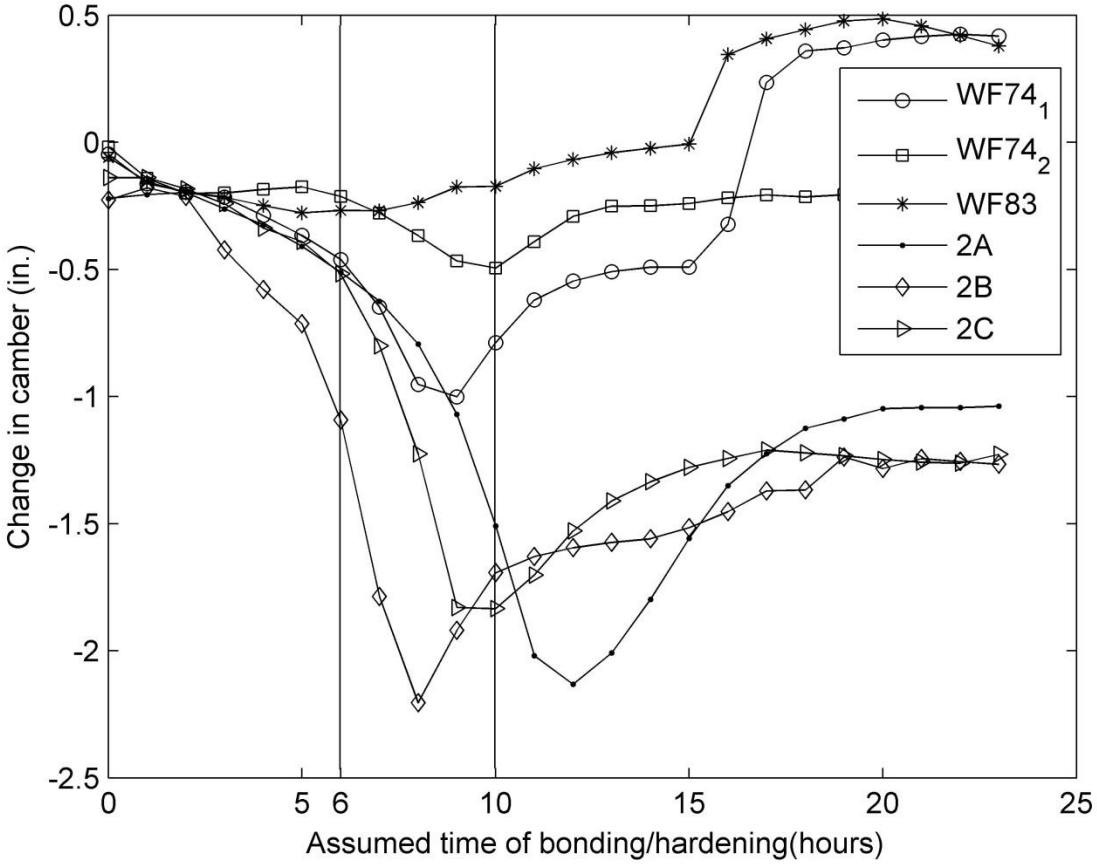

Figure 7-11. Total Change in Camber due to Curing Temperatures

The changes in stress and camber were about twice as large in the CPM girders as they were in the CTC girders. This was expected based on the different curing methods in the two fabrication plants, and the weather condition at the times of casting and curing. On average, if the bonding time is 10h, the CTC girders lost 3.61 ksi and their upward camber decreased by 0.58 in., whereas the two numbers for the CPM girders were 7.33 ksi and 1.10 in. Those lead to larger temperature gradients for the CPM girders than for the CTC girders.

Tables 7-3 and 7-4 combine the changes in stress in the strands from casting to releasing for the six girders investigated for bonding times of 6h and 10h. Table 7-3 and 7-4 split the effect of Temperature Gradient into two components: effect of temperature gradient from bonding to uniform, and then from uniform to release. The reason was that the temperature gradient at

bonding was used to calculate the camber change as the girder cools to a uniform temperature. However, the temperature in the girder at release was not uniform, but was hotter in the bottom and cooler in the top of the girder. This was opposite to the temperature gradient at bonding, when the girder was hotter in the top and cooler in the bottom of the girder. Therefore, the change in camber of the girder due to temperature gradient from bonding to release should be a combination of the changes in camber due to temperature gradient from bonding to the time of uniform temperature and the time of uniform temperature to release. Because the changes of strand stress due caused by temperature gradient is relatively small, the study considered only the amount of prestressing loss from bonding to uniform and ignored the loss from uniform to release.

Table 7-3. Calculated Changes in Stress in Strands (ksi) for Bonding Time of 6h

Girder	Effect of Heating Strands (ksi)	Effect of Temperature Gradient (ksi)		Total (ksi)
		From bonding to uniform (ksi)	From uniform to release	
WF74_1	-2.35	0.42	Ignore	-1.93
WF74_2	-0.95	0.39	Ignore	-0.55
WF83	-2.85	0.94	Ignore	-1.91
2A	-2.81	0.18	Ignore	-2.63
2B	-7.24	0.90	Ignore	-6.33
2C	-3.61	0.42	Ignore	-3.19
Average				**-2.76**

Table 7-4. Calculated Changes in Stress in Strands (ksi) for Bonding Time of 10h

Girder	Effect of Heating Strands (ksi)	Effect of Temperature Gradient		Total (ksi)
		From bonding to uniform (ksi)	From uniform to release	
WF74_1	-6.15	0.87	Ignore	-5.28
WF74_2	-2.81	1.54	Ignore	-1.28
WF83	-6.21	1.94	Ignore	-4.27
2A	-5.38	0.11	Ignore	-5.26
2B	-9.84	0.47	Ignore	-9.37
2C	-7.94	0.58	Ignore	-7.36
Average				**-5.47**

Similarly, Tables 7-5 and 7-6 combine the changes in camber from casting to release for bonding times of 6h and 10h.

Table 7-5. Calculated Changes in Camber (in.) for Bonding Time of 6h

Girder	Effect of Heating Strands (in.)	Effect of Temperature Gradient		Total (in.)
		From bonding to uniform (in.)	From uniform to release (in.)	
WF74_1	-0.08	-0.39	-0.25	-0.21
WF74_2	-0.04	-0.17	-0.06	-0.16
WF83	-0.09	-0.18	0.59	-0.86
2A	-0.07	-0.44	-0.49	-0.02
2B	-0.19	-0.90	-0.67	-0.43
2C	-0.10	-0.42	-0.57	0.05
Average				**-0.27**

Table 7-6. Calculated Changes in Camber (in.) for Bonding Time of 10h

Girder	Effect of Heating Strands	Effect of Temperature Gradient		Total (in.)
		From bonding to uniform	From uniform to release	
WF74_1	-0.20	-0.59	-0.25	-0.54
WF74_2	-0.12	-0.37	-0.06	-0.44
WF83	-0.19	0.02	0.59	-0.77
2A	-0.14	-1.37	-0.49	-1.02
2B	-0.26	-1.43	-0.67	-1.03
2C	-0.21	-1.62	-0.57	-1.26
Average				**-0.84**

7.2.4 Camber Comparison

The accuracy of these estimations can be evaluated by comparing the calculated cambers with and without thermal effect and measured cambers at release. All camber prediction used measured concrete strength and followed the AASHTO 2005 models for creep, shrinkage, and the AASHTO 2005 refined method for prestress loss. Assuming that the concrete started bonding to the strands at 6 hours from casting, Table 7-7 compares the measured camber at release with

calculated camber with and without thermal effects. Table 7-8 does the same things, but assumes that bonding occurs 10h from casting.

Table 7-7. Camber Comparison with Assuming Bonding at 6h after Casting

Girder	Comparison time	Calc. camber	Calc. camber with thermal	Meas. Camber	Calc without Thermal/ Meas	Calc with Thermal/ Meas
WF74_1	Release	3.02	2.81	2.63	**1.15**	**1.07**
	2h after release	3.25	2.25	3.00	**1.08**	**0.75**
	6 hours from release	3.26	2.24	2.94	**1.11**	**0.76**
	9 hours from release	3.27	2.27	3.00	**1.09**	**0.76**
WF74_2	Release	2.98	2.82	2.50	**1.19**	**1.13**
WF83	Release	2.90	2.04	2.50	**1.16**	**0.82**
	2h after release	2.89	1.99	2.78	**1.04**	**0.72**
	6 hours from release	2.83	1.90	2.80	**1.01**	**0.68**
	9 hours from release	2.83	1.92	3.06	**0.92**	**0.63**
2A	Release	3.38	3.36	2.50	**1.35**	**1.34**
2B	Release	3.45	3.02	2.57	**1.34**	**1.18**
2C	Release	3.46	3.51	2.60	**1.33**	**1.35**

Table 7-8. Camber Comparison with Assuming Bonding at 10h after Casting

Girder	Comparison time	Calc. camber	Calc. camber with thermal	Meas. Camber	Calc without Thermal/ Meas	Calc with Thermal/ Meas
WF74_1	Release	3.02	2.48	2.63	**1.15**	**0.94**
	2h after release	3.25	1.92	3.00	**1.08**	**0.64**
	6 hours from release	3.26	1.93	2.94	**1.11**	**0.66**
	9 hours from release	3.27	1.94	3.00	**1.09**	**0.65**
WF74_2	Release	2.98	2.54	2.50	**1.19**	**1.02**
WF83	Release	2.90	2.13	2.50	**1.16**	**0.85**
	2h after release	2.89	2.09	2.78	**1.04**	**0.75**
	6 hours from release	2.83	1.99	2.80	**1.01**	**0.71**
	9 hours from release	2.83	2.01	3.06	**0.92**	**0.66**
2A	Release	3.38	2.36	2.50	**1.35**	**0.94**
2B	Release	3.45	2.42	2.57	**1.34**	**0.94**
2C	Release	3.46	2.20	2.60	**1.33**	**0.85**

Figures 7-12 and 7-13 plot the ratio between calculated cambers and measured cambers vs time. While Figure 7-12 shows the ratios at release for all investigated girders, Figure 7-13 presents the ratios of calculated camber and measured camber with and without thermal effect for Girder WF74_1 and Girder WF83 at several times after release. All calculations used the actual concrete strength and the AASHTO 2005 models for creep, shrinkage, and the AASHTO 2005 refined method for prestress loss.

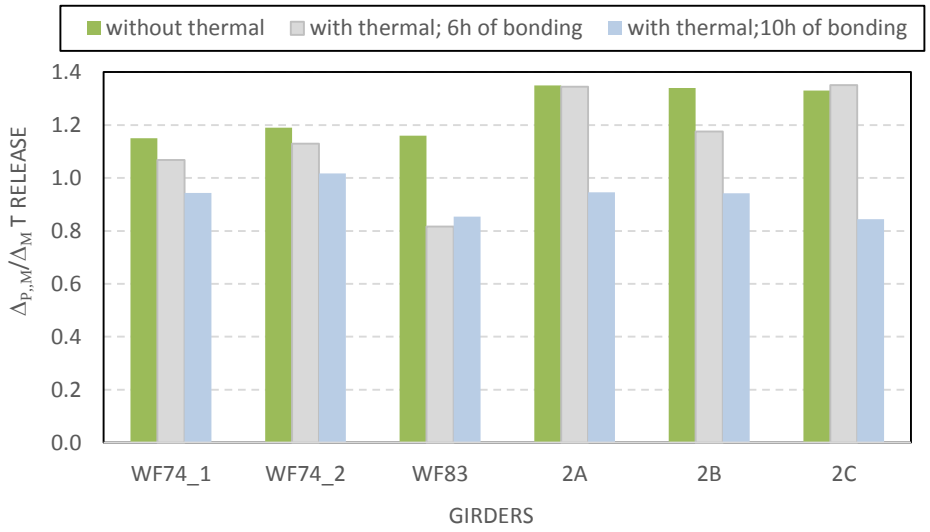

Figure 7-12. Ratio between Calculated Camber and Measured Camber at Release for All Girders.

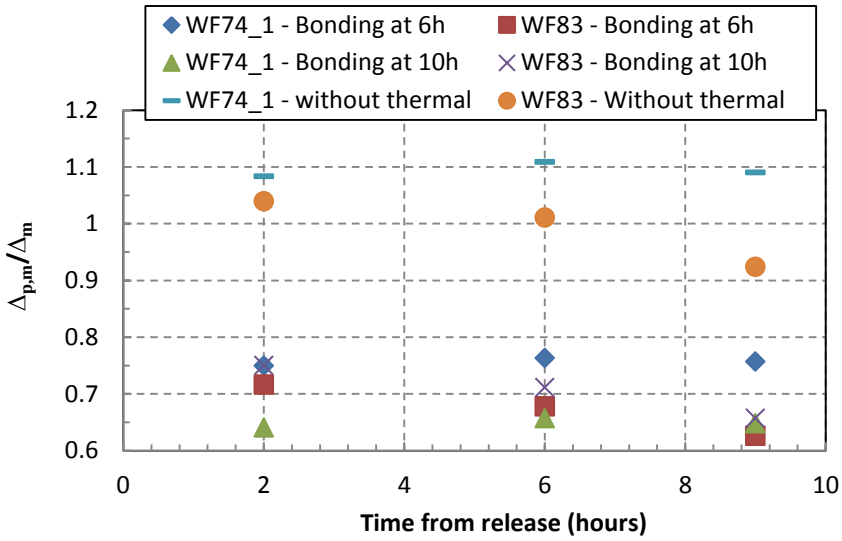

Figure 7-13. Ratio between Calculated Camber with and without Thermal and Measured Camber at 2h, 6h and 9h after Release - Girder WF74_1 and Girder WF83.

As shown in Figure 7-12, the ratios between calculated camber and measured camber of Girders WF74_2, 2A, 2B, 2C (Group 1) were closer to 1 when the thermal effects were included. This means counting for the thermal effects gives better prediction. However, as shown in the Figure 7-12 and 7-13, for two weekday girders cast at CTC, Girder WF74_1 and Girder WF83 (Group 2), accounting for the thermal effects did not help, and even made predictions worse. It is hard to explain why. One possible explanation could be that for all four girders in the Group 1 including 3 girders cast at the CPM and 1 weekend girder of the CTC, the time from stressing to de-stressing was longer than 24 hours. However, for two weekend girders in the Group 2, that time was about 16 hours. Therefore, the CTC weekday girders may gain maturity faster than the CPM girders may. Also, bonding might occur sooner than 6h after casting. To investigate this possibility, the maturities of the 5 weekday girders were computed as functions of time and are plotted in Figure 7-14.

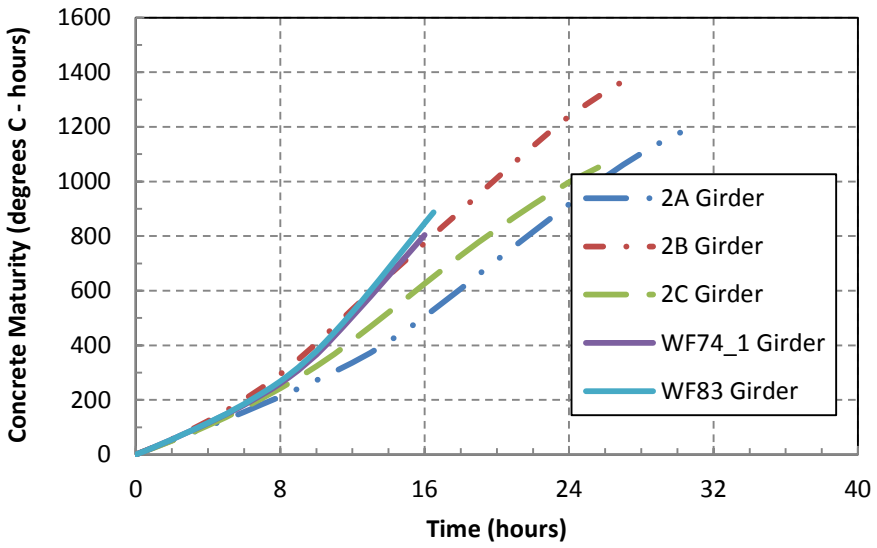

Figure 7-14 Concrete Maturity of the Girders

Figure 7-14 indicates that the maturity gain rates of the CTC girders and the CPM girder were quite similar, and cannot explain the discrepancy.

7.3 Summary

This chapter researched the effect of curing temperature on release camber by using data of temperature and camber from two WF74 and one WF83 girders cast at Concrete Technology Corporation (CTC) and data from three other W74G girders cast at Central Premix Corporation (CPM) from Barr et al. (2000). The chapter focused on analyzing the effect of heating strand before it bonded to the concrete, and the effect on camber of a temperature gradient at hardening. The accuracy of methods of estimations was evaluated by comparing the calculated camber with and without thermal effect to measured camber. Camber predictions that included thermal effects were successful for four of the six girders investigated, , implying that thermal effects may be causes of the discrepancy between measured and predicted camber at release.

The study led to following conclusions:

- High curing temperatures change the strand stress and the camber in prestressed concrete girders. The magnitude of those changes depends on the temperature

history of the girder at stressing time and during curing. The different temperatures in the strand between stressing and bonding times reduce the strand stress.

- As the girder cools to ambient temperature, the girder experiences a thermal gradient that is equal and opposite to the thermal gradient in the girder at the bonding time, causing a change in camber. Assuming that the bonding time is 10 hours from casting, for six analyzed girders, the upward camber decreased by 0.84 in., which corresponds to 30% of the average measured camber.
- The AASHTO 2005 specifications overestimate service bottom tensile stress in the girders. For six researched girders, on average, the stress decreased by 5.47 ksi (Table 7-4), which corresponds to 2.70% of jacking stress, or two times prestressing loss due to relaxation.
- For the other two girders (CTC weekday girders), the results were contrary to expectations, and further research is needed to determine the reasons.

8 SUMMARY

The goal of the study described in this thesis was to improve the methods of predicting camber in precast, prestressed concrete girders, with an emphasis on determining the effect of temperature on camber both during curing and in service. To achieve this goal, data from various girders cast in Washington State, Minnesota State and Georgia State were considered.

Detailed data were collected on the behavior of nine WF100 girders from the Alaska Way Viaduct project, fabricated by Concrete Technology Corporation (CTC) in Tacoma, Washington. Data were also collected for 146 girders by Rosa (2007) from two fabricators in Washington State. Of the 146 girders, 103 were fabricated by Concrete Technology Corporation (CTC), and the other 43 were cast by Central Premix Prestress Co. (CPM), in Spokane, Washington. Those girders varied in cross section, length, concrete strength, curing history and number of prestressing strands. The data on release concrete strength, release camber and long-term camber of the combined 155 girders (9 + 146) were used to calibrate the models of the effects of using actual concrete strength and the effect of the elastic modulus on camber. Optimization factors were recommended for implementation into current camber prediction models.

Detailed data on daily camber variations were collected for two WF100 girders, fabricated by CTC. This data included measurements of variations in internal temperatures within the two girders. Additional less-detailed data were collected for 22 girders fabricated by others, including data from five girders monitored by Barr et al. (2000), 14 girders monitored by Cullen at el. (2012), and 3 girders monitored by Hinkle at el. (2006). Those girders were cast in three states: Washington, Minnesota and Georgia. The girders had a variety of depths, lengths, curing times and times of measurement. Camber was monitored several times on specific days for each of the 24 girders (2 +22) to evaluate the effect of daily temperature variations on camber. Two models were proposed for estimating the camber change during service due to changes in temperature caused by external thermal effects, such as solar radiation and changes in ambient temperature.

The last set of data was collected for two WF74 girders and a WF83 girder from CTC, and three W74 girders fabricated at CPM from Barr et al. (2000). The concrete properties and

internal temperatures during curing were available for these girders. The purpose of measuring internal temperatures was to evaluate the effect of high curing temperatures on release camber. This research has resulted in a better understanding of the behavior of prestressed concrete girders during curing and at early ages.

8.1 Conclusions

A number of factors influence the camber of a prestressed concrete girder. From the results obtained in this study, the following conclusions can be drawn for improving predictions of camber in precast, prestressed concrete bridge girders.

1. *Concrete Strength:* Using the measured, rather than the design, compressive strength improves camber predictions, especially for the long-term camber. Since the measured concrete strength is unknown at the time of design, the estimated concrete strength can be estimated by multiplying the design concrete strength by 1.08 at release and by 1.18 at 28 days.
2. *Concrete Elastic Modulus:* Camber estimates using the elastic modulus from the AASHTO 2006 and ACI 363 recommendations tended to overestimate the measured camber. The NCHRP 496 method of calculating the elastic modulus led to better predictions of camber.
3. *Effects of temperature variations on daily cambers*: Girder camber is significantly affected by daily variations in the girder temperature distribution. These effects should be considered in estimating the camber.
4. *Effect of curing temperature on release camber:* Thermal effects are potentially major causes of the discrepancies between measured and predicted release cambers.
    - High curing temperature changes the level of strand stress. Generally, strands are stressed at ambient temperature. However, at the time of bonding (assumed to occur between 6 hours and 10 hours after casting), the concrete temperature increases rapidly as a result of the curing heat and cement hydration. The heated strands cannot expand because they are fixed at the two ends, causing the strands lose some stress.
    - The AASHTO 2006 model for predicting prestress loss leads to an overestimate of the service bottom tensile stress in the girders because it ignores a

component of the prestressing loss caused by curing temperature. The magnitude of this component can be up to 4.5 times the component due to relaxation, as was the case in Girder 2B (Chapter 7). However, this source of prestressing loss is not included in the AASHTO 2006 calculations, whereas the prestressing losses due to relaxation are included. This difference is not rational because the loss due to thermal effects is much larger.

- High curing temperatures change the level of camber for two reasons. Firstly, a high curing temperature causes the strand to expand thermally and thus to lose stress, which in turn leads to a reduction in camber. Secondly, if a temperature gradient occurs at the time of bonding, as the girder later cools to ambient temperature, the change in thermal gradient is equal and opposite to the absolute thermal gradient in the girder at the bonding time, causing a change in camber (Chapter 7). The two effects, the effect of heating strands and the effect of temperature gradient due to curing temperature, combine to influence camber. For the six analyzed girders, if bonding occurred at 10 hours after casting, the upward camber decreased by 0.84 in., on average, which corresponds to 30% of the average measured camber.

8.2 Recommendations

8.2.1 Recommendations for Practice

The following recommendations are made for practice:

1. The camber calculations should be based on the actual, rather the design, concrete strength. If the true strength is unavailable, it may by estimated (for girders in Washington State) as 1.08 and 1.18 times the design strength at release and 28 days respectively.
2. If the AASHTO (2006), the ACI 363 or the NCHRP 496 methods are used to estimate the elastic modulus for girders cast in Washington State, the following modification factors are recommended:

Table 8-1. Recommended Modification Factors for Elastic Modulus Calculations

Model	Release	Long term
AASHTO 2006	1.18	0.98
ACI 363	1.35	1.10
NCHRP 496	1.08	0.93

3. The Temperature History Model and the Peak Temperature Model (Chapter 6) are both recommended for estimating the camber change due to daily variations in temperature. They require knowledge only of the air temperature during a 24-hour period, which is typically available from meteorological records.

The governing equation for the Temperature History Model is:

$$\phi(t) = A_0 \frac{\alpha}{H} (T(t) - T_{min}) \qquad (8-1)$$

The governing equation for the Peak Temperature Model is:

$$\phi(t) = A_1 \frac{\alpha}{H} \frac{(T_{max} - T_{min})\left(1 - \cos\left(\frac{(t - t_0)}{24} 2\pi\right)\right)}{2} \qquad (8-2)$$

In these equations, the coefficient of thermal expansion is taken as $6.5*10^{-6}$ in./in./deg. F. The calibration factors: $A_0 = 1.25$, $A_1 = 1.24$ and $t_0 = 5$ hours are recommended for Washington and Minnesota girders. For girders in other states, more measured data are needed to calibrate the models.

8.2.2 Recommendations for Future Work

- This study evaluated several effects that influence camber. However, each variation influences the others. Therefore, the interactions between those effects should be investigated to predict camber better.
- Additional measurements of internal temperatures during curing and initial camber should be made to investigate the effect of curing temperature on initial camber of weekday girders.

REFERENCES

AASHTO (2005). "*LRFD Bridge Design Specifications*" 3th ed., American Association of StateHighway and Transportation Officials, Washington, DC.

AASHTO (2006). "*LRFD Bridge Design Specifications*" 3th ed. – 2006 Interim revisions, American Association of StateHighway and Transportation Officials, Washington, DC.

ACI Committee 363. "*State of the Art Report on High-Strength Concrete*" American Concrete Institute, Detroit, MI, 1992.

ACI Committee 209 (2008). " *ACI 209.2R-08 Guide for Modeling and Calculating Shrinkage and Creep in Hardened Concrete.*" American Concrete Institute, Farmington Hills, MI.

ACI Committee 318 (2008). "*ACI 318-08 Building Code Requirements for Structural Concrete and Commentary.*" American Concrete Institute, Farmington Hills, MI.

Tadros, M.K., Seguirant, S.J. (2003), Gallt, J.G. (2003). "*NCRHP Report 496 Prestress Loss in Pretensioned High- Strength Concrete Bridge.*" Transportation Research Board, DC.

Rosa, M.A., Stanton, J.F., Eberhard, M.O. (2007). "*Improving Predictions for Camber in Precast, Prestressed Concrete Bridge Girders.*" Concrete Bridge Conference.

Barr, P.J., Stanton, J.F., Eberhard, M.O. (2005). *"Effects of Temperature Variations on Precast, Prestressed Concrete Bridge Girders."* Journal of Bridge Engineering, Vol. 10(2), 186-194.

French, C.E., Neill, C.O. (2012). "*Validation of Prestressed Concrete I-Beam Deflection and Camber Estimates.*" MnDOT Final Report 2012-16, Minnesota Department of Transportation Research Service, St. Paul, MN.

Neill, C.O. (2011). "*Validation of Prestressed Concrete I-Beam Deflection and Camber Estimates.*" MSCE Thesis, Univ. of Minnesota, MN.

Barr, P.J. (2000). "*Consistent Crudeness in Prestressed Concrete Girder Design.*" PhD Dissertation, Univ. of Washington, Seattle, WA.

Hinkle, S.D. (2006). "*Investigation of Time-Dependent Deflection in Long Span, High Strength, Prestressed Concrete Bridge Beams.*" MSCE Thesis, the Virginia Polytechnic Institute and State University, Blacksburg, VA.

Tadros, M.K., Fawzy, F., Hanna, K.E. (2011). "Precast, Prestressed Girder Camber Variability." *PCI Journal,* (Winter 2011), 135-154.

Brown, K.M. (1998). "*Camber Growth Prediction in Precast Prestressed Concrete Bridge Girders.*" PhD Dissertation, Univ. of Idaho, Moscow, ID.

Pauw, A. (1960). "*Static Modulus of Elasticity of Concrete as Affected by Density*." ACI Journal, Vol. 32(6), 679-687.

Woolf, D., French, C.E. (1998). "*A Camber Study of MnDOT Prestressed Concrete I-Girders*" MnDOT Final Report 1998-08, Minnesota Department of Transportation, St. Paul, MN.